RNAchat: Integrating machine learning algorithms to identify metapathways based on clinical and multi-omics data

Mingcan Tang[1,2]

1. James Watt School of Engineering, University of Glasgow, UK
2. School of computing science, University of Glasgow, UK

ABSTRACT

Background: Understanding the global interactions among cellular pathways and types is essential for unraveling the complex biological mechanisms that underlie various diseases. While many existing studies have primarily focused on omics data, they often fail to integrate clinical heterogeneity, which is crucial for a comprehensive understanding of disease biology. Although significant progress has been made in researching crosstalks between inter-pathways and inter-cells, and tools like CellChat have emerged to analyze these interactions, they have notable limitations. These include the assumption that mRNA expression directly reflects protein activity, a heavy reliance on pre-established ligand-receptor interactions, and an inability to connect “chats” with clinical phenotypes. Furthermore, existing methods have limitations in distinguishing between paracrine signaling (interactions between different cell types) and autocrine signaling (self-signaling within the same cell type). These limitations hinder the ability to translate molecular insights into phenotypic outcomes, thereby limiting clinical applicability. To provide another solution for these challenges, we introduce RNAchat, a novel approach that utilizes machine learning techniques to identify metapathways for crosstalks among pathways at not only the bulk level but also cell types at the single-cell level, incorporating both clinical and multi-omics data.

Results: RNAchat provides another solution by providing an interactive, reproducible platform designed to analyse metapathways between inter-pathways and inter-cell types using multi-omics level data in a clinical context. This tool enables researchers to integrate diverse datasets, conduct exploratory analyses, and identify cooperated pathways. The platform facilitates hypothesis generation and produces intuitive visualizations to support further investigation.

As a proof of concept, we applied RNAchat to connect omics data to pain, drug resistance in rheumatoid arthritis (RA), disease severity to RA and Heart Failure (HF). We discovered cooperated molecular pathways associated with different treatments using SHAP (Shapley Additive Explanations) values. Then, we demonstrated how to use it to find cellular interactions at single cell level. Last but not the least, we further extended crosstalk exploration between host and parasites and found potential novel important pathways interaction not mentioned by previous studies.

Conclusion: We introduce RNAchat, a computational platform designed to identify pathway communications with clinical and multi-omics data in real-time. This tool supports both user-generated and publicly available datasets, offering a robust solution and enhancing our understanding of complex diseases such as RA and HF. The platform is available at https://github.com/tangmingcan/RNAchat.

Keywords: bulk RNA, single cell RNA, patient clinic data, multi-omics, machine learning, crosstalk, synergic effect, metapathways

BACKGROUND

Autoimmune and autoinflammatory diseases incorporate a heterogeneous group of chronic diseases with substantial morbidity and mortality, thereby posing significant health challenges. While there have been substantial advances in the treatment of RA and related rheumatic immune-mediated conditions, based on improved understanding of the underlying disease pathogenesis, there remains significant unmet clinical needs. Treatment responses remain unpredictable and inadequate response is common; some patients may respond to drugs with one mode of action, while others may respond to another drug or not at all [1]. Furthermore, although recently with the development of machine learning, signatures were found by many previous studies connecting to drug resistance/pain in RA, it still lacks a solid theory to inter-connect patients' clinical heterogeneity and multi-omic evidence with a generalised drug-independent treatment outcome [2–4].

RNAcare[5] was developed based on tools of DEG analysis such as Phantasus[6], CFViSA[7], AmiC[8], using Django, Regularisation Regression[9,10] and distributed framework for accelerating the analysis process. It provides insightful results in terms of pain, fatigue and drug response for RA treatment. However, it didn't consider interaction between metagenes; RNAcompare is the development of RNAcare, focusing on addressing the issues of heterogeneous data and suggesting its own solution for tissue-cross, omic-cross, batch-cross, tech-cross and disease-cross data. But it still has limitations: It found crosstalk/synergy effects passively by SHAP dependence plot, and it limits to only two metagenes; used Pearson Correlation matrix for variable selection while potentially retaining overlapped metagenes with same biologic function; didn't consider crosstalk among pathways/cell types in a single cell background.

At the same time, softwares such as CellChat[11] have appeared to analyze these interactions at the single cell level. Still, they have notable limitations. These include the assumption that mRNA expression directly reflects protein activity, a heavy reliance on pre-established ligand-receptor interactions, and an inability to infer/prioritise direct functional effects based on clinical outcome. Furthermore, existing methods struggle to distinguish between paracrine signaling (interactions between different cell types) and autocrine signaling (self-signaling within the same cell type) at single cell level.

MetaPathways[12] is a bioinformatics software designed for functional annotation and metabolic pathway reconstruction from metagenomics and metatranscriptomic data. It is particularly useful for analyzing microbial communities and understanding their metabolic capabilities. However, it only focuses on metabolic and biochemical pathway interactions among microbes; still an unsupervised in nature, which means it lacks a pre-defined functional target.

To address these complexities, we introduce RNAchat. This development of RNAcompare offers an automated pipeline that seamlessly integrates clinical and multi-omics data for clinicians, facilitating the identification of metapathways across inter-pathways/inter-cells through advanced machine learning algorithms. By enabling comprehensive, multi-levels analyses, RNAchat aims to enhance our understanding of disease pathogenesis and inform the development of more effective, personalized treatment strategies.

IMPLEMENTATION

The overall aim of RNAchat is to provide a web-based tool simplifying the identification of interactions among pathways based on multi-omics and clinical data and showing the analysis workflow in tabs as outlined in Figure 1 which will be described later in more detail. RNAchat was developed in Python, utilizing several open-source packages. The webserver was built using the Django framework, adhering to the FAIR[13] (Findable, Accessible, Interoperable, and Reusable) principle. The platform employs the Plotly graphics system for generating interactive visualisations on the fly. The platform can be installed locally from https://github.com/tangmingcan/RNAchat.

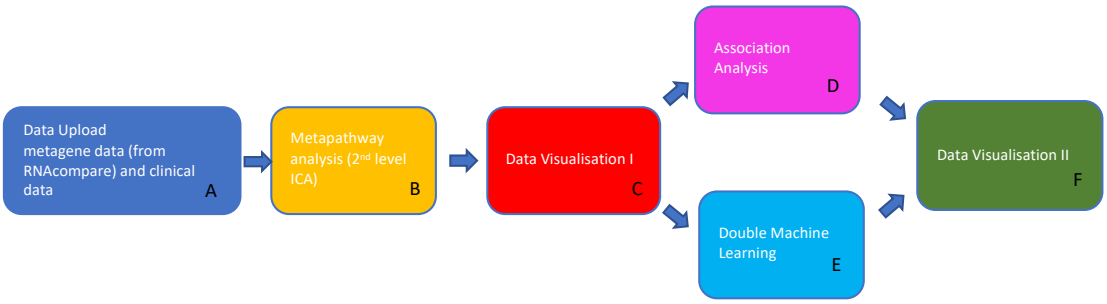

Figure 1- RNAchat work flow. (A) In the first tab, user can upload processed metagene data from RNAcompare and clinical data; (B) Metapathway analysis where data was processed by Independent Component Analysis (ICA) again. (C) Data Visualisation I for the 2nd level ICA processed data to check relationships and expression level of metapathways; (C) Association Analysis based on metapathways; (D) Double Machine Learning (DML) analysis based on metapathways; (E) Data Visualisation II for cooperated metagenes in the metapathways and cooperated cell types (only for single cell data).

To enable several users working on the system, Django is used to allow group and authentication management. System administrators can easily assign group roles to specific users, enabling them roles to only view and operate the permitted data.

Datasets

We introduced the following RA, HF, single cell and malaria datasets (Table 2) – Optimal management of RA patients requiring Biologic Therapy (ORBIT[14]), Pathobiology of Early Arthritis Cohort (PEAC[15]), RA-MAP[16] as part of the IMID-Bio-UK consortium, GSE135055[17] , RV infection scRNA-seq[18] , GSE288146 [19] and GSE289197 [20].

Cohort name	Number of participants	Data type	tissue type	#clinical feature
PEAC1	49	Bulk RNA-seq (harmonised with ORBIT)	Whole Blood	7
PEAC2	67	Bulk RNA-seq	Whole Blood	1
	53	Bulk RNA-seq	Synovium	1
ORBIT	139	Bulk RNA-seq (harmonised with PEAC1)	Blood	16
RA-MAP	63	Relative fluorescence units(RFU)	Plasma	1
	34	Microarray	Whole Blood	1
GSE135055	18	Bulk RNA-seq-FPKM	Left ventricular heart tissue	2
RV infection scRNA-seq	4 batches	Single cell RNA-seq	primary human bronchial organoids	1*
GSE288146	2 batches	Single cell RNA-seq	Plasmodium	0
GSE289197	79	Bulk RNA-seq	Whole Blood	1

Table 1. Overview of PEAC, ORBIT, RA-MAP, GSE135055 and RV infection scRNA-seq used in RNAchat. For RV infection scRNA-seq data, we put cell types in the clinical data.

The Pathobiology of Early Arthritis Cohort (PEAC) was established with the aim to create an extensively phenotyped cohort of patients with early inflammatory arthritis, including RA, linked to detailed pathobiological data. The clinical and transcriptomic data can be found on EBI ArrayExpress with accession E-MTAB-6141. When analysing with ORBIT, we used processed PEAC1, downloaded directly from RNAcare after its own qualification control; When analysing based on two tissues, we used the original PEAC from the source mentioned.

ORBIT was a study comparing Rituximab to anti-TNF treatments. Blood was taken from patients before drug treatment. RNA-Seq data are being submitted to Array Express as pseudo-anonymized data.

The RA-MAP Consortium is a UK industry-academic collaboration to investigate clinical and biological predictors of disease outcome and treatment response in RA, using deep clinical and multi-omic phenotyping. The raw data were retrieved from accessions GSE97810 and GSE97948 on ArrayExpress. The clinical data can be found here: https://doi.org/10.6084/m9.figshare.c.5491611.v1

GSE135055 was a study about Heart Failure (HF), collected from left ventricular heart tissue from 21 HF patients and 9 healthy donors as study cohort and generated multi-level transcriptomic data. We just used 18 patients with Dilated Cardiomyopathy (DCM), a condition where the heart's left ventricle (the main pumping chamber) becomes enlarged and weakened, reducing its ability to pump blood effectively.

RV infection scRNA-seq data about rhinovirus infection in primary human bronchial organoids comprises four conditions: exposure to cigarette-smoke extract (CSE), rhinovirus (RV) infection, the combination of rhinovirus and cigarette smoke (RVCSE), and a control condition (mock). Although rhinovirus infection has been investigated[18], the goal of our study was to further probe cellular communication to viral infection from each airway epithelial cell type in the presence or absence of a common environmental insult that is known to impact the outcome of rhinovirus infection: cigarette smoke. The data is available on Dryad[21].

Malaria pathogenesis, encompassing parasite invasion, egress, and antigenic variation, relies on the coordinated activity of numerous proteins, yet their molecular regulatory mechanisms remain poorly understood. GSE288146 was an experiment for the intrinsic mechanism of PfAP2-V regulation in P. falciparum by scRNA-seq analysis. Here we just used the baseline data.

GSE289197 is transcript data detailing human transcription in severe malaria cases and uncomplicated malaria controls in a Mali study. Severe malaria cases were either cerebral malaria, severe malarial anemia, or concurrent cerebral malaria and severe malarial anemia disease.

Clinical data used from the cohorts

RA disease activity was assessed using the validated DAS (Disease Activity Score using 28 joint counts) score, which was calculated from the original recorded 28 joint counts plus a blood marker of inflammation, typically the erythrocyte sedimentation rate (ESR) or the C-reactive protein (CRP) level[22]; DAS score in RA-MAP is standardised; Pain VAS[23] is short for pain Visual Analog Scale (VAS) for self-reported pain, which is a unidimensional measure of general pain intensity, used to measure patients' current pain level. The pain VAS is not specific to RA and has been widely used in a range of patient populations, including those with other rheumatic diseases, patients with chronic pain, cancer, or even cases with allergic rhinitis[24], which provides an possibility for integration of different diseases for our later discussion.

HYNA (New York Heart Association[25]) is a system used to classify the severity of HF based on a patient's symptoms and physical activity limitations. It has four functional classes: Class I: No symptoms and no limitations in ordinary physical activity; Class II: Mild symptoms and slight limitation during ordinary activities; Class III: Significant limitation in activity due to symptoms; comfortable only at rest; Class IV: Severe limitations; symptoms present even at rest.

To combine the disease severity of both diseases, we min-maximised each severity index (DAS in PEAC+ORBIT and HYNA in GSE135055) to 0-1 respectively, and then multiplied by 100. The second step is not necessary.

For RV infection scRNA-seq data, we put cell type of each record in the clinical data.

All this clinical information is stored on csv files and, after curation, loaded into RNAchat.

For GSE289197, the number of parasitemia in the whole blood was used to measure the infection.

A - Data upload

The user has the option to import preprocessed data from RNAcompare, or upload their own iCA pre-processed data on the fly combined with clinical data which may include cell type information for scRNA analysis. Clinical data are uploaded as a table.

B – Metapathway Analysis

Based on the first-level independent component analysis (ICA[26]) processed data, we perform a second-level ICA on the metagenes. We hypothesize that the pathways represented by metagenes interact with one another, forming higher-order structures referred to as metapathways. Following the second-level ICA, we can extract the components of these metapathways, each composed of multiple metagenes. In the case of single-cell RNA sequencing (scRNA-seq) data, individual cell types are treated as specialized metagenes during the decomposition process. Consequently, the resulting metapathways may incorporate cell type information, reflecting ICA-derived correlations between cell types and pathways within the same metapathway. If a metapathway contains only a single cell type, it is indicative of autocrine signaling; if multiple cell types are present, it suggests paracrine signaling. Conversely, metapathways devoid of cell type representation correspond to generalized pathway interactions that are not cell type-specific.

Metapathways can be directly downloaded after processing.

C - Data Visualisation I

In this section, users will perceive the relationships of metapathways. We provide 2 ways: Pearson Correlation Matrix[27] and matrixplot scaled by metapathways/batches. When uses want to compare the expression level of different metapathways within the same tissue and omics level, the option of ‘scaled by metapathways’ is recommended; otherwise, ‘scaled by batches’ is recommended.

D - Associatioin Analysis

Here, the user has the option to associate selected clinical data parameters with metapathway data in order to study phenotypes based on part or all of datasets. We provide Random Forests[28], XGBoost[29] and LightGBM[30] with its corresponding parameters for basic tuning. The data will be split into training and test (20%) datasets by default. AUC-ROC[31] or MSE[32] will be shown according to different cases. This module will provide SHAP[33] feature importance plot and SHAP dependence plot.

E - Double Machine Learning (DML) Analysis

We used DML introduced from RNAcompare to bypass data hamalisation for comparsion between different batches/tissues/omics levels. Causal Forests[34] is recommended because it can estimate conditional treatment heterogeneity between batches, which can allow us to explore whether the most contributing factor (hub metapathways) in a given condition is the most important compared to protective mechanisms. Notably, the most significant contributor identified by Association analysis may differ from feature importance rankings obtained using Causal Forests.

F – Data Visualisation II

In this section, user can use network plot to visualise the interactions among metagenes/cell types for finding the most frequent/significant metagenes/cell types.

Results

Here we present the first tool that allows users without bioinformatics skill to integrate clinical and multi-omics data, establish an automated pipeline, and look for crosstalks between inter-pathways/ inter-cell types by integrated machine learning algorithms.

Case Study 1: Drug-Specific Interferon Metapathways Underlie Treatment Response Heterogeneity in RA

First, we applied Random Forests association analysis to drug response (0-nonresponse, 1-response) in RNAcompare after ICA based on 3rd level granularity data defined in RNAcompare. We can see metagene_3 shows positively related to drug response in Figure 2-A. We did enrichment analysis and found it was enriched in IFN signalling in Figure 2-B. We then did 2nd level ICA analysis based on metagenes which we called as metapathway analysis. Figure 2-C shows after 2nd time ICA, metagenes were decomposed into metapathways for inter-pathway interactions. We can see meta_2 includes metagene_3_1st standing for metagene_3 mentioned before. Also, we think meta_2 includes related metapathways cooperating with metagene_3_1st, which are explained in Table 2-A in metapathway_2(All). Next, we used the same data and did metapathway (2nd level ICA) analysis based on anti-TNF and Rituximab treatment separately, showed in Figure 2-D-E, and looked for metapathways containing metagene_3_1st. We found in Figure 2-D, metagene_3_1st belongs to meta_6, while in Figure 2-E, metagene_3_1st belongs to meta_3. We did the similar enrichment analysis for metapathway_6(Anti-TNF) and metapathway_3(Rituximab). Interestingly, we found the two metapathways were slightly different: metapathway for Rituximab exhibits more related to type II IFN. This may be partly because the thresholds we used to select candidate metagenes during generalised metapathway analysis. However, it cannot be fully explained by this reason because the order of the metagenes in the list also matters, since metagene_14_1st exists in Rituximab rather than Anti-TNF group. We could only contribute this to selection bias/ heterogeneity at the baseline.
Figure 3-A shows SHAP importance plot for the whole dataset based on metapathways. We can see metapathway_1 is the most positively related to

pain this time, while metapathway_3 exhibits complexity. When we separately plotted the importance for Rituxmab (Figure 3-B) and anti-TNF (Figure 3-C), we found metapathway_3 exhibits the characteristic of type I IFN in both plots, namely lower expression of metapathway_3 in Figure 3-B exhibits good response to Rituximab, and higher expression of metapathway_3 in Figure 3-C exhibits good response to anti-TNF, which can explain the complexity in Figure 3-A, why red dots are symmetrically distributed for metapathway_3. This seems a contradiction based on the presumption in RNAcompare that metagene_3_1st behaved more like type II IFN.

Of Note, after comparing 3 plots in Figure 3, we can see the introduction of Rituximab activates metapathway_1, making it more important to pain, because metapathway_1 includes metagene_2_1st, which is L1CAM/Notch related pathway (see Table 2-A Metapathway_3(Rituximab))[5,35]. Therefore, this explains the contradiction that during the 1st ICA level analysis, the effect was contributed to metagene_3_1st for Rituximab responders.

One plausible explanation is before B cell depletion, HSP90AA1 stabilizes survival pathways in B-cells, ensuring that they function properly within the immune system (Rho GTPase cycle and B cell receptor signaling)[36,37]. After B cell depletion under Rituximab, HSP90AA1 could shift the major role to stabilize Type II IFN signaling components[36–38], possibly amplifying inflammation and immune responses, leading to further activation of immune cells that could maintain or enhance autoimmune processes.

Figure 3-D shows the relationship between metagenes based on metapathways: each circle (node) represents a metagene; each line (edge) connects metagenes within the same metapathway; the size of link is proportional to its frequency across all pathways, another perspective of visualising hub metagenes. The interaction between (metagene_17_1st, metagene_8_1st) seems to appear frequently, representing the interaction between class I MHC mediated antigen processing presentation and B cell receptor signalling[39]; (metagene_15_1st, metagene_8_1st) represent the interaction between EJC-independent NMD and B cell signalling[40].

A

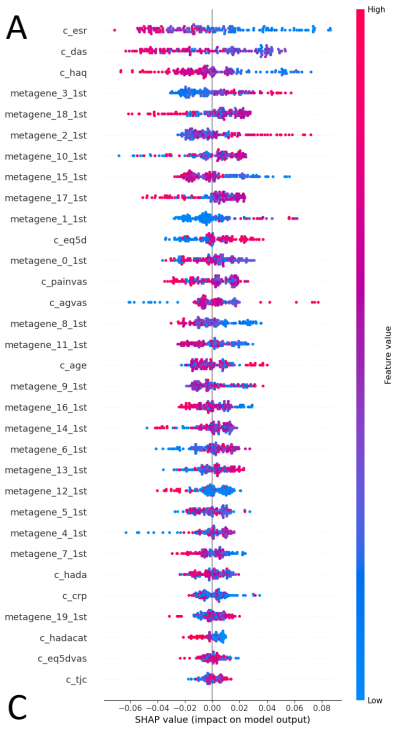

B

Name	PValue
REACTOME_INTERFERON_SIGNALING	1.476452e-46
REACTOME_INTERFERON_ALPHA_BETA_SIGNALING	1.071163e-45
REACTOME_INTERFERON_GAMMA_SIGNALING	9.851463e-32
WP_IMMUNE_RESPONSE_TO_TUBERCULOSIS	7.511500e-17
WP_TYPE_II_INTERFERON_SIGNALING	1.861285e-16
WP_TYPE_II_INTERFERON_SIGNALING_IFNG	4.031285e-13

C

	inputs
meta_0	[metagene_1_1st, metagene_0_1st, metagene_10_1st, metagene_4_1st, metagene_7_1st]
meta_1	[metagene_2_1st, metagene_0_1st, metagene_13_1st, metagene_6_1st]
meta_2	[metagene_16_1st, metagene_14_1st, metagene_7_1st, metagene_3_1st, metagene_17_1st, metagene_8_1st, metagene_0_1st]
meta_3	[metagene_18_1st, metagene_17_1st, metagene_4_1st, metagene_8_1st, metagene_10_1st]
meta_4	[metagene_19_1st, metagene_17_1st, metagene_4_1st, metagene_14_1st, metagene_9_1st, metagene_8_1st]
meta_5	[metagene_8_1st, metagene_15_1st, metagene_6_1st, metagene_19_1st, metagene_7_1st]
meta_6	[metagene_6_1st, metagene_17_1st, metagene_15_1st, metagene_8_1st]

D

	inputs
meta_0	[metagene_2_1st, metagene_0_1st, metagene_14_1st, metagene_5_1st, metagene_6_1st]
meta_1	[metagene_12_1st, metagene_14_1st, metagene_11_1st, metagene_9_1st, metagene_13_1st, metagene_15_1st, metagene_10_1st, metagene_18_1st]
meta_2	[metagene_16_1st, metagene_14_1st, metagene_7_1st, metagene_17_1st, metagene_8_1st]
meta_3	[metagene_18_1st, metagene_17_1st, metagene_8_1st, metagene_4_1st]
meta_4	[metagene_8_1st, metagene_15_1st, metagene_6_1st, metagene_19_1st, metagene_7_1st, metagene_1_1st, metagene_18_1st]
meta_5	[metagene_19_1st, metagene_17_1st, metagene_14_1st, metagene_9_1st, metagene_4_1st, metagene_8_1st, metagene_15_1st, metagene_5_1st]
meta_6	[metagene_6_1st, metagene_17_1st, metagene_15_1st, metagene_8_1st, metagene_3_1st]

E

	inputs
meta_0	[metagene_1_1st, metagene_10_1st, metagene_0_1st, metagene_11_1st, metagene_12_1st, metagene_4_1st, metagene_14_1st, metagene_18_1st]
meta_1	[metagene_2_1st, metagene_13_1st, metagene_0_1st, metagene_16_1st, metagene_10_1st, metagene_6_1st]
meta_2	[metagene_18_1st, metagene_4_1st, metagene_17_1st, metagene_13_1st, metagene_8_1st, metagene_14_1st, metagene_7_1st, metagene_10_1st]
meta_3	[metagene_16_1st, metagene_14_1st, metagene_7_1st, metagene_8_1st, metagene_17_1st, metagene_3_1st, metagene_2_1st]
meta_4	[metagene_19_1st, metagene_17_1st, metagene_4_1st, metagene_9_1st, metagene_14_1st, metagene_8_1st]
meta_5	[metagene_8_1st, metagene_15_1st, metagene_9_1st, metagene_11_1st, metagene_19_1st, metagene_16_1st]
meta_6	[metagene_17_1st, metagene_6_1st, metagene_15_1st, metagene_5_1st]

Figure 2. (A)SHAP importance plot for metagenes. (B) Enrichment analysis of metagene_3_1st; (C) Componets of metapathway analysis for all data; (D) Components of metapathway analysis for only Anti-TNF; (E) Components of metapathway analysis for ony Rituximab;

Metagene 2nd level	Metagene 1st level	Enrichment result	Explaination
Metapathway_2(All)	16	REACTOME_RHO_GTPASE_CYCLE	I IFN
	14	REACTOME_MHC_CLASS_II_ANTIGEN_PRESENTATION KEGG_ALLOGRAFT_REJECTION	II IFN
	7	REACTOME_TOLL_LIKE_RECEPTOR_CASCADES REACTOME_SIGNALING_BY_INTERLEUKINS	
	17	REACTOME_CLASS_I_MHC_MEDIATED_ANTIGEN_PROCESSING_PRESENTATION	I IFN
	8	REACTOME_RHO_GTPASE_CYCLE WP_B_CELL_RECEPTOR_SIGNALING	I IFN
	0	REACTOME_RESPONSE_TO_ELEVATED_PLATELET_CYTOSOLIC_CA2 REACTOME_FORMATION_OF_FIBRIN_CLOT_CLOTTING_CASCADE	
Metapathway_6(Anti-TNF)	6	REACTOME_NONSENSE_MEDIATED_DECAY_NMD	I IFN
	17	REACTOME_CLASS_I_MHC_MEDIATED_ANTIGEN_PROCESSING_PRESENTATION	I IFN, II IFN
	15	REACTOME_EUKARYOTIC_TRANSLATION_ELONGATION REACTOME_NONSENSE_MEDIATED_DECAY_NMD_INDEPENDENT_OF_THE_EXON_JUNCTION_COMPLEX_EJC	I IFN
	8	REACTOME_RHO_GTPASE_CYCLE WP_B_CELL_RECEPTOR_SIGNALING	I IFN
Metapathway_3(Rituximab)	16	REACTOME_RHO_GTPASE_CYCLE	I IFN
	14	REACTOME_MHC_CLASS_II_ANTIGEN_PRESENTATION KEGG_ALLOGRAFT_REJECTION	II IFN
	7	REACTOME_TOLL_LIKE_RECEPTOR_CASCADES REACTOME_SIGNALING_BY_INTERLEUKINS	
	8	REACTOME_RHO_GTPASE_CYCLE WP_B_CELL_RECEPTOR_SIGNALING	I IFN
	17	REACTOME_CLASS_I_MHC_MEDIATED_ANTIGEN_PROCESSING_PRESENTATION	I IFN, II IFN
	2	REACTOME_L1CAM_INTERACTIONS BIOCARTA_AHSP_PATHWAY	II IFN

Table 2 Metapathway analysis.

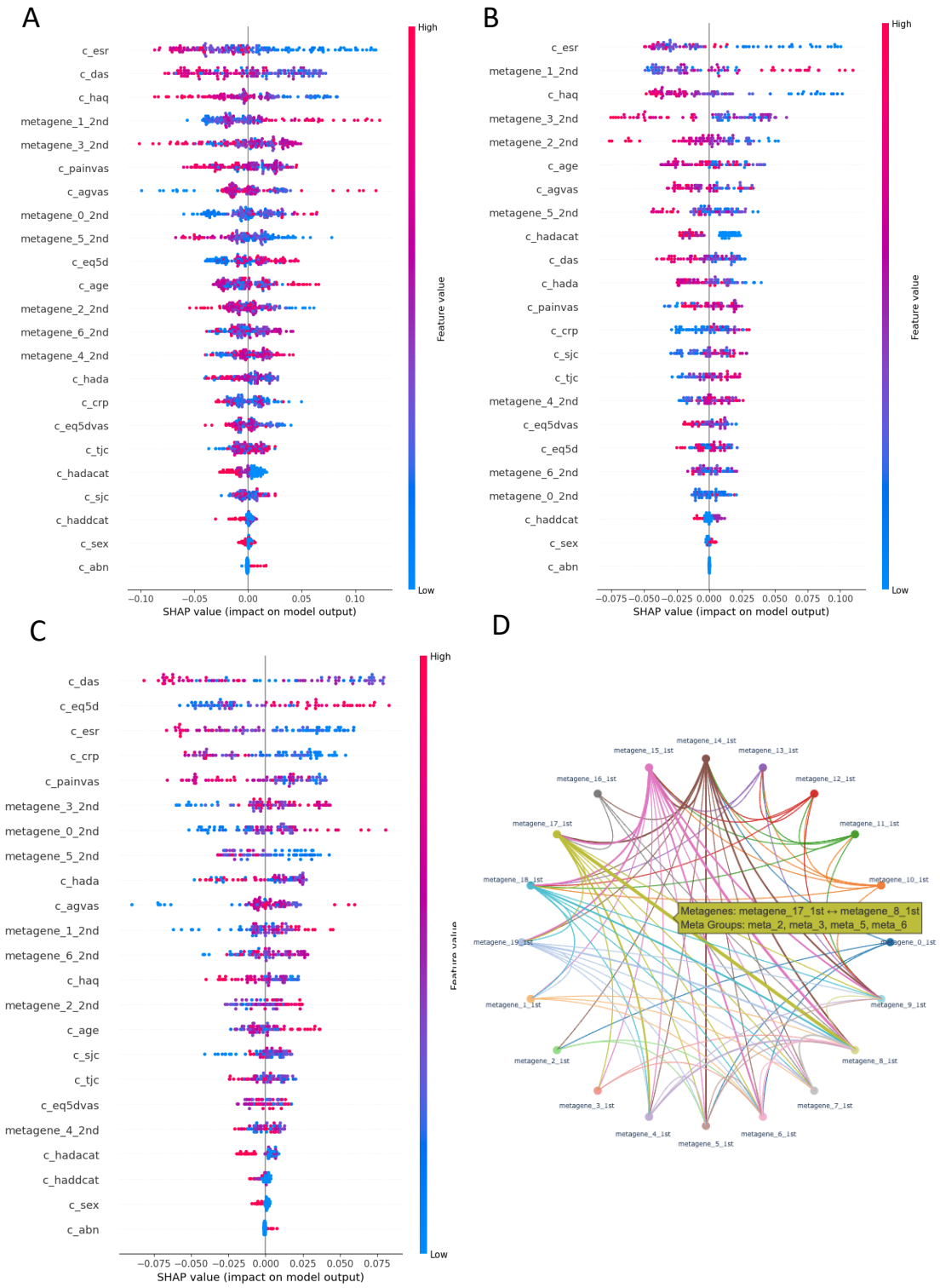

Figure 3. (A) SHAP importance plot for metapathways based on all data; (B) SHAP importance plot for metapathways based on Rituximab; (C) SHAP importance plot for metapathways based on anti-TNF; (D) Relationship of metagenes;

Conclusion: Through 2nd level ICA analysis, we found cooperated pathways and explained the most important metapathways to the

treatment outcome. Besides, we found its activated pathway after introducing Rituximab.

Case Study 2: Immune Feedback Loops to pain at transcriptomic level: The Role of Type II IFN and Complement Cascade

In this case, we will adopt Causal Forests based on cohort-ICA similar to cases in RNAcompare. But this time we didn't use Pearson Correlation matrix for variable selection.

Figure 4-A shows the SHAP importance of metapathways to pain. Figure 4-B shows their components after Enrichment analysis. (metagene_0_orb, metagene_3_pea) grouped together in metapathway_2 as expected because they are identical.

We can see the most important metapathway is metapathway_0, including 2 metagenes, metagene_3_orb and metagene_5_orb. The 2nd important metapathway is metapathway_9. After that we noticed complement cascade in metapathway_1 acting as a feedback hub, and linking innate immune responses (alpha defensins) and coagulation/thrombosis (platelet activation).

C3 and C5 activation are crucial steps in the complement cascade, and their activation has significant implications for immune responses, particularly in inflammation and immune complex-mediated diseases like RA[41]. Using RNAcare, we drew the heatmap plot for ORBIT. As we expected in Figure 4-C, non-respondent group shows high expression with signatures of complement cascade pathway, identical with the result in RNAcompare.

Next, we drew a Pearson Correlation Matrix to explore the relationship among metapathways in Figure 4-D. We can see metapathway_0 and metapathway_9 are negatively correlated. Notably, metapathway_9 is enriched in type II IFN. Therefore, our assumption is under Rituximab and its induction of type II IFN, metapathway_9 proliferate the damage from metapathway_0, while relieving the pain.

To further prove this assumption, we did a matrixplot scaled by each pathway in Figure 4-E. As we see, the mean expression of metapathway_0 in responder group (ORBIT) is lower than that in non-responder group (ORBIT). Since we already known that responder group had higher expression of type II IFN (RNAcompare), the result proves our assumption. Besides, we also see metapathway_7 (complement cascade related pathway) is higher in non-response group. We can also prove it in density plots in Figure 4-FG.

Different from non-responders, for Rituximab responders in metapathway_6, the participation of type II IFN can activate the cooperation of IL10 signaling and complement cascade in the negative feedback loop, relieving the pain from metapathway_7[42,43].

Figure 4-E shows the interactions between metagenes. (metagene_2_pea, metagene_8_orb) represents the most frequent one between antigen presentation and TLR signaling[44] ; (metagene_2_pea, metagene_5_pea) stands for the one between nkcells pathway and alpha defensin[45].

Besides, we also think the involvement of type II IFN have two roles: on one hand, they can drive pain progression within the same level, to make the tissue less damaged; on the other hand, they can act in a negative feedback loop to prevent excessive inflammation and pain sensitization between different layers (tissues/omics layers).

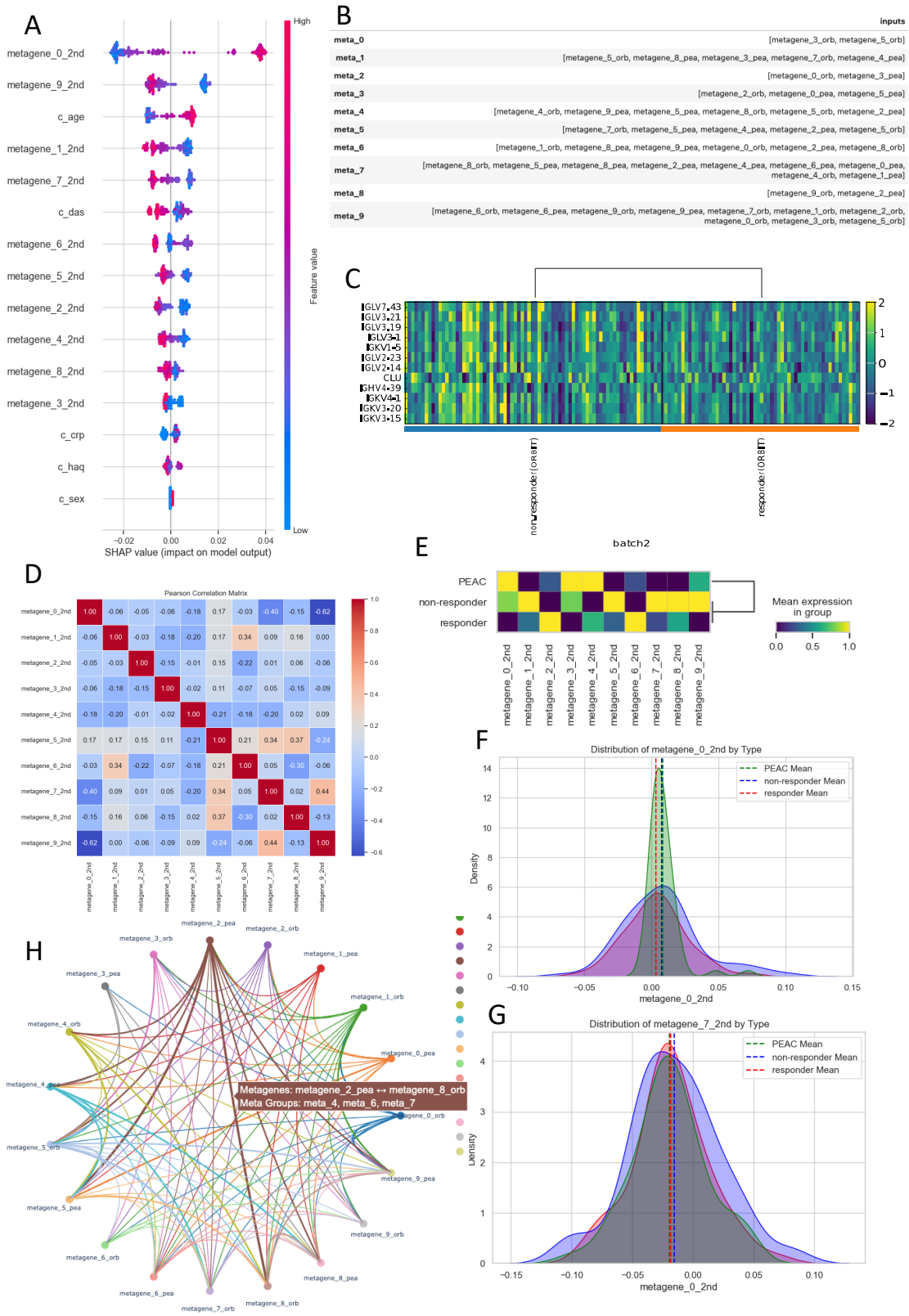

Figure 4. (A) SHAP importance of metapathways; (B) Componets of metapathways; (C) Signatures of complement cascade pathway; (D) Pearson Correlation Matrix of metapathways; (E) Matrixplot of 3 batches scaled by metagenes; (F) Distribution of metapathway_0 of 3 batches; (G) Distribution of metapathway_7 of 3 batches. (H) Relationship of metagenes.

Metagene 2nd level	Metagene 1st level	Enrichment result	Signatures
metapathway_0	3_orb	REACTOME_NONSENSE_MEDIATED_DECAY_NMD REACTOME_SELENOAMINO_ACID_METABOLISM	FAU
	5_orb	REACTOME_RESPONSE_TO_ELEVATED_PLATELET_CYTOSOLIC_CA2 REACTOME_COMMON_PATHWAY_OF_FIBRIN_CLOT_FORMATION	PROS1, F13A1
metapathway_9	6_orb	WP_OSTEOPONTIN_SIGNALING PID_AVB3_OPN_PATHWAY	MMP9
	6_pea	KEGG_MEDICUS_REFERENCE_TCR_PLCG_ITPR_SIGNALING_PATHWAY	CD247,GRAP2,PLCG1,LAT,FYN,ZAP70,ITPR3,LCK
	9_orb	BIOCARTA_CTL_PATHWAY BIOCARTA_NKCELLS_PATHWAY KEGG_MEDICUS_REFERENCE_ANTIGEN_PROCESSING_AND_PRESENTATION_BY_MHC_CLASS_I_MOLECULES	HLA-B, HLA-C,B2M, HLA-E
	9_pea	WP_ALLOGRAFT_REJECTION BIOCARTA_CTL_PATHWAY BIOCARTA_AHSP_PATHWAY	GZMB, AHSP
	7_pea	KEGG_ALLOGRAFT_REJECTION	FAS,CD28,CD86,CD40,CD40LG,HLA-DMB,HLA-DOA
	1_orb	BIOCARTA_AHSP_PATHWAY WP_HEMATOPOIETIC_STEM_CELL_DIFFERENTIATION REACTOME_ERYTHROCYTES_TAKE_UP_CARBON_DIOXIDE_AND_RELEASE_OXYGEN	
	2_orb	REACTOME_ANTIMICROBIAL_PEPTIDES REACTOME_ALPHA_DEFENSINS	DEFA1, DEFA3, DEFA4
	0_orb	REACTOME_INTERFERON_SIGNALING REACTOME_INTERFERON_GAMMA_SIGNALING REACTOME_INTERFERON_ALPHA_BETA_SIGNALING	MX1, STAT1, STAT2, CXCL10
	3_orb	REACTOME_NONSENSE_MEDIATED_DECAY_NMD REACTOME_SELENOAMINO_ACID_METABOLISM	FAU
	5_orb	REACTOME_RESPONSE_TO_ELEVATED_PLATELET_CYTOSOLIC_CA2 REACTOME_COMMON_PATHWAY_OF_FIBRIN_CLOT_FORMATION	PROS1, F13A1
metapathway_1	5_orb	REACTOME_RESPONSE_TO_ELEVATED_PLATELET_CYTOSOLIC_CA2 REACTOME_COMMON_PATHWAY_OF_FIBRIN_CLOT_FORMATION	PROS1, F13A1
	8_pea	REACTOME_FCGR_ACTIVATION REACTOME_COMPLEMENT_CASCADE	IGLV7-43, IGLV3-21, PROS1
	3_pea	REACTOME_INTERFERON_SIGNALING REACTOME_INTERFERON_GAMMA_SIGNALING REACTOME_INTERFERON_ALPHA_BETA_SIGNALING	MX1, STAT1, STAT2, CXCL10
	7_orb	REACTOME_NEUTROPHIL_DEGRANULATION KEGG_HEMATOPOIETIC_CELL_LINEAGE	
	4_pea	PID_ATF2_PATHWAY PID_NFAT_TFPATHWAY PID_REG_GR_PATHWAY	FOS, CXCL8
Metapathway_7	8_orb	REACTOME_TOLL_LIKE_RECEPTOR_CASCADES	S100A8, S100A9, LY96
	5_pea	REACTOME_ANTIMICROBIAL_PEPTIDES REACTOME_ALPHA_DEFENSINS REACTOME_NEUTROPHIL_DEGRANULATION	DEFA1, DEFA3, DEFA4
	8_pea	REACTOME_FCGR_ACTIVATION REACTOME_COMPLEMENT_CASCADE	IGLV7-43, IGLV3-21, PROS1
	2_pea	REACTOME_ANTIGEN_PRESENTATION_FOLDING_ASSEMBLY_AND_PEPTIDE_LOADING_OF_CLASS_I_MHC BIOCARTA_CTL_PATHWAY BIOCARTA_NKCELLS_PATHWAY	HLA-B, HLA-C, B2M, HLA-E
	4_pea	PID_ATF2_PATHWAY PID_AP1_PATHWAY REACTOME_SIGNALING_BY_NTRKS PID_REG_GR_PATHWAY	FOS, CXCL8
	6_pea	KEGG_MEDICUS_REFERENCE_TCR_PLCG_ITPR_SIGNALING_PATHWAY	
	0_pea	REACTOME_P2Y_RECEPTORS	P2RY1,P2RY2,P2RY6,P2RY12,P2RY14
	4_orb	PID_IL12_2PATHWAY KEGG_NATURAL_KILLER_CELL_MEDIATED_CYTOTOXICITY BIOCARTA_CTL_PATHWAY	GZMB
	1_pea	REACTOME_NONSENSE_MEDIATED_DECAY_NMD REACTOME_SELENOAMINO_ACID_METABOLISM	RPL21, RPL23A, RPL29, RPL39, RPL41, RPLP0, RPS2, RPS3A, RPS15, RPS15A, RPSA, RPL14, RPS26
Metapathway_6	1_orb	BIOCARTA_AHSP_PATHWAY WP_HEMATOPOIETIC_STEM_CELL_DIFFERENTIATION REACTOME_ERYTHROCYTES_TAKE_UP_CARBON_DIOXIDE_AND_RELEASE_OXYGEN	
	8_pea	REACTOME_FCGR_ACTIVATION REACTOME_COMPLEMENT_CASCADE	IGLV7-43, IGLV3-21, PROS1

	9_pea	WP_ALLOGRAFT_REJECTION BIOCARTA_CTL_PATHWAY BIOCARTA_AHSP_PATHWAY	GZMB, AHSP
	0_orb	REACTOME_INTERFERON_ALPHA_BETA_SIGNALING REACTOME_INTERFERON_GAMMA_SIGNALING	MX1, STAT1, STAT2, CXCL10
	2_pea	REACTOME_ANTIGEN_PRESENTATION_FOLDING_ASSEMBLY_AND_PEPTIDE_LOADING_OF_CLASS_I_MHC BIOCARTA_CTL_PATHWAY BIOCARTA_NKCELLS_PATHW	HLA-B, HLA-C, B2M, HLA-E
	8_orb	PID_TOLL_ENDOGENOUS_PATHWAY REACTOME_INTERLEUKIN_10_SIGNALING	S100A8,S100A9,LY96; IL1R2,IL1R1,PTGS2

Table 3. Metapathway analysis.

Case Study 3: Synovium vs. Blood: Distinct Immune Feedback Loops in RA Pain Regulation

In this case, we applied Causal Forests, connecting different tissues to pain using PEAC. Figure 5-A shows SHAP importance. Figure 5-B shows metagene members for each metapathways. Figure 5-C shows the relationships among metapathways. We can see Group 1: (metapathway_3, metapathway_4, metapathway_5, metapathway_8, metapathway_9) negatively correlated with Group 2: (metapathway_1, metapathway_2). Figure 5-D shows the matrix plot scaled by tissue types.

Combining Figure 5-CD, we can see Group1 is more active at synovium level while Group 2 is more active at whole blood level.

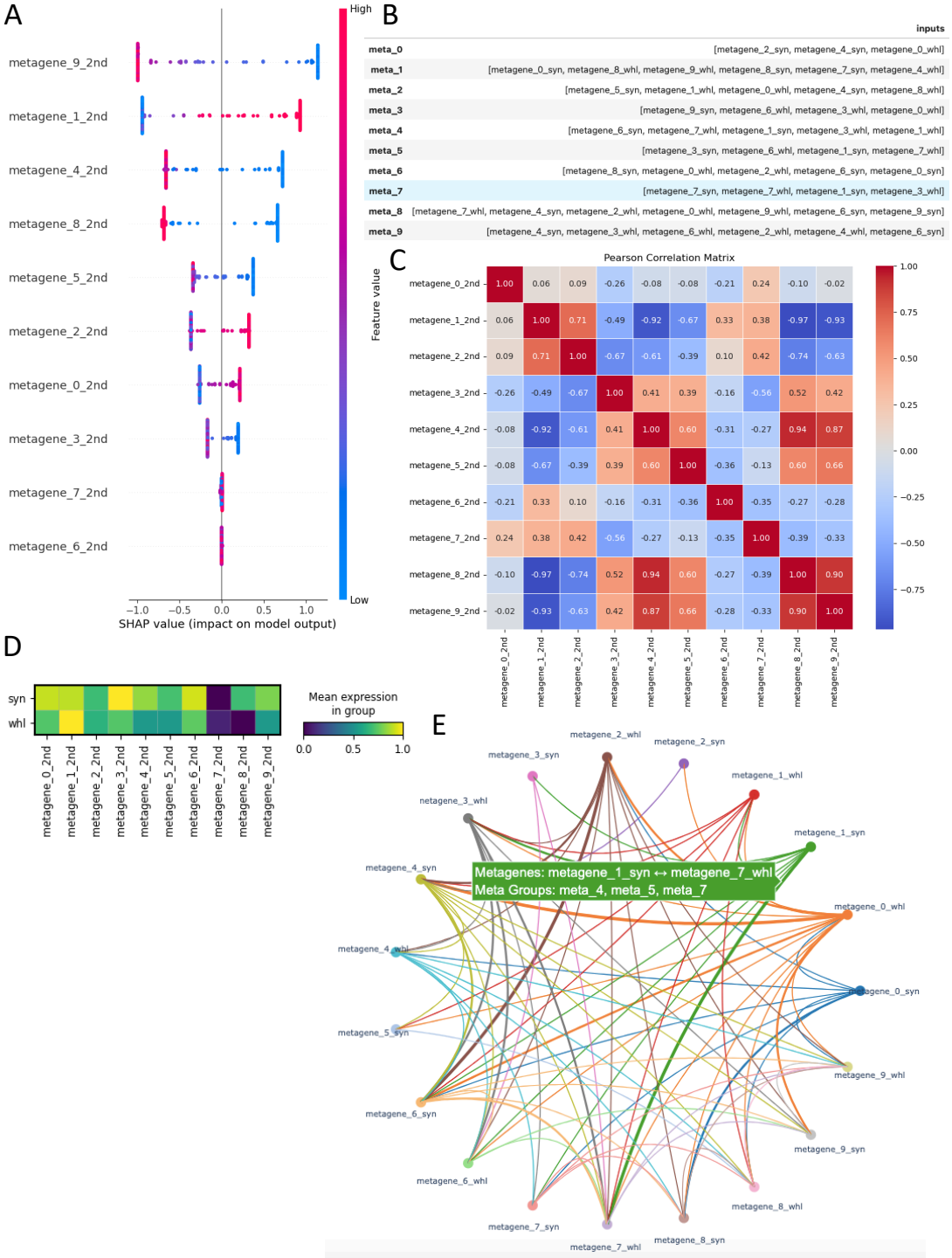

Figure 5. (A) SHAP importance plot; (B) Components of metapathway analysis; (C) Pearson Correlation Matrix of metapathways; (D) Matrix plot scaled by batches; (E) Relationship f metagenes.

metagene_2nd_level	metagene_1st_level	Enrichment result	Signatures
metapathway_9	4_syn	KEGG_MEDICUS_REFERENCE_GF_RTK_PI3K_SIGNALING_PATHWAY WP_COMPLEMENT_SYSTEM WP_COMPLEMENT_AND_COAGULATION_CASCADES	EREG CFI,CFD,C4A,ADIPOQ, CFI,F3,CFD
	3_whl	REACTOME_ANTIMICROBIAL_PEPTIDES	CTSG, LTF
	6_whl	WP_NEURAL_CREST_CELL_MIGRATION_DURING_DEVELOPMENT REACTOME_NERVOUS_SYSTEM_DEVELOPMENT	EPHB4,MMP9
	2_whl	BIOCARTA_CCR5_PATHWAY WP_BURN_WOUND_HEALING	CCL2
	4_whl	REACTOME_NEUTROPHIL_DEGRANULATION KEGG_MEDICUS_REFERENCE_ANTIGEN_PROCESSING_AND_PRESENTATION_BY_MHC_CLASS_I_MOLECULES BIOCARTA_CTL_PATHWAY	B2M
	6_sny	REACTOME_O_LINKED_GLYCOSYLATION PID_INTEGRIN1_PATHWAY REACTOME_RESPONSE_TO_ELEVATED_PLATELET_CYTOSOLIC_CA2	THBS1
metapathway_1	0_syn	REACTOME_TNFR2_NON_CANONICAL_NF_KB_PATHWAY WP_INFLAMMATORY_RESPONSE_PATHWAY KEGG_CYTOKINE_CYTOKINE_RECEPTOR_INTERACTION	TNFRSF13C, BIRC3, CD27, TNFRSF18, ZAP70, LCK, CCL5
	8_whl	BIOCARTA_AHSP_PATHWAY REACTOME_ERYTHROCYTES_TAKE_UP_CARBON_DIOXIDE_AND_RELEASE_OXYGEN WP_QUERCETIN_AND_NFKB_AP1_INDUCED_APOPTOSIS	HBA1, PTGS2
	9_whl	WP_INTERACTIONS_OF_NATURAL_KILLER_CELLS_IN_PANCREATIC_CANCER	KLRK1, CCL5
	8_syn	WP_TOLLLIKE_RECEPTOR_SIGNALING WP_OSTEOCLAST_SIGNALING	CXCL10,SPP1
	7_syn	PID_INTEGRIN4_PATHWAY WP_BURN_WOUND_HEALING	LAMA1
	4_whl	KEGG_MEDICUS_REFERENCE_ANTIGEN_PROCESSING_AND_PRESENTATION_BY_MHC_CLASS_I_MOLECULES BIOCARTA_CTL_PATHWAY	B2M
metapathway_4	6_syn	REACTOME_O_LINKED_GLYCOSYLATION PID_INTEGRIN1_PATHWAY REACTOME_RESPONSE_TO_ELEVATED_PLATELET_CYTOSOLIC_CA2	THBS1
	7_whl	REACTOME_NEGATIVE_REGULATION_OF_THE_PI3K_AKT_NETWORK WP_PI3KAKT_SIGNALING	FGF23,NRG1,FLT3
	1_syn	REACTOME_ANTIMICROBIAL_PEPTIDES PID_IL1_PATHWAY WP_PHOTODYNAMIC_THERAPYINDUCED_NFKB_SURVIVAL_SIGNALING	S100A9,PI3,LCN2, IL1B
	3_whl	REACTOME_ANTIMICROBIAL_PEPTIDES	CTSG,LTF,LCN2
	1_whl	REACTOME_RESPONSE_TO_ELEVATED_PLATELET_CYTOSOLIC_CA2 REACTOME_FORMATION_OF_FIBRIN_CLOT_CLOTTING_CASCADE	PROS1
metapathway_8	7_whl	REACTOME_NEGATIVE_REGULATION_OF_THE_PI3K_AKT_NETWORK WP_PI3KAKT_SIGNALING	FGF23,NRG1,FLT3
	4_syn	KEGG_MEDICUS_REFERENCE_GF_RTK_PI3K_SIGNALING_PATHWAY WP_COMPLEMENT_SYSTEM WP_COMPLEMENT_AND_COAGULATION_CASCADES	EREG CFI,CFD,C4A, ADIPOQ, CFI,F3,CFD
	2_whl	WP_BURN_WOUND_HEALING PID_TCR_CALCIUM_PATHWAY WP_GLUCOCORTICOID_RECEPTOR_PATHWAY	CCL2, JUN,PTGS2
	0_whl	WP_TYPE_II_INTERFERON_SIGNALING REACTOME_INTERFERON_ALPHA_BETA_SIGNALING WP_SPINAL_CORD_INJURY	STAT1, ISG15, OAS1, CXCL10, CCL2, TNFSF13B, CXCL10
	9_whl	WP_INTERACTIONS_OF_NATURAL_KILLER_CELLS_IN_PANCREATIC_CANCER	KLRK1,CCL5
	6_syn	REACTOME_O_LINKED_GLYCOSYLATION PID_INTEGRIN1_PATHWAY REACTOME_RESPONSE_TO_ELEVATED_PLATELET_CYTOSOLIC_CA2	THBS1
	9_syn	REACTOME_INITIAL_TRIGGERING_OF_COMPLEMENT KEGG_COMPLEMENT_AND_COAGULATION_CASCADES WP_T_CELL_MODULATION_IN_PANCREATIC_CANCER	C1QA,CFD,TNFRSF4,LGALS9 KLRK1,CCL5
metapathway_5	3_syn	REACTOME_ERBB2_ACTIVATES_PTK6_SIGNALING REACTOME_CONSTITUTIVE_SIGNALING_BY_ABERRANT_PI3K_IN_CANCER	ERBB3,EREG,PTK6

	6_whl	WP_NEURAL_CREST_CELL_MIGRATION_DURING_DEVELOPMENT REACTOME_NERVOUS_SYSTEM_DEVELOPMENT	EPHB4,MMP9
	1_syn	REACTOME_ANTIMICROBIAL_PEPTIDES PID_IL1_PATHWAY WP_PHOTODYNAMIC_THERAPYINDUCED_NFKB_SURVIVAL_SIGNALING	S100A9,PI3,LCN2, IL1B
	7_whl	REACTOME_NEGATIVE_REGULATION_OF_THE_PI3K_AKT_NETWORK WP_PI3KAKT_SIGNALING	FGF23,NRG1,FLT3
metapathway_2	5_syn	REACTOME_ACTIVATED_NOTCH1_TRANSMITS_SIGNAL_TO_THE_NUCLEUS REACTOME_PLATELET_ADHESION_TO_EXPOSED_COLLAGEN	JAG2,NOTCH1 VWF,GP1BA
	1_whl	REACTOME_RESPONSE_TO_ELEVATED_PLATELET_CYTOSOLIC_CA2 REACTOME_FORMATION_OF_FIBRIN_CLOT_CLOTTING_CASCADE	PROS1
	0_whl	WP_TYPE_II_INTERFERON_SIGNALING REACTOME_INTERFERON_ALPHA_BETA_SIGNALING WP_SPINAL_CORD_INJURY	STAT1, ISG15, OAS1, CXCL10, CCL2, TNFSF13B,,CXCL10
	4_syn	KEGG_MEDICUS_REFERENCE_GF_RTK_PI3K_SIGNALING_PATHWAY WP_COMPLEMENT_SYSTEM WP_COMPLEMENT_AND_COAGULATION_CASCADES	EREG CFI,CFD,C4A,ADIPOQ, CFI,F3,CFD
	8_whl	BIOCARTA_AHSP_PATHWAY REACTOME_ERYTHROCYTES_TAKE_UP_CARBON_DIOXIDE_AND_RELEASE_OXYGEN WP_QUERCETIN_AND_NFKB_AP1_INDUCED_APOPTOSIS	HBA1, PTGS2
Metapathway_3	9_syn	REACTOME_INITIAL_TRIGGERING_OF_COMPLEMENT KEGG_COMPLEMENT_AND_COAGULATION_CASCADES WP_T_CELL_MODULATION_IN_PANCREATIC_CANCER	C1QA,CFD,TNFRSF4,LGALS9 KLRK1,CCL5
	6_whl	WP_NEURAL_CREST_CELL_MIGRATION_DURING_DEVELOPMENT REACTOME_NERVOUS_SYSTEM_DEVELOPMENT	EPHB4,MMP9
	3_whl	REACTOME_ANTIMICROBIAL_PEPTIDES	CTSG, LTF
	0_whl	WP_TYPE_II_INTERFERON_SIGNALING REACTOME_INTERFERON_ALPHA_BETA_SIGNALING WP_SPINAL_CORD_INJURY	STAT1, ISG15, OAS1, CXCL10, CCL2, TNFSF13B, CXCL10

Table 4. Metapathway analysis.

- **Group 1 (G1)** - Synovium-level

G1 consists of pathways related to growth factor signaling, PI3K activation, synovial remodeling, immune activation, and nerve interaction, all of which can contribute to pain in RA:

1. From metapathway_4 and metapathway_5, we know that hub metapathways are more related to PI3K signalling, antimicrobial peptides, and fibrin clot formation.
2. metapathway_4 and metapathway_5 are the 1st level proliferation including IL-1 pathway; metapathway_3 is 2nd level proliferation including type II IFN; metapathway_9 and metapathway_8 are the positive feedback loops;
3. metapathway_3 is the most enriched in synovium tissue in Figure 5-D, including nervous system development, which means the proliferation from synovium to the nerve.

- **Group 2 (G2)** - Blood-level

1. metapathway_1 is the proliferation and metapathway_2 is the negative feedback loop;
2. REACTOME_TNFR2_NON_CANONICAL_NF_KB_PATHWAY

Non-canonical NF-κB signaling via TNFR2 is often protective like IL-10, especially in Tregs (Regulatory T Cells) and immune resolution mechanisms to supports Tregs' suppressive function, while activating PI3K/Akt signaling[46].

3. WP_INFLAMMATORY_RESPONSE_PATHWAY
   This pathway may buffer excessive inflammation by regulating cytokine signaling. Instead of promoting chronic inflammation, it helps restore immune balance, potentially reducing pain.
4. WP_QUERCETIN_AND_NFKB_AP1_INDUCED_APOPTOSIS
   Pro-apoptotic mechanisms in blood may limit inflammatory cell survival in synovium, reducing pain-driving immune responses.
5. PID_INTEGRIN4_PATHWAY & WP_BURN_WOUND_HEALING
   Involved in tissue repair and immune regulation, potentially counteracting chronic inflammation in the synovium[47].

G2 appears to have immune-regulatory, apoptotic, and anti-inflammatory properties that could act as a compensatory mechanism to suppress excessive inflammation and pain from G1. G1 pathways in the synovium drive inflammation and pain, while G2 pathways in blood counteract excessive inflammation and promote immune regulation. This suggests that therapies enhancing G2 (e.g., TNFR2 agonists, apoptosis inducers, or regulatory immune modulators) could help reduce RA pain. The inflammatory environment in the synovium allows for positive feedback loops, where complement activation enhances PI3K signaling, promoting fibroblast proliferation and tissue inflammation. This feedback contributes to the chronic inflammation. In the bloodstream, the immune system is more regulated by mechanisms like Tregs. Here, TNFR2 signaling enhances Treg expansion, which suppresses complement activation and PI3K signaling to prevent excessive immune responses, thus creating a negative feedback loop. This difference in the feedback loops can be understood as a tissue-specific response to the immune system's need for either promotion of inflammation (in synovium) or immune regulation (in blood).

Until now, we can explain the phenomenon in RNAcare why L1CAM is downregulated to pain in blood, but upregulated to pain in DRG.

Besides, we found in terms of crosstalk, CCL2 recruits monocytes/macrophages from the bloodstream into inflamed tissues, including the synovium in RA, acting as a bridge from the bloodstream to the synovium, drawing immune cells into the joint space, thereby initiating and amplifying inflammation; CCL5 promotes the retention and activation of T cells and macrophages in the synovium, sustaining inflammation, acting as a feedback signal, maintaining chronic inflammation by keeping immune cells in the synovium and further activating them[48]. Hence, Targeting CCL2 (blocking monocyte recruitment) might help reduce immune cell infiltration; Targeting CCL5 (disrupting retention and activation of immune cells) could break the chronic inflammation loop. And during the feedback loop CCL5 may potentially increase the risk of getting pancreatic cancer for RA patients[49].

Meanwhile, we found the progression of pain in rheumatoid arthritis (RA) following the sequence: blood → synovium → dorsal root ganglion (DRG). The CCL2/CCR2 axis has been implicated in peripheral inflammatory pain sensitization. Research indicates that CCL2 can act directly on DRG neurons, leading to increased neuronal excitability and pain hypersensitivity[50].

Finally, Figure 5-E shows the interaction plot among metagenes based on Figure 5-B. As we see, (metagene_1_syn, metagene_7_whl) crosstalks frequently, representing the crosstalk between antimicrobial peptides (alpha defensins) in blood and PI3K/AKT signalling in synovium[51]; (metagene_2_whl, metagene_6_syn) crosstalks frequently, representing the crosstalk between glucocorticoid receptor pathway in blood and O-linked glycosylation in synovium[52]; (metagene_0_whl, metagene_4_syn) crosstalks frequently, representing the crosstalk between IFN signaling and complement system pathway/ medicus reference GF RTK PI3K signalling[53].

Conclusion: Through combining different tissues, we know the relationship between different metapathways, the progression direction related to pain, the mechanism for RA to recruit/retain immune cells and the hub metapathways.

Case Study 4: Cross-Omics Regulation of Pain: The Role of type II IFN, IL-6, and IL-10 in RA

In this case, we applied Causal Forests, connecting different omics data to pain using RA-MAP.

Figure 6-A shows SHAP importance. Figure 6-B shows metagene members for each metapathways. Figure 6-C shows the relationships among metapathways. We can see G1: (metapathway_0, metapathway_9); G2: (metapathway_6, metapathway_7, metapathway_8); G3: (metapathway_1, metapathway_2, metapathway_3, metapathway_4). Figure 6-D shows the matrix plot scaled by omics types. Combining Figure 6-CD, we can see in proteomics is active in G3 and transcripts is active in G2. Given the relevance to pain, we propose the following explanation:

- **metapathway_0 as a Hub Metapathway**

It contains platelet activation, fibrin clot formation, and peptide ligand binding receptor pathways, which are highly interconnected with inflammatory and immune responses. Platelet activation and coagulation (e.g., GPVI-mediated activation cascade, intrinsic pathway of fibrin clot formation) are key contributors to inflammation and pain in RA.

This suggests it acts as a central regulatory network for inflammatory and immune activation, which then influences metapathway_0, metapathway_8, and metapathway_1.

- **metapathway_9 (Inflammation and Immune Activation)**

Promoted by metapathway_0, antimicrobial peptides and NF-κB activation (via TRAF6) indicate a strong link to innate immune responses and chronic inflammation, which drive pain.

- **metapathway_8 (Adaptive Immunity and Chronic Inflammation)**

TNFR2 and T-cell receptor signaling point to adaptive immune activation, contributing to sustained inflammation and synovial damage in RA; NF-κB activation (TRAF6-mediated and non-canonical TNFR2)[54] and type II IFN[55] links it back to pain sensitization.

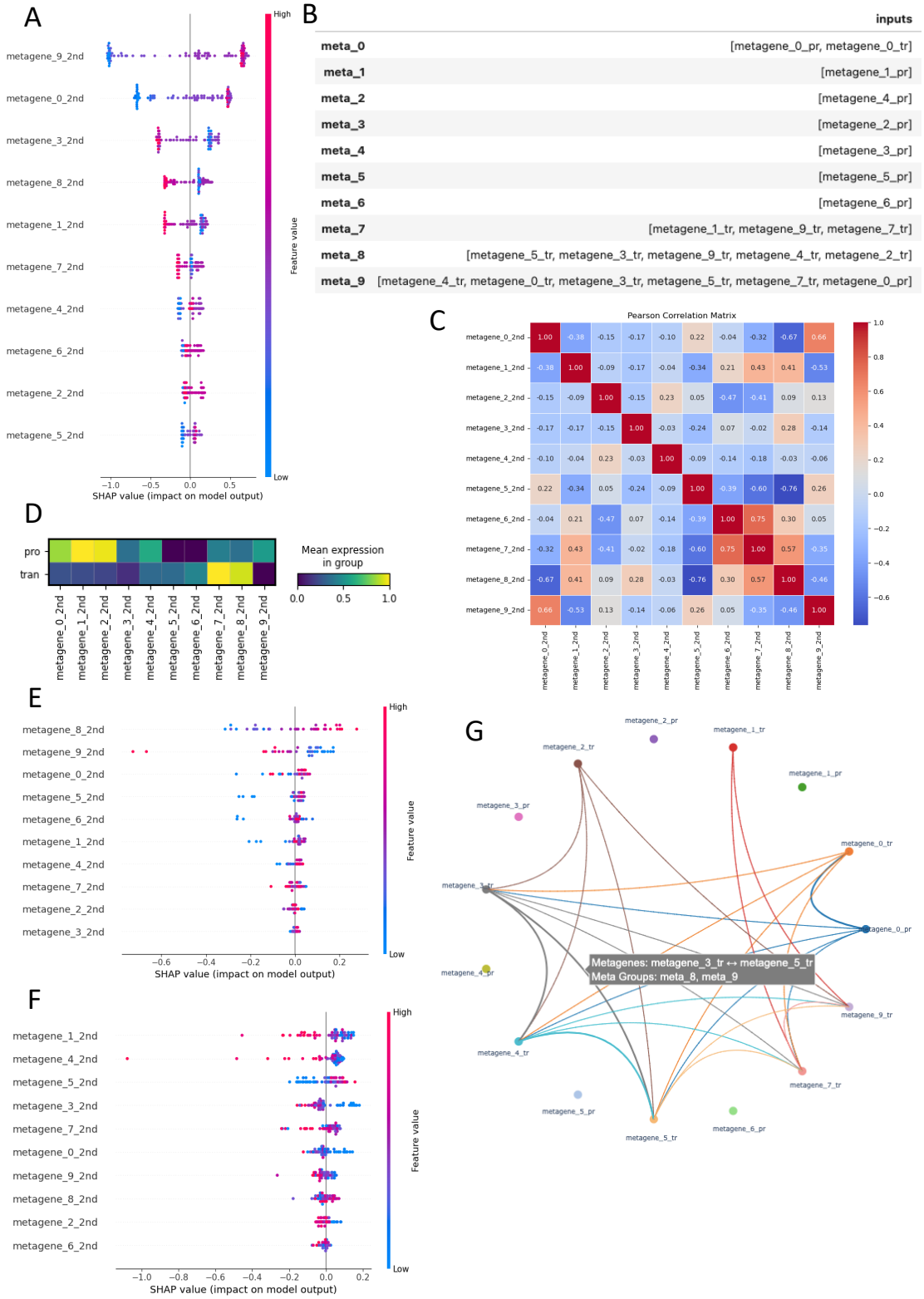

Figure 6. (A) SHAP importance plot; (B) Components of metapathway analysis; (C) Pearson Correlation Matrix of metapathways; (D) Matrix plot scaled by batches; (E) SHAP importance plot for only transcriptomic level based on association analysis; (F) SHAP importance plot for only proteomic level based on association analysis; (G) Relationship of metagenes.

metagene_2nd_level	metagene_1st_level	Enrichment result	Signatures
metapathway_9	4_tr	REACTOME_ANTIMICROBIAL_PEPTIDES	CTSG,ELANE,LTF,PRTN3,LCN2,BPI
	0_tr	REACTOME_RESPONSE_TO_ELEVATED_PLATELET_CYTOSOLIC_CA2 REACTOME_INTRINSIC_PATHWAY_OF_FIBRIN_CLOT_FORMATION	SELP,PF4,THBS1,SPARC,VWF,ITGA2B,PROS1,SERPINE2,VWF,GP1BA
	3_tr	REACTOME_REGULATION_OF_SIGNALING_BY_CBL REACTOME_TRAF6_MEDIATED_NF_KB_ACTIVATION	YES1,PIK3CA, HMGB1,S100A12
	5_tr	KEGG_CYTOKINE_CYTOKINE_RECEPTOR_INTERACTION	CCL23,LEP,IL10,TNFSF15
	7_tr	BIOCARTA_ARF_PATHWAY REACTOME_GPVI_MEDIATED_ACTIVATION_CASCADE	PIK3CA,PIK3CG
	0_pr	REACTOME_RESPONSE_TO_ELEVATED_PLATELET_CYTOSOLIC_CA2 REACTOME_INTRINSIC_PATHWAY_OF_FIBRIN_CLOT_FORMATION REACTOME_PEPTIDE_LIGAND_BINDING_RECEPTORS	PPBP,PDGFA,PDGFB,SPARC,TF,PF4,APP,CCL5
metapathway_0	0_pr	REACTOME_RESPONSE_TO_ELEVATED_PLATELET_CYTOSOLIC_CA2 REACTOME_INTRINSIC_PATHWAY_OF_FIBRIN_CLOT_FORMATION REACTOME_PEPTIDE_LIGAND_BINDING_RECEPTORS	PPBP,PDGFA,PDGFB,SPARC,TF,PF4,APP,CCL5
	0_tr	REACTOME_RESPONSE_TO_ELEVATED_PLATELET_CYTOSOLIC_CA2 REACTOME_INTRINSIC_PATHWAY_OF_FIBRIN_CLOT_FORMATION	SELP,PF4,THBS1,SPARC,VWF,ITGA2B,PROS1,SERPINE2,VWF,GP1BA
metapathway_3	2_pr	WP_EXTRAFOLLICULAR_AND_FOLLICULAR_B_CELL_ACTIVATION_BY_SARSCOV2	BCL6,SLAMF7
metapathway_8	5_tr	KEGG_CYTOKINE_CYTOKINE_RECEPTOR_INTERACTION	CCL23,LEP,IL10,TNFSF15
	3_tr	REACTOME_REGULATION_OF_SIGNALING_BY_CBL REACTOME_TRAF6_MEDIATED_NF_KB_ACTIVATION	YES1,PIK3CA, HMGB1,S100A12
	9_tr	REACTOME_TNFR2_NON_CANONICAL_NF_KB_PATHWAY KEGG_T_CELL_RECEPTOR_SIGNALING_PATHWAY	CD27,CD40LG,PLCG1
	4_tr	REACTOME_ANTIMICROBIAL_PEPTIDES	CTSG,ELANE,LTF,PRTN3,LCN2,BPI
	2_tr	WP_ALLOGRAFT_REJECTION	IFNG,FASLG,GNLY,GZMB
metapathway_1	1_pr	REACTOME_COMMON_PATHWAY_OF_FIBRIN_CLOT_FORMATION REACTOME_FORMATION_OF_FIBRIN_CLOT_CLOTTING_CASCADE WP_IL6_SIGNALING	SERPINA5,FGA,MAP2K4,JAK2
metapathway_7	1_tr	REACTOME_ACTIVATED_TAK1_MEDIATES_P38_MAPK_ACTIVATION	UBB,MAP2K3
	9_tr	REACTOME_TNFR2_NON_CANONICAL_NF_KB_PATHWAY KEGG_T_CELL_RECEPTOR_SIGNALING_PATHWAY	CD27,CD40LG,PLCG1
	7_tr	BIOCARTA_ARF_PATHWAY REACTOME_GPVI_MEDIATED_ACTIVATION_CASCADE	PIK3CA,PIK3CG
metapathway_4	3_pr	REACTOME_INTERLEUKIN_10_SIGNALING WP_OVERVIEW_OF_PROINFLAMMATORY_AND_PROFIBROTIC_MEDIATORS	CXCL10,TNFRSF1B, CXCL11,MMP9

Table 5. Metapathway analysis.

- **metapathway_1 (Resolution Mechanism via IL-6 and Fibrin Clot Formation)**

IL-6 signaling and fibrin clot formation suggest a role in transitioning inflammation toward resolution, aligning with the crosstalk between IL-6 and IFN-γ in immune regulation[56,57].

- **metapathway_7 (Adaptive Immunity and Chronic Inflammation)**

It shares similarities with metapathway_8.

- **(metapathway_8 & metapathway_7) & metapathway_1 act as complementary modulators to metapathway_0 & metapathway_9 for transcriptomic and proteomic level respectively.**

type II IFN (transcriptomic level) and IL-6 (proteomic level) regulate the immune response, acting as negative feedback loop and preventing excessive pain sensitization while TNFR2 non-canonical NF-κB pathway supports Tregs' suppressive function; Therefore, metapathway_1 is the pain buffer at proteomic level and metapathway_7& metapathway_8 is the pain buffer at transcriptomic level.

Figure 6-E is the SHAP importance for only transcriptomic level and Figure 6-F is the SHAP importance for only proteomic level. As what we expected before, in Figure 6-E, metapathway_8 buffered metapathway_9 and metapathway_0, contributing the most pain; while in Figure 6-F, metapathway_1and metapathway_4 buffered metapathway_9 and metapathway_0. The negative feedback loop at different omics levels is a protective mechanism.

Figure 6-G shows the interaction plot among metagenes based on Figure 6-B: (metagene_3_tr, metagene_5_tr) represents interaction between TRAF6 mediated NFKB activation and cytokine receptor signaling[58].

Interestingly, we notice the different roles between metapathway_1 and metapathway_4 in the two omics lays in Figure 6-EF to pain. It is because they act as pain regulators not only at the same omics level but also across levels. Then, we checked the enrichment result of metapathway_4 which is enriched in IL-10 signaling. IL-10 signaling is a well-known negative feedback mechanism that dampens excessive inflammation, which could prevent sustained pain sensitization[59].

Conclusion: Through combining different omics data, we know the relationship between different metapathways correlated to pain. At the transcriptomic level, type II IFN often acts as a negative feedback loop by inducing immune-

modulatory responses; at the proteomic level, IL-6 and IL-10 appear to play a more dominant role in negative feedback compared to type II IFN.

We can see in blood tissue, feedback loop is always negative across different omics. The pain buffer serves as a protective mechanism to modulate pain, helping to maintain balance and prevent excessive pain perception. If this buffer is removed or disrupted, the body can lose its ability to regulate pain properly, leading to increased pain sensitivity or chronic pain. Many pain treatments aim to target this buffer but must do so carefully to avoid removing protective feedback because pain in this situation is helpful to prevent further tissue damage.

Case Study 5: Divergent Buffering Strategies in RA and HF: The Role of IFN Signaling in Disease Severity

In this case, we applied Causal Forests, connecting different diseases to disease score using HF and RA data.

Figure 7-A shows SHAP importance. Figure 7-B shows metagene members for each metapathways. Figure 7-C shows the relationships among metapathways. We can see G1: (metapathway_0, metapathway_9), G2: (metapathway_1, metapathway_8) are negatively correlated. Figure 7-D shows the matrix plot scaled by disease types. Combing Figure 7-A and Table 6, we know the hub pathways is (metapathway_6, metapathway_7) (HF related), (alpha defensins, REACTOME_RESPONSE_TO_ELEVATED_PLATELET_CYTOSOLIC_CA2) (RA related) and metapathway_0 (shared). Although metapathway_6 and metapathway_7 shared almost the same metapathways, ICA separates them as different components, which will be analysed later; metapathway_9 further proliferates metapathway_0 in both RA and HF by IFN signaling; For RA only, metapathway_1 and metapathway_8 are the negatively related to metapathway_0 because metapathway_9 suppressed their interactions with metapathway_0 (Table 3) and they can only be proliferated by type II IFN (6_op, 7_op).

As we see in Figure 7-E, metapathway_8 and metapathway_1 contribute the most pain to RA patients, protects the patients against from the damage of REACTOME_RESPONSE_TO_ELEVATED_PLATELET_CYTOSOLIC_CA2 while metapathway_9 is the most enriched for RA in Figure 7-D, protecting the patients from the damage of metapathway_6, metapathway_7 and metapathway_0.

In Figure 7-F, we find metapathway_5 is top 1, ranking before metapathway_6 and metapathway_7. Therefore, we assumed metapathway_5 is also a buffer considering its negative relationship with metapathway_6 and metapathway_7 in Figure 7-C. We checked its enrichment result in Table 6 and found it is enriched in type I IFN as well as its Gene Ontology Molecular Function including “oxidoreduction-driven active transmembrane transporter activity” with signatures COX7B, COX8A, UQCRC1, NDUFS5, COX6B1, related to signatures in metapathway_6(Table 6). However, generally speaking, the negative regulation is not as good as RA under type II IFN because metapathway_6 and metapathway_7 are still top-listed in Figure 7-EF and

metapathway_7 is still high expressed in Figure 7-D. Under the same logic, metapathway_2 and metapathway_3 are better severity buffers enriched in type I IFN but already overwhelmed in Figure 7-D. Furthermore, metapathway_2 (6_hf) is more aligned with IFN-I's negative feedback mechanisms because it focuses on translation repression, stress responses, and inflammatory mRNA degradation, while metapathway_3 (5_hf) has additional immune activation components, such as binding and uptake of ligands by scavenger receptors. So, the difference of the two diseases is different metapathways regulate the damage of the tissue, and it seems that RA patients have more ways to buffer the damage.

Figure 7-G shows the interactions between metagenes, we can see the most frequent one (metagene_3_hf, metagene_4_op) represents for the interaction between Response of EIF2AK4 (GCN2) to Amino Acid Deficiency and Nonsense-Mediated Decay (NMD) in both diseases[60].

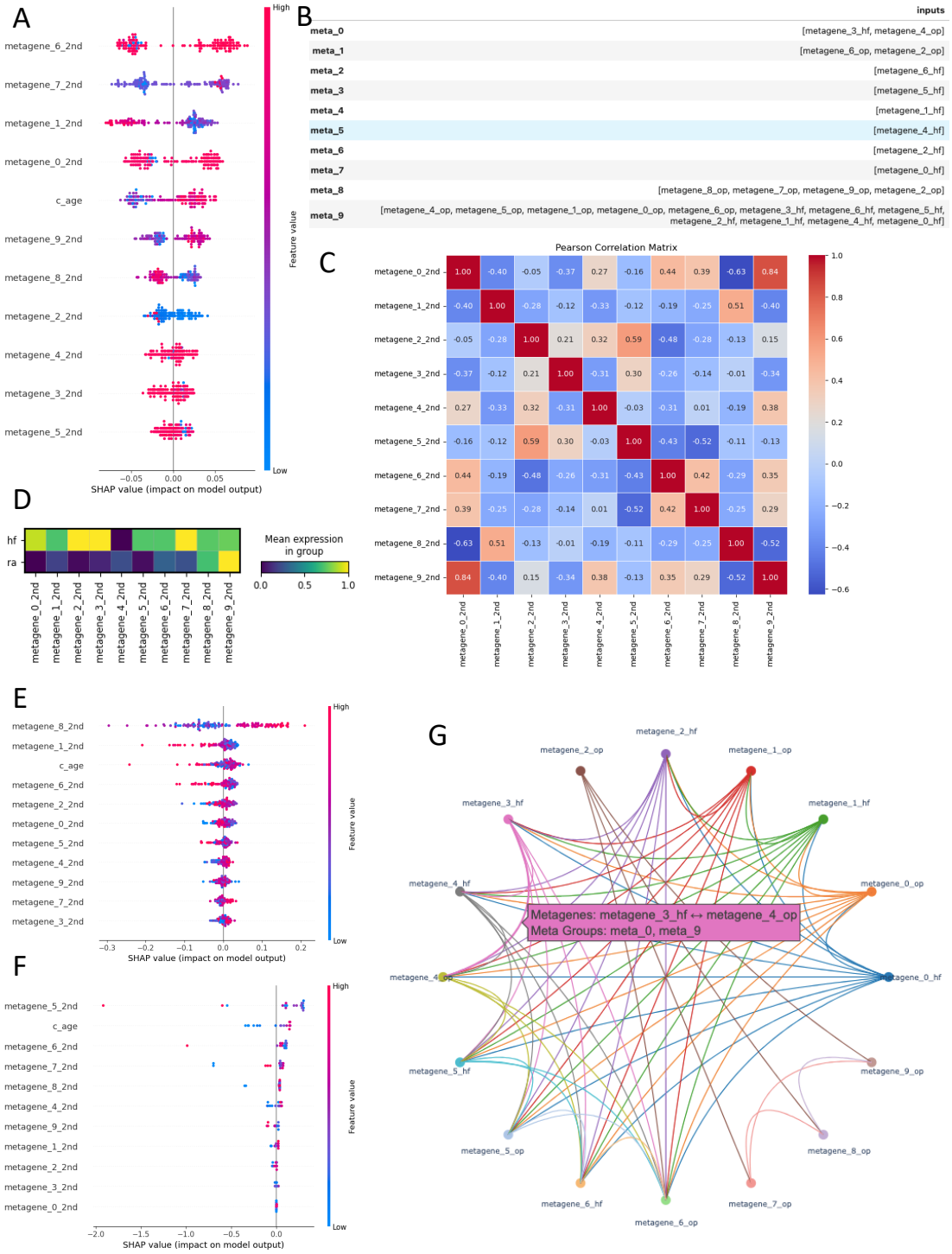

Figure 7. (A) SHAP importance plot; (B) Components of metapathway analysis; (C) Pearson Correlation Matrix of metapathways; (D) Matrix plot scaled by diseases; (E) SHAP importance plot for only RA based on association analysis; (F) SHAP importance plot for only HF based on association analysis; (G) Relationship of metagenes.

metagene_2nd_level	metagene_1st_level	Enrichment result	Signatures
metapathway_6	2_hf	KEGG_OXIDATIVE_PHOSPHORYLATION KEGG_PARKINSONS_DISEASE WP_NONALCOHOLIC_FATTY_LIVER_DISEASE KEGG_ALZHEIMERS_DISEASE KEGG_HUNTINGTONS_DISEASE KEGG_OXIDATIVE_PHOSPHORYLATION REACTOME_RESPIRATORY_ELECTRON_TRANSPORT	COX7B,COX7C,COX17,NDUFA1,NDUFA4,UQCRFS1,NDUFAB1,NDUFB1,NDUFB2,NDUFB4,NDUFB10,COX5B,SDHB
metapathway_7	0_hf	KEGG_OXIDATIVE_PHOSPHORYLATION KEGG_PARKINSONS_DISEASE WP_NONALCOHOLIC_FATTY_LIVER_DISEASE KEGG_ALZHEIMERS_DISEASE KEGG_HUNTINGTONS_DISEASE REACTOME_RESPIRATORY_ELECTRON_TRANSPORT	NDUFA13,CS,COX5A,SLC25A4,ETFA,ETFB,COX7C,COX8A,UQCRC1,NDUFA4,UQCRC2,UQCRFS1,IDH2,NDUFAB1,NDUFB2,NDUFB4,NDUFB10,NDUFS3,NDUFS5,GOT1,SDHB,NDUFS6,GOT2
metapathway_1	6_op	BIOCARTA_AHSP_PATHWAY WP_HEMATOPOIETIC_STEM_CELL_DIFFERENTIATION REACTOME_CLASS_I_MHC_MEDIATED_ANTIGEN_PROCESSING_PRESENTATION	AHSP,GATA1,RIOK3,PIM1,KCNH2,KLF1,LYL1,MXI1,MKRN1,UBA52,UBB,FBXO9,UBE2H,MRC2,FBXO7,PSMF1,NEDD4L,SIAH2,RNF14,RNF123,UBE2O,CDC34,RNF182
	2_op	REACTOME_PLATELET_ACTIVATION_SIGNALING_AND_AGGREGATION REACTOME_RESPONSE_TO_ELEVATED_PLATELET_CYTOSOLIC_CA2 KEGG_FOCAL_ADHESION	PDGFA,ITGA2B,ITGB1,ITGB3,ITGB5,VWF
metapathway_0	3_hf	REACTOME_RESPONSE_OF_EIF2AK4_GCN2_TO_AMINO_ACID_DEFICIENCY REACTOME_NONSENSE_MEDIATED_DECAY_NMD	
	4_op	REACTOME_RESPONSE_OF_EIF2AK4_GCN2_TO_AMINO_ACID_DEFICIENCY REACTOME_SELENOAMINO_ACID_METABOLISM REACTOME_NONSENSE_MEDIATED_DECAY_NMD	
metapathway_9	4_op	REACTOME_RESPONSE_OF_EIF2AK4_GCN2_TO_AMINO_ACID_DEFICIENCY REACTOME_SELENOAMINO_ACID_METABOLISM REACTOME_NONSENSE_MEDIATED_DECAY_NMD	
	5_op	REACTOME_ALPHA_DEFENSINS	DEFA1,DEFA3,DEFA4
	1_op	KEGG_NATURAL_KILLER_CELL_MEDIATED_CYTOTOXICITY PID_IL12_2PATHWAY	
	0_op	REACTOME_INTERFERON_ALPHA_BETA_SIGNALING REACTOME_INTERFERON_GAMMA_SIGNALING	
	6_op	BIOCARTA_AHSP_PATHWAY WP_HEMATOPOIETIC_STEM_CELL_DIFFERENTIATION REACTOME_CLASS_I_MHC_MEDIATED_ANTIGEN_PROCESSING_PRESENTATION	AHSP,GATA1,RIOK3,PIM1,KCNH2,KLF1,LYL1,MXI1,MKRN1,UBA52,UBB,FBXO9,UBE2H,MRC2,FBXO7,PSMF1,NEDD4L,SIAH2,RNF14,RNF123,UBE2O,CDC34,RNF182
	3_hf	REACTOME_RESPONSE_OF_EIF2AK4_GCN2_TO_AMINO_ACID_DEFICIENCY REACTOME_NONSENSE_MEDIATED_DECAY_NMD	
	6_hf	REACTOME_RESPONSE_OF_EIF2AK4_GCN2_TO_AMINO_ACID_DEFICIENCY REACTOME_NONSENSE_MEDIATED_DECAY_NMD REACTOME_SRP_DEPENDENT_COTRANSLATIONAL_PROTEIN_TARGETING_TO_MEMBRANE KEGG_MEDICUS_REFERENCE_TRANSLATION_INITIATION WP_CYTOPLASMIC_RIBOSOMAL_PROTEINS REACTOME_NONSENSE_MEDIATED_DECAY_NMD_INDEPENDENT_OF_THE_EXON_JUNCTION_COMPLEX_EJC	
	5_hf	REACTOME_NONSENSE_MEDIATED_DECAY_NMD WP_CYTOPLASMIC_RIBOSOMAL_PROTEINS REACTOME_RESPONSE_OF_EIF2AK4_GCN2_TO_AMINO_ACID_DEFICIENCY REACTOME_NONSENSE_MEDIATED_DECAY_NMD_INDEPENDENT_OF_THE_EXON_JUNCTION_COMPLEX_EJC REACTOME_BINDING_AND_UPTAKE_OF_LIGANDS_BY_SCAVENGER_RECEPTORS REACTOME_SRP_DEPENDENT_COTRANSLATIONAL_PROTEIN_TARGETING_TO_MEMBRANE	
	2_hf	KEGG_OXIDATIVE_PHOSPHORYLATION KEGG_PARKINSONS_DISEASE WP_NONALCOHOLIC_FATTY_LIVER_DISEASE KEGG_ALZHEIMERS_DISEASE KEGG_HUNTINGTONS_DISEASE	COX7B,COX7C,COX17,NDUFA1,NDUFA4,UQCRFS1,NDUFAB1,NDUFB1,NDUFB2,NDUFB4,NDUFB10,COX5B,SDHB
	1_hf	REACTOME_NONSENSE_MEDIATED_DECAY_NMD REACTOME_SELENOAMINO_ACID_METABOLISM REACTOME_INFLUENZA_INFECTION	RPL23,RPL37A,RPS28,RPL41,RPS11
	4_hf	REACTOME_INFLUENZA_INFECTION REACTOME_NONSENSE_MEDIATED_DECAY_NMD	RPL23,RPS20,RPS26,RPL37A,RPS28,RPLP2,RPL12,RPS8,RPS11,RPL18,RPL18A
	0_hf	KEGG_OXIDATIVE_PHOSPHORYLATION KEGG_PARKINSONS_DISEASE WP_NONALCOHOLIC_FATTY_LIVER_DISEASE KEGG_ALZHEIMERS_DISEASE KEGG_HUNTINGTONS_DISEASE	

metapathway_8	8_op	WP_LEUKOTRIENE_METABOLIC_PATHWAY WP_GLUCOCORTICOID_RECEPTOR_PATHWAY WP_LEUKOTRIENE_METABOLIC_PATHWAYWP_VIWP_VITAMIN_D_RECEPTOR_PATHWAY	
	7_op	KEGG_ALLOGRAFT_REJECTION	
	9_op	KEGG_NOTCH_SIGNALING_PATHWAY	NOTCH1,NOTCH2,NUMBL,CIR1,CREBBP,NCOR2,MAML1,EP300,MAML3
	2_op	REACTOME_PLATELET_ACTIVATION_SIGNALING_AND_AGGREGATION REACTOME_RESPONSE_TO_ELEVATED_PLATELET_CYTOSOLIC_CA2 KEGG_FOCAL_ADHESION	PDGFA,ITGA2B,ITGB1,ITGB3,ITGB5,VWF
metapathway_5	4_hf	REACTOME_INFLUENZA_INFECTION REACTOME_NONSENSE_MEDIATED_DECAY_NMD	RPL23,RPS20,RPS26,RPL37A,RPS28,RPLP2,RPL12,RPS8,RPS11,RPL18,RPL18A

Table 6. Metapathway analysis.

Conclusion: based on our framework, we found difference in the similarity of the two totally different diseases RA and HF. We found type I IFN alone can also call a negative feedback loop and act as a buffer for disease severity, especially for HF, but not as good as type IL-10 or type II IFN for RA[61,62].

Case Study 6: Deciphering Pre-Ciliated Cell Plasticity and Multicellular Stress Response Under RVCSE Exposure

In this case we used the case from Causal identification of single-cell experimental perturbation effects with CINEMA-OT[18] for single cell illustration. In the original paper, CINEMA-OT applies ICA in the context of cell types, with the goal of identifying cell-type-specific signals from complex multi-omics data. This is the reason why the author mentioned at the same time that the default setting of FastICA has low tolerance for ICA convergence, which harms CINEMA-OT little in practice[63]. Besides, in the original paper the authors found Pre-ciliated cells co-exposed to both viral infection and CSE showed synergistic induction of genes encoding secreted proteins that are typically associated with secretory cells in resting cultures, including SCGB3A1, LCN2, BPIFB1, SLPI, and WFDC2. However, they didn't further explore the mechanism and its interaction with other cell types.

We did metapathway analysis combining cell types and 1st level cohort-ICA processed data with 20 components for 4 different batches: MOCK, RV, CSE and RVCSE. Currently, RNAcompare only supports 2 batches, so we did this case manually. In our use case, we used ICA to decompose components without thinking cell types at first. Then we introduced the 2nd level ICA, and combined the output with cell types together, treating cell types as one interaction term with metapathways. Through this way, we bypassed the limitation and addressed the question mentioned above.

The first 5 metapathways are shown in Figure 8-A. We can see for example metapathway_0 includes the interactions among Doublets, Pre-ciliated, Ionocyte and Brush+PNEC cells with their communications via related pathways. Figure 8-B is just the cell types we extracted from the metapathways, based on which, we drew the inter-cell communication plot in Figure 8-C. The size of the cell types can basically represent the synergy score: cell_type_Pre-ciliated(9) means Pre-ciliated cells exist in 9 metapathways. Therefore, we can easily identify the hub cell type(s): Brush+PNEC(11), Ionocyte(9) and Pre-ciliated(9) based on 4 batches. We

then drew the Pearson Correlation matrix of metapathways in Figure 8-D for later use.

We manually trained the model based on the 4 batches together. Figure 8-E-G are SHAP importance plot for CSE(labelled 1) vs others(labelled 0), RV(labelled 1) vs others(labelled 0), RVCSE(labelled 1) vs others(labelled 0) based on 1% test data.

After comparision of the 3 plots, we can easily see metapathway_9 and metapathway_17 are suppressed while metapathway_12 is promoted under RVCSE vs others. metapathway_9 is the interaction among Brush+PNEC, Pre-ciliated and Cycling basal; metapathway_17 is the interaction between Ionocyte and Pre-ciliated; metapathway_12 is Ionocyte. We then checked them with Figure 8-E-G and found metapathway_9 is suppressed by metapathway_19; metapathway_17 is suppressed by metapathway_4. Since the original paper only mentioned synergy effect with Pre-ciliated under RVCSE, we only analyse metapathway_19 here.

Table 7 shows the enrichment results for the related metapathways:

- Metapathway Feedback Loop:

Metapathway_9 includes IFN signaling and complement activation, forming a regulatory feedback loop during inflammatory stimuli; It also includes metagene_16_cse, which is defined by antimicrobial peptide (AMP) signatures (BPIFB1, LCN2), consistent with innate immune activation in the original paper.

- Pre-Ciliated Cell Plasticity Under Stress (RVCSE):

Under combined respiratory virus (RV) and cigarette smoke extract (CSE) exposure, pre-ciliated cells undergo functional reprogramming:

Phase 1: Their secretion of inflammation-induced AMPs (metagene_13_rv) is suppressed by the proliferation process from metapathway_19.

Phase 2: They shift toward producing secretory granule lumen proteins (BPIFA1[64], LTF[65], LCN2[66]), which mediate intercellular communication characterised by the pathway REACTOME_CELL_CELL_COMMUNICATION. This secretory transition activates neighboring secretory cells, driving enhanced antigen processing and T cell activation to bring innate and adaptive immunity.

- Multicellular Stress Response Orchestration:

Pre-ciliated cells further recruit Basal, Doublet, and Hillock cells to amplify antimicrobial defences. These cells secrete proliferative AMPs (S100A7, S100A8, S100A9, PI3), which (1) directly neutralize pathogens (e.g., via S100A proteins' metal chelation[67]); (2) amplify epithelial stress signaling (e.g., PI3's protease inhibition[68]).

Besides, we also checked metapathway_7, enriched in IFN signalling, aligning with the description in the original paper under RV.

.

A

	inputs
meta_0	[cell_type_Doublet, cell_type_Pre-ciliated, cell_type_Ionocyte, metagene_12_r4, metagene_10_r2, metagene_14_r2, metagene_11_r4, cell_type_Brush+PNEC, metagene_17_r1]
meta_1	[cell_type_Basal, metagene_12_r4, metagene_15_r1, cell_type_Pre-ciliated, metagene_9_r3, metagene_10_r4, metagene_8_r1, metagene_19_r2, metagene_12_r3, cell_type_Ionocyte, metagene_1_r2, metagene_10_r2, metagene_18_r4, metagene_16_r2, metagene_18_r2, metagene_12_r1, metagene_7_r3, metagene_3_r2, metagene_4_r4, cell_type_Ciliated]
meta_2	[cell_type_Hillock, metagene_13_r1, metagene_6_r2, metagene_10_r4, metagene_15_r2, cell_type_Pre-ciliated, metagene_19_r2, metagene_17_r3, metagene_9_r3, metagene_18_r4, metagene_16_r4, cell_type_Ionocyte]
meta_3	[metagene_11_r3, metagene_6_r1, metagene_13_r4, metagene_17_r2, metagene_15_r2, metagene_10_r4, cell_type_Brush+PNEC, metagene_14_r4, metagene_6_r4, metagene_14_r2, cell_type_Pre-ciliated, metagene_12_r2, metagene_9_r4, metagene_19_r2, metagene_9_r1, metagene_4_r3, metagene_5_r1, metagene_9_r2, metagene_7_r4, metagene_2_r2, metagene_16_r2, metagene_4_r1, metagene_12_r1, metagene_8_r4, metagene_1_r4]
meta_4	[cell_type_Secretory, metagene_15_r2]

B

```
['cell_type_Doublet', 'cell_type_Pre-ciliated', 'cell_type_Ionocyte', 'cell_type_Brush+PNEC']
['cell_type_Basal', 'cell_type_Pre-ciliated', 'cell_type_Ionocyte', 'cell_type_Ciliated']
['cell_type_Hillock', 'cell_type_Pre-ciliated', 'cell_type_Ionocyte']
['cell_type_Brush+PNEC', 'cell_type_Pre-ciliated']
['cell_type_Secretory']
['cell_type_Cycling basal', 'cell_type_Ionocyte', 'cell_type_Pre-ciliated', 'cell_type_Ciliated']
['cell_type_Ciliated', 'cell_type_Brush+PNEC', 'cell_type_Cycling basal', 'cell_type_Ionocyte', 'cell_type_Basal']
['cell_type_Ionocyte', 'cell_type_Pre-ciliated']
['cell_type_Brush+PNEC', 'cell_type_Pre-ciliated']
['cell_type_Brush+PNEC', 'cell_type_Pre-ciliated', 'cell_type_Cycling basal']
['cell_type_Pre-ciliated', 'cell_type_Brush+PNEC']
['cell_type_Myoepithelial']
['cell_type_Ionocyte']
['cell_type_Brush+PNEC', 'cell_type_Cycling basal']
['cell_type_Brush+PNEC']
['cell_type_Brush+PNEC', 'cell_type_Myoepithelial', 'cell_type_Ionocyte']
['cell_type_Brush+PNEC']
['cell_type_Ionocyte', 'cell_type_Myoepithelial']
[]
['cell_type_Brush+PNEC', 'cell_type_Cycling basal', 'cell_type_Basal', 'cell_type_Doublet', 'cell_type_Hillock']
```

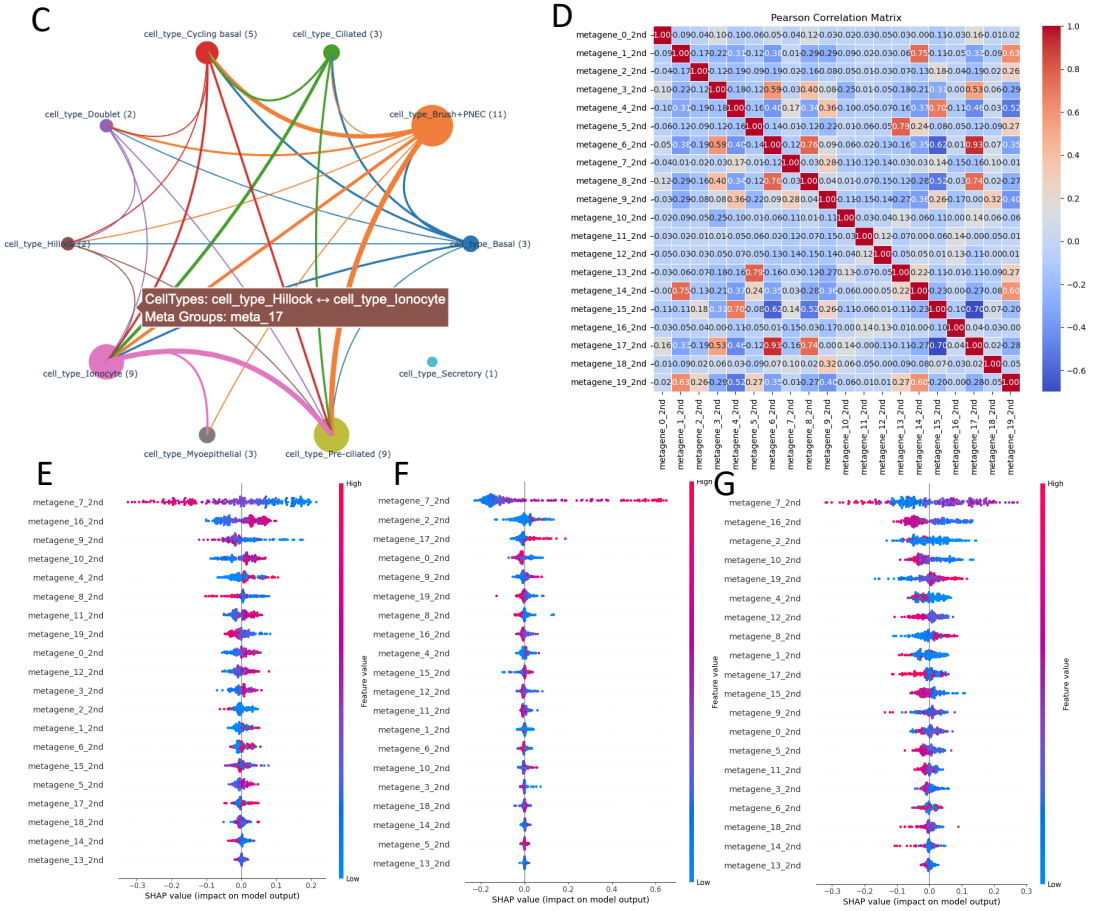

Figure 8. (A) Components of metapathway analysis; (B) Components of metapathway analysis for only cell types; (C) Relationship of cell types; (D) Pearson Correlation Matrix of metapathways; (E) SHAP importance plot for CSE vs others; (F) SHAP importance plot for RV vs others; (G) SHAP importance plot for RVCSE vs others;

metagene_2nd_level	metagene_1st_level	Enrichment result	Signatures	cell type interaction
metapathway_9	18_rvcse	REACTOME_M_PHASE REACTOME_MITOTIC_PROMETAPHASE REACTOME_RHO_GTPASES_ACTIVATE_FORMINS		Brush+PNEC, Pre-ciliated, Cycling basal
	16_cse	REACTOME_ANTIMICROBIAL_PEPTIDES WP_COMPLEMENT_SYSTEM	BPIFB1,LTF,LCN2,BPIFA1	
	14_mock	BIOCARTA_INFLAM_PATHWAY REACTOME_PEPTIDE_LIGAND_BINDING_RECEPTORS		
	13_rv	REACTOME_ANTIMICROBIAL_PEPTIDES REACTOME_REGULATION_OF_TLR_BY_ENDOGENOUS_LIGAND	S100A7,S100A8,S100A9,PI3	
	16_rv	WP_COMPLEMENT_ACTIVATION WP_CYTOKINES_AND_INFLAMMATORY_RESPONSE KEGG_ANTIGEN_PROCESSING_AND_PRESENTATION		
	14_rv	BIOCARTA_MHC_PATHWAY BIOCARTA_BLYMPHOCYTE_PATHWAY		
	16_rvcse	REACTOME_POST_TRANSLATIONAL_MODIFICATION_SYNTHESIS_OF_GPI_ANCHORED_PROTEINS		
	7_mock	BIOCARTA_FIBRINOLYSIS_PATHWAY WP_ENDOCHONDRAL_OSSIFICATION		
	8_rvcse	REACTOME_INTERFERON_ALPHA_BETA_SIGNALING WP_TYPE_II_INTERFERON_SIGNALING		
	5_cse	REACTOME_INTERFERON_GAMMA_SIGNALING		
	4_rv	REACTOME_NEURONAL_SYSTEM REACTOME_G_ALPHA_I_SIGNALLING_EVENTS		
	13_cse	REACTOME_INTEGRIN_CELL_SURFACE_INTERACTIONS		
	4_cse	REACTOME_INTRAFLAGELLAR_TRANSPORT REACTOME_RECRUITMENT_OF_NUMA_TO_MITOTIC_CENTROSOMES		
	17_mock	REACTOME_CILIUM_ASSEMBLY KEGG_MEDICUS_REFERENCE_RETROGRADE_AXONAL_TRANSPORT		
	9_mock	REACTOME_CILIUM_ASSEMBLY REACTOME_ORGANELLE_BIOGENESIS_AND_MAINTENANCE		
	7_rvcse	KEGG_MEDICUS_REFERENCE_RETROGRADE_AXONAL_TRANSPORT		
	9_rvcse	BIOCARTA_MHC_PATHWAY BIOCARTA_TCRA_PATHWAY		
	17_rvcse	REACTOME_NEUTROPHIL_DEGRANULATION REACTOME_ANTIMICROBIAL_PEPTIDES WP_ALLOGRAFT_REJECTION	LCN2, SLPI, BPIFB1	
	19_rvcse	REACTOME_TRANSPORT_OF_INORGANIC_CATIONS_ANIONS_AND_AMINO_ACIDS_OLIGOPEPTIDES WP_NUCLEAR_RECEPTORS_METAPATHWAY (peptidase regulator activity)	WFDC2, SLPI	
	11_rvcse	REACTOME_CELL_CELL_COMMUNICATION REACTOME_CELL_JUNCTION_ORGANIZATION		
metapathway_19	12_cse	REACTOME_DISSOLUTION_OF_FIBRIN_CLOT PID_MYC_REPRESS_PATHWAY		Brush+PNEC, Cycling basal, Basal, Doublet, Hillock
	15_mock	REACTOME_FORMATION_OF_THE_CORNIFIED_ENVELOPE REACTOME_DISSOLUTION_OF_FIBRIN_CLOT		
	10_rv	REACTOME_FORMATION_OF_THE_CORNIFIED_ENVELOPE REACTOME_CELL_CELL_COMMUNICATION		
	12_rvcse	REACTOME_FORMATION_OF_THE_CORNIFIED_ENVELOPE REACTOME_KERATINIZATION		
	13_rv	REACTOME_FORMATION_OF_THE_CORNIFIED_ENVELOPE REACTOME_ANTIMICROBIAL_PEPTIDES	S100A7,S100A8,S100A9,PI3	
	8_rvcse	REACTOME_INTERFERON_ALPHA_BETA_SIGNALING WP_TYPE_II_INTERFERON_SIGNALING		
	18_mock	REACTOME_ORGANELLE_BIOGENESIS_AND_MAINTENANCE REACTOME_INTRAFLAGELLAR_TRANSPORT		
	4_rv	WP_INFLAMMATORY_RESPONSE_PATHWAY		
	15_rvcse	REACTOME_INTERLEUKIN_10_SIGNALING		
	17_rv	BIOCARTA_MHC_PATHWAY		
	11_rvcse	REACTOME_CELL_CELL_COMMUNICATION WP_ALPHA_6_BETA_4_INTEGRIN_SIGNALING_PATHWAY		
	6_rvcse	REACTOME_MITOTIC_PROMETAPHASE REACTOME_DNA_REPAIR		
	12_rv	REACTOME_OPIOID_SIGNALLING KEGG_CALCIUM_SIGNALING_PATHWAY		
	4_cse	REACTOME_INTRAFLAGELLAR_TRANSPORT		
	9_mock	REACTOME_CILIUM_ASSEMBLY REACTOME_ANCHORING_OF_THE_BASAL_BODY_TO_THE_PLASMA_MEMBRANE		

	16_mock	REACTOME_CILIUM_ASSEMBLY WP_CILIOPATHIES		
	16_rvcse	REACTOME_POST_TRANSLATIONAL_MODIFICATION_SYNTHESIS_OF_GPI_ANCHORED_PROTEINS		
	5_rv	REACTOME_INTRAFLAGELLAR_TRANSPORT		
	7_rv	REACTOME_CILIUM_ASSEMBLY REACTOME_REGULATION_OF_PLK1_ACTIVITY_AT_G2_M_TRANSITION		
	1_rvcse	REACTOME_INTRAFLAGELLAR_TRANSPORT		
	13_cse	REACTOME_INTEGRIN_CELL_SURFACE_INTERACTIONS		
	7_rvcse	REACTOME_CILIUM_ASSEMBLY REACTOME_INTRAFLAGELLAR_TRANSPORT		
	5_mock	REACTOME_INTERFERON_ALPHA_BETA_SIGNALING		
	2_rv	KEGG_CALCIUM_SIGNALING_PATHWAY REACTOME_OPIOID_SIGNALLING		
	14_rvcse	REACTOME_CILIUM_ASSEMBLY REACTOME_FORMATION_OF_THE_CORNIFIED_ENVELOPE		
	18_rvcse	REACTOME_CILIUM_ASSEMBLY REACTOME_INTRAFLAGELLAR_TRANSPORT		
	17_mock	REACTOME_CILIUM_ASSEMBLY KEGG_P53_SIGNALING_PATHWAY		
	5_rvcse	REACTOME_INTERFERON_ALPHA_BETA_SIGNALING		
metapathway_4	15_rv	KEGG_MEDICUS_REFERENCE_ANTIGEN_PROCESSING_AND_PRESENTATION_BY_MHC_CLASS_II_MOLECULES BIOCARTA_BLYMPHOCYTE_PATHWAY	HLA-DRB1,HLA-DRB5	Secretory
metapathway_7	6_rv	REACTOME_INTERFERON_SIGNALING		Ionocyte, Pre-ciliated
	5_mock	REACTOME_INTERFERON_SIGNALING REACTOME_ANTIMICROBIAL_PEPTIDES		
	5_cse	REACTOME_INTERFERON_SIGNALING		
	17_rv	BIOCARTA_MHC_PATHWAY		
	9_rvcse	BIOCARTA_MHC_PATHWAY		
	8_rvcse	WP_MATRIX_METALLOPROTEINASES REACTOME_INTERFERON_ALPHA_BETA_SIGNALING WP_TYPE_II_INTERFERON_SIGNALING		
	9_rv	REACTOME_INTERFERON_SIGNALING		
	11_rvcse	REACTOME_CELL_CELL_COMMUNICATION		
	10_rvcse	REACTOME_INTERFERON_ALPHA_BETA_SIGNALING WP_CILIOPATHIES REACTOME_CILIUM_ASSEMBLY		
metapathway_16	1_rv	REACTOME_SENSORY_PERCEPTION_OF_TASTE REACTOME_G_ALPHA_Q_SIGNALLING_EVENTS		Brush+PNEC
	2_rvcse	REACTOME_G_ALPHA_Q_SIGNALLING_EVENTS REACTOME_G_ALPHA_I_SIGNALLING_EVENTS		
	9_cse	REACTOME_ACTIVATION_OF_KAINATE_RECEPTORS_UPON_GLUTAMATE_BINDING		
	8_mock	REACTOME_NEURONAL_SYSTEM REACTOME_SENSORY_PERCEPTION_OF_TASTE		
	4_cse	REACTOME_INTRAFLAGELLAR_TRANSPORT		
	9_mock	REACTOME_CILIUM_ASSEMBLY		
	10_rvcse	REACTOME_CILIUM_ASSEMBLY		
metapathway_2	13_mock	REACTOME_CILIUM_ASSEMBLY WP_GANGLIO_SERIES_SPHINGOLIPID_METABOLISM REACTOME_INTRAFLAGELLAR_TRANSPORT		Hillock, Pre-ciliated, Ionocyte
	6_rv	REACTOME_INTERFERON_ALPHA_BETA_SIGNALING WP_TYPE_II_INTERFERON_SIGNALING		
	10_rvcse	REACTOME_CILIUM_ASSEMBLY REACTOME_ANCHORING_OF_THE_BASAL_BODY_TO_THE_PLASMA_MEMBRANE		
	15_rv	BIOCARTA_MHC_PATHWAY KEGG_MEDICUS_REFERENCE_ANTIGEN_PROCESSING_AND_PRESENTATION_BY_MHC_CLASS_II_MOLECULES		
	19_rv	WP_CILIOPATHIES REACTOME_INOSITOL_PHOSPHATE_METABOLISM		
	17_cse	WP_PROSTAGLANDIN_AND_LEUKOTRIENE_METABOLISM_IN_SENESCENCE_WP5122 WP_GABA_RECEPTOR_SIGNALING		
	9_cse	REACTOME_NEURONAL_SYSTEM KEGG_TASTE_TRANSDUCTION		
	18_rvcse	REACTOME_INTERLEUKIN_10_SIGNALING BIOCARTA_MHC_PATHWAY		
	16_rvcse	REACTOME_POST_TRANSLATIONAL_MODIFICATION_SYNTHESIS_OF_GPI_ANCHORED_PROTEINS		

Table 7. Metapathway analysis.

Case Study 7: Cross-Species Metapathway Crosstalk Identifies Keratinization as a Novel Biomarker for Malaria Susceptibility

In this case, we combined GSE288146 and GSE289197 to explore the crosstalk of metapathways for host-parasite interaction where we used customised pipeline of RNAchat.

We first manually did the 1st level ICA decomposition on the two datasets separately (10 components each) and combined them with an outer join. Then we filled the missing values with 0 for the two species after outer join. Through metapathway analysis of both human and Plasmodium-derived pathways, we identified two major mechanisms by which the parasite interacts with host: metapathway_0 and metapathway_4, representing 2 different stages of infection: (Immune Modulation and Metabolic Adaptation) and (Host-Cell Structure Remodeling and Direct Cellular Interference).

A

	inputs
meta_0	[metagene_4_hum, metagene_9_hum, metagene_0_hum, metagene_4_plas, metagene_2_hum, metagene_3_plas, metagene_6_plas, metagene_8_plas]
meta_1	[metagene_6_hum]
meta_2	[metagene_3_hum]
meta_3	[metagene_2_hum, metagene_4_hum, metagene_5_hum, metagene_8_hum]
meta_4	[metagene_0_hum, metagene_1_plas, metagene_5_hum, metagene_2_plas, metagene_0_plas, metagene_4_hum, metagene_9_plas]
meta_5	[metagene_7_hum, metagene_5_hum, metagene_9_hum, metagene_4_hum]
meta_6	[metagene_1_hum, metagene_9_hum, metagene_8_hum, metagene_5_hum, metagene_4_hum]

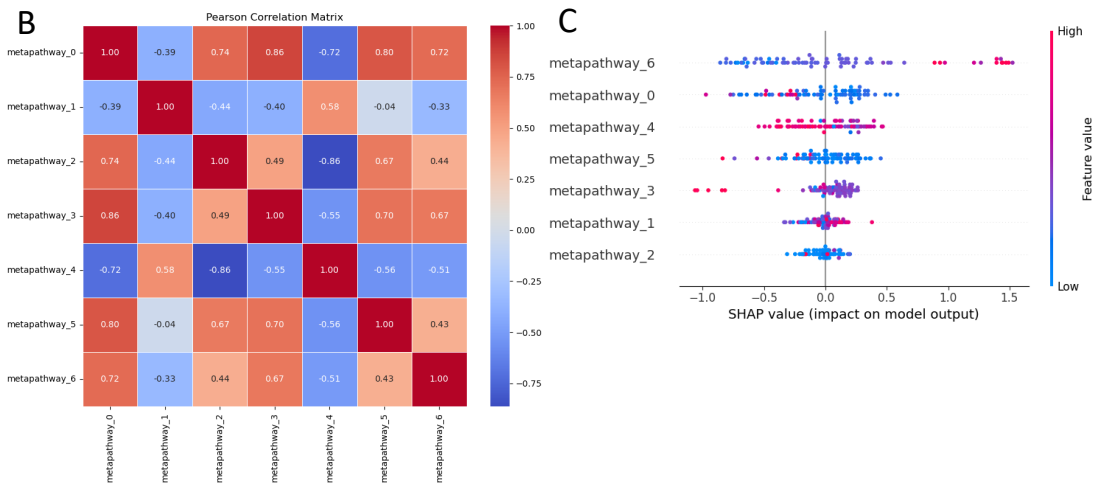

Figure 9. (A) Components of metapathway analysis; (B) Pearson Correlation Matrix of metapathways.

metagene_2nd_level	metagene_1st_level	Enrichment result
metapathway_0	4_hum	REACTOME_GAP_JUNCTION_TRAFFICKING_AND_REGULATION
	9_hum	icosanoid transport regulation of fatty acid transport cellular response to steroid hormone stimulus
	0_hum	REACTOME_NEUTROPHIL_DEGRANULATION REACTOME_SRP_DEPENDENT_COTRANSLATIONAL_PROTEIN_TARGETING_TO_MEMBRANE REACTOME_EUKARYOTIC_TRANSLATION_INITIATION
	4_plas	structural constituent of chromatin protein dimerization activity
	2_hum	adaptive thermogenesis regulation of peptide hormone secretion
	3_plas	structural constituent of ribosome structural molecule activity RNA binding Peptide chain elongation Selenoamino acid metabolism Nonsense-Mediated Decay (NMD) Eukaryotic Translation Initiation
	6_plas	Cellular response to heat stress Regulation of HSF1-mediated heat shock response Protein processing in endoplasmic reticulum
	8_plas	PKMTs methylate histone lysines
metapathway_4	0_hum	REACTOME_NEUTROPHIL_DEGRANULATION REACTOME_SRP_DEPENDENT_COTRANSLATIONAL_PROTEIN_TARGETING_TO_MEMBRANE REACTOME_EUKARYOTIC_TRANSLATION_INITIATION
	1_hum	cadherin binding exonuclease activity
	5_hum	heart looping erythrocyte differentiation myeloid cell homeostasis
	2_plas	protein dimerization activity symbiont-containing vacuole membrane extracellular membrane-bounded organelle
	0_plas	host cell cytoplasm host intracellular part
	4_hum	REACTOME_GAP_JUNCTION_TRAFFICKING_AND_REGULATION
	9_plas	extracellular region
metapathway_2	3_hum	oxygen binding
metapathway_1	6_hum	REACTOME_NEUTROPHIL_DEGRANULATION REACTOME_NONSENSE_MEDIATED_DECAY_NMD
metapathway_6	1_hum	cadherin binding exonuclease activity
	9_hum	icosanoid transport regulation of fatty acid transport
	8_hum	REACTOME_KERATINIZATION REACTOME_FORMATION_OF_THE_CORNIFIED_ENVELOPE
	5_hum	erythrocyte differentiation myeloid cell homeostasis
	4_hum	fatty acid metabolic process erythrocyte differentiation
metapathway_3	2_hum	adaptive thermogenesis regulation of peptide hormone secretion
	4_hum	REACTOME_GAP_JUNCTION_TRAFFICKING_AND_REGULATION
	5_hum	heart looping erythrocyte differentiation myeloid cell homeostasis
	8_hum	REACTOME_KERATINIZATION REACTOME_FORMATION_OF_THE_CORNIFIED_ENVELOPE

metapathway_5	7_hum	WP_IL3_SIGNALING_PATHWAY WP_IL5_SIGNALING_PATHWAY WP_VEGFAVEGFR2_SIGNAL
	5_hum	heart looping erythrocyte differentiation
	9_hum	icosanoid transport regulation of fatty acid transport
	4_hum	REACTOME_GAP_JUNCTION_TRAFFICKING_AND_REGULATION

Table 8. Metapathway analysis.

In Table 8, we can see metapathway_6, metapathway_3 and metapathway_5 are the downstream stage of malaria infection. metapathway_1 was the immune response.

We then extracted the patients' data alone and did Random Forests (0.1 test split) to their number of parasitemia (log1p-ed) in the blood (Figure 9-C) with test MSE 2.4652. As we see metapathway_0 and metapathway_4 present a complementary mechanism to keep the number of parasitemia at a fixed level while metapathway_6 took the dominant. Currently there are many papers trying to cure malaria with solutions related to metapathway_0 and metapathway_4[69–71]. However, no paper talks about metapathway_6 related to keratinization. Paper found that serum lipids can regulate keratinization[72–74]. Therefore, we think keratinization level reflects malaria susceptibility in terms of the following genes related to lipid metabolism: LIPM[75], LIPK[76], LIPN[77].

Discussion

RNAchat represents a paradigm shift in analyzing pathway and cell-cell communication by integrating clinical heterogeneity with multi-omics data through machine learning. Unlike existing tools such as CellChat or MetaPathways, which focus narrowly on predefined ligand-receptor interactions or microbial metabolic pathways, RNAchat prioritizes identifying clinically actionable metapathways—cooperative molecular modules that bridge omics layers and correlate with patient outcomes. Here, we discuss how RNAchat addresses critical gaps in the field, its biological and clinical implications, and its limitations.

- Clinical Integration as a Key Advancement

Most pathway analysis tools operate in a vacuum, dissecting molecular interactions without linking them to clinical phenotypes. RNAchat closes this gap by combining unsupervised ICA decomposition with supervised ML models to directly associate metapathways with outcomes like drug resistance, pain severity, or disease progression. By anchoring findings in clinical data, RNAchat transforms pathway analysis from a descriptive exercise into a predictive and actionable framework.

- Overcoming Limitations of Direction-Centric Tools

A key distinction between RNAchat and tools like CellChat is the lack of explicit directionality in inferred interactions. While CellChat prioritizes directional ligand-receptor signaling, it relies on curated databases that omit non-canonical interactions and cannot prioritize pathways based on functional outcomes. RNAchat circumvents these limitations by focusing on cooperative metapathways—groups of co-regulated genes that jointly influence clinical phenotypes.

- Biological Discoveries Enabled by RNAchat

1. Therapy-Specific Metapathways

RNAchat uncovered that the same metagene (e.g., IFN-related *metagene*) participates in divergent metapathways depending on treatment context.

2. Tissue-Specific Pathway Regulation

By comparing synovium and blood, RNAchat revealed that pain-associated feedback loops are negatively buffered in blood but dysregulated in synovial

tissue. This suggests that systemic biomarkers may poorly reflect local disease mechanisms, advocating for tissue-targeted therapies.

3. Conserved Stress-Response Strategies of HF

RNAchat identified IFN signaling as a universal stress-response hub across RA and HF, but with disease-specific buffering strategies.

- Technical Innovations and Limitations

1. Strengths

Hypothesis-Free Discovery: RNAchat's ICA-based approach avoids biases from pre-defined databases, enabling identification of novel interactions (e.g., EJC-independent NMD and BCR signaling crosstalk).

Bulk and Single-Cell Compatibility: Unlike CellChat, RNAchat operates on bulk and single-cell data, distinguishing paracrine/autocrine signaling in bulk via differential pathway enrichment (e.g., synovium vs. blood).

Explainable ML: SHAP values provide intuitive prioritization of metapathways.

2. Limitations

Directionality: While RNAchat identifies cooperative metapathways, it cannot infer directional cell-cell communication. We propose combining RNAchat with CellChat in single-cell datasets to resolve this.

Validation Dependency: RNAchat's predictions require external experimental validation, though we mitigated this by cross-referencing high-impact studies.

- Future Directions

RNAchat's modular design allows expansion into new domains:

Non-Immune Diseases: Applying RNAchat to cancer or neurodegeneration could reveal conserved stress-response metapathways.

Therapeutic Discovery: drug targeting for the prioritised metapathways.

Dynamic Modeling: Integrating time-series data to track metapathway evolution during treatment.

- Conclusion

RNAchat redefines pathway analysis by placing clinical heterogeneity at the core of multi-omics integration. Its ability to identify therapy-specific metapathways and resolve feedback mechanisms like the "pain buffer"

provides a roadmap for personalized medicine. While tools like CellChat remain valuable for directional signaling, RNAchat addresses a critical unmet need: translating pathway crosstalk into clinically actionable insights. As precision medicine advances, RNAchat's framework will prove indispensable for dissecting the molecular basis of treatment response and disease heterogeneity.

REFERENCES

1. Sharma, S.D., and Bluett, J. (2024). Towards Personalized Medicine in Rheumatoid Arthritis. Preprint at Dove Medical Press Ltd, https://doi.org/10.2147/OARRR.S372610 https://doi.org/10.2147/OARRR.S372610.
2. Salehi, F., Lopera Gonzalez, L.I., Bayat, S., Kleyer, A., Zanca, D., Brost, A., Schett, G., and Eskofier, B.M. (2024). Machine Learning Prediction of Treatment Response to Biological Disease-Modifying Antirheumatic Drugs in Rheumatoid Arthritis. J Clin Med *13*. https://doi.org/10.3390/jcm13133890.
3. Lee, S., Kang, S., Eun, Y., Won, H.H., Kim, H., Lee, J., Koh, E.M., and Cha, H.S. (2021). Machine learning-based prediction model for responses of bDMARDs in patients with rheumatoid arthritis and ankylosing spondylitis. Arthritis Res Ther *23*. https://doi.org/10.1186/s13075-021-02635-3.
4. Bouget, V., Duquesne, J., Hassler, S., Cournède, P.H., Fautrel, B., Guillemin, F., Pallardy, M., Broët, P., Mariette, X., and Bitoun, S. (2022). Machine learning predicts response to TNF inhibitors in rheumatoid arthritis: results on the ESPOIR and ABIRISK cohorts. RMD Open *8*. https://doi.org/10.1136/rmdopen-2022-002442.
5. Tang, M., Haese-Hill, W., Morton, F., Goodyear, C., Porter, D., Siebert, S., and Otto, T.D. (2025). RNAcare: Integrating Clinical Data with Transcriptomic Evidence using Rheumatoid Arthritis as a Case Study. Preprint, https://doi.org/10.1101/2025.01.31.635914 https://doi.org/10.1101/2025.01.31.635914.
6. Kleverov, M., Zenkova, D., Kamenev, V., Sablina, M., Artyomov, M.N., and Sergushichev, A.A. (2024). Phantasus, a web application for visual and interactive gene expression analysis. *13*, 85722. https://doi.org/10.7554/eLife.
7. Wang, N., Li, Y., Han, S., Zhang, Y., Yang, J., Yin, Z., Deng, C., Liu, Z., Wu, Y., Wu, W., et al. (2024). CFViSA: A comprehensive and free platform for visualization and statistics in omics-data. Comput Biol Med *171*, 108206. https://doi.org/10.1016/J.COMPBIOMED.2024.108206.
8. Hauptman, N., Pižem, J., and Jevšinek Skok, D. (2024). AmiCa: Atlas of miRNA-gene correlations in cancer. Comput Struct Biotechnol J *23*, 2277–2288. https://doi.org/10.1016/J.CSBJ.2024.05.030.

9. Ridge regression https://en.wikipedia.org/wiki/Ridge_regression.
10. Tibshiranit, R. (1996). Regression Shrinkage and Selection via the Lasso.
11. Jin, S., Guerrero-Juarez, C.F., Zhang, L., Chang, I., Ramos, R., Kuan, C.H., Myung, P., Plikus, M. V., and Nie, Q. (2021). Inference and analysis of cell-cell communication using CellChat. Nat Commun *12*. https://doi.org/10.1038/s41467-021-21246-9.
12. Konwar, K.M., Hanson, N.W., Pagé, A.P., and Hallam, S.J. (2013). MetaPathways: A modular pipeline for constructing pathway/genome databases from environmental sequence information. BMC Bioinformatics *14*. https://doi.org/10.1186/1471-2105-14-202.
13. Wilkinson, M.D., Dumontier, M., Aalbersberg, Ij.J., Appleton, G., Axton, M., Baak, A., Blomberg, N., Boiten, J.W., da Silva Santos, L.B., Bourne, P.E., et al. (2016). Comment: The FAIR Guiding Principles for scientific data management and stewardship. Sci Data *3*. https://doi.org/10.1038/sdata.2016.18.
14. Porter, D., van Melckebeke, J., Dale, J., Messow, C.M., McConnachie, A., Walker, A., Munro, R., McLaren, J., McRorie, E., Packham, J., et al. (2016). Tumour necrosis factor inhibition versus rituximab for patients with rheumatoid arthritis who require biological treatment (ORBIT): an open-label, randomised controlled, non-inferiority, trial. The Lancet *388*, 239–247. https://doi.org/10.1016/S0140-6736(16)00380-9.
15. Lliso-Ribera, G., Humby, F., Lewis, M., Nerviani, A., Mauro, D., Rivellese, F., Kelly, S., Hands, R., Bene, F., Ramamoorthi, N., et al. (2019). Synovial tissue signatures enhance clinical classification and prognostic/treatment response algorithms in early inflammatory arthritis and predict requirement for subsequent biological therapy: Results from the pathobiology of early arthritis cohort (PEAC). Ann Rheum Dis *78*, 1642–1652. https://doi.org/10.1136/annrheumdis-2019-215751.
16. Isaacs, J.D., Brockbank, S., Pedersen, A.W., Hilkens, C., Anderson, A., Stocks, P., Lendrem, D., Tarn, J., Smith, G.R., Allen, B., et al. (2022). RA-MAP, molecular immunological landscapes in early rheumatoid arthritis and healthy vaccine recipients. Sci Data *9*. https://doi.org/10.1038/s41597-022-01264-y.

17. Hua, X., Wang, Y.Y., Jia, P., Xiong, Q., Hu, Y., Chang, Y., Lai, S., Xu, Y., Zhao, Z., and Song, J. (2020). Multi-level transcriptome sequencing identifies COL1A1 as a candidate marker in human heart failure progression. BMC Med *18*. https://doi.org/10.1186/s12916-019-1469-4.
18. Dong, M., Wang, B., Wei, J., Antonio, A.H., Perry, C.J., Frey, A., Ouerghi, F., Foxman, E.F., Ishizuka, J.J., Dhodapkar, R.M., et al. (2023). Causal identification of single-cell experimental perturbation effects with CINEMA-OT. Nat Methods *20*, 1769–1779. https://doi.org/10.1038/s41592-023-02040-5.
19. The Plasmodium falciparum ApiAP2 transcription factor PfAP2-V controls parasite proliferation and virulence in intra-erythrocytic developmental cycle (2025).
20. Travassos M, S.R.S.E.S.J. (2025). Transcript data from a severe malaria study. https://www.ncbi.nlm.nih.gov/geo/query/acc.cgi?acc=GSE289197.
21. Dong, M. et al. (2023). Causal identification of single-cell experimental perturbation effects with CINEMA-OT. Dryad. https://doi.org/10.5061/dryad.4xgxd25g1.
22. Nielung, L., Christensen, R., Danneskiold-Samsøe, B., Bliddal, H., Holm, C.C., Ellegaard, K., Slott Jensen, H., and Bartels, E.M. (2015). Validity and Agreement between the 28-Joint Disease Activity Score Based on C-Reactive Protein and Erythrocyte Sedimentation Rate in Patients with Rheumatoid Arthritis. Arthritis *2015*, 1–6. https://doi.org/10.1155/2015/401690.
23. British Pain Society (2019). Outcome Measures. https://www.britishpainsociety.org/static/uploads/resources/files/Outcome_Measures_January_2019.pdf.
24. Klimek, L., Bergmann, K.C., Biedermann, T., Bousquet, J., Hellings, P., Jung, K., Merk, H., Olze, H., Schlenter, W., Stock, P., et al. (2017). Visual analogue scales (VAS) - Measuring instruments for the documentation of symptoms and therapy monitoring in case of allergic rhinitis in everyday health care. Allergo Journal *26*, 36–47. https://doi.org/10.1007/s40629-016-0006-7.
25. Specifications Manual for Joint Commission National Quality Measures (v2016B) https://manual.jointcommission.org/release/TJC2016B/DataElem0439.html.

26. Comon, P. (1994). Independent component analysis, A new concept? Signal Processing *36*, 287–314. https://doi.org/10.1016/0165-1684(94)90029-9.
27. Pearson correlation coefficient https://en.wikipedia.org/wiki/Pearson_correlation_coefficient.
28. Breiman, L. (2001). Random Forests.
29. Chen, T., and Guestrin, C. (2016). XGBoost: A scalable tree boosting system. In Proceedings of the ACM SIGKDD International Conference on Knowledge Discovery and Data Mining (Association for Computing Machinery), pp. 785–794. https://doi.org/10.1145/2939672.2939785.
30. Ke, G., Meng, Q., Finley, T., Wang, T., Chen, W., Ma, W., Ye, Q., and Liu, T.-Y. LightGBM: A Highly Efficient Gradient Boosting Decision Tree.
31. Bradley, A.P. (1997). The use of the area under the ROC curve in the evaluation of machine learning algorithms. Pattern Recognit *30*, 1145–1159. https://doi.org/10.1016/S0031-3203(96)00142-2.
32. Mean squared error https://en.wikipedia.org/wiki/Mean_squared_error.
33. Lundberg, S.M., Allen, P.G., and Lee, S.-I. A Unified Approach to Interpreting Model Predictions.
34. Athey, S., Tibshirani, J., and Wager, S. (2019). Generalized random forests. Ann Stat *47*, 1179–1203. https://doi.org/10.1214/18-AOS1709.
35. Issa, Y., Nummer, D., Seibel, T., Müerköster, S.S., Koch, M., Schmitz-Winnenthal, F.H., Galindo, L., Weitz, J., Beckhove, P., and Altevogt, P. (2009). Enhanced L1CAM expression on pancreatic tumor endothelium mediates selective tumor cell transmigration. J Mol Med *87*, 99–112. https://doi.org/10.1007/s00109-008-0410-7.
36. Guo, A., Lu, P., Lee, J., Zhen, C., Chiosis, G., and Wang, Y.L. (2017). HSP90 stabilizes B-cell receptor kinases in a multi-client interactome: PU-H71 induces CLL apoptosis in a cytoprotective microenvironment. Oncogene *36*, 3441–3449. https://doi.org/10.1038/onc.2016.494.
37. Walter, R., Pan, K.-T., Doebele, C., Comoglio, F., Tomska, K., Bohnenberger, H., Young, R.M., Jacobs, L., Keller, U., Engelke, M., et al. HSP90 promotes Burkitt lymphoma cell survival by maintaining tonic B-cell receptor signaling. https://doi.org/10.1182/blood-2016-06.

38. Albakova, Z. (2024). HSP90 multi-functionality in cancer. Preprint at Frontiers Media SA, https://doi.org/10.3389/fimmu.2024.1436973 https://doi.org/10.3389/fimmu.2024.1436973.
39. Lee, J.A., Sinkovits, R.S., Mock, D., Rab, E.L., Cai, J., Yang, P., Saunders, B., Hsueh, R.C., Choi, S., Subramaniam, S., et al. (2006). Components of the antigen processing and presentation pathway revealed by gene expression microarray analysis of following B cell antigen receptor (BCR) stimulation. BMC Bioinformatics *7*. https://doi.org/10.1186/1471-2105-7-237.
40. Lambert, J.M., Ashi, M.O., Srour, N., Delpy, L., and Saulière, J. (2020). Mechanisms and regulation of nonsense-mediated mRNA decay and nonsense-associated altered splicing in lymphocytes. Preprint at MDPI AG, https://doi.org/10.3390/ijms21041335 https://doi.org/10.3390/ijms21041335.
41. Kehrel, B.E., Horn, M., Brodde, M.F., Jurk, K., Niemann, S., and Van, H.K. (2004). 605 Alpha-Defensins NHP-1 and NHP-2 Induce Strong Platelet-Activation Leading to CD40L Expression.
42. Freitas do Rosario, A.P., and Langhorne, J. (2012). T cell-derived IL-10 and its impact on the regulation of host responses during malaria. Int J Parasitol *42*, 549–555. https://doi.org/10.1016/J.IJPARA.2012.03.010.
43. Koch, N., Jung, M., Sabat, R., Krätzschmar, J., Döcke, W.-D., Asadullah, K., Volk, H.-D., and Grütz, G. (2009). IL-10 protects monocytes and macrophages from complement-mediated lysis. J Leukoc Biol *86*, 155–166. https://doi.org/10.1189/jlb.0708443.
44. Watts, C., West, M.A., and Zaru, R. (2010). TLR signalling regulated antigen presentation in dendritic cells. Curr Opin Immunol *22*, 124–130. https://doi.org/10.1016/J.COI.2009.12.005.
45. Chalifour, A., Jeannin, P., Gauchat, J.F., Blaecke, A., Malissard, M., N'Guyen, T., Thieblemont, N., and Delneste, Y. (2004). Direct bacterial protein PAMP recognition by human NK cells involves TLRs and triggers α-defensin production. Blood *104*, 1778–1783. https://doi.org/10.1182/blood-2003-08-2820.
46. Yang, S., Wang, J., Brand, D.D., and Zheng, S.G. (2018). Role of TNF-TNF receptor 2 signal in regulatory T cells and its therapeutic implications. Preprint

at Frontiers Media S.A., https://doi.org/10.3389/fimmu.2018.00784 https://doi.org/10.3389/fimmu.2018.00784.

47. Yu, D., Lu, Z., Nie, F., and Chong, Y. (2024). Integrins regulation of wound healing processes: insights for chronic skin wound therapeutics. Preprint at Frontiers Media SA, https://doi.org/10.3389/fcimb.2024.1324441 https://doi.org/10.3389/fcimb.2024.1324441.

48. Yang, T., Deng, Z., Xu, L., Li, X., Yang, T., Qian, Y., Lu, Y., Tian, L., Yao, W., and Wang, J. (2022). Macrophages-aPKCι-CCL5 Feedback Loop Modulates the Progression and Chemoresistance in Cholangiocarcinoma. Journal of Experimental and Clinical Cancer Research *41*. https://doi.org/10.1186/s13046-021-02235-8.

49. Chang, C.C., Chiou, C.S., Lin, H.L., Wang, L.H., Chang, Y.S., and Lin, H.C. (2015). Increased risk of acute pancreatitis in patients with rheumatoid arthritis: A population-based cohort study. PLoS One *10*. https://doi.org/10.1371/journal.pone.0135187.

50. Dansereau, M.A., Midavaine, É., Bégin-Lavallée, V., Belkouch, M., Beaudet, N., Longpré, J.M., Mélik-Parsadaniantz, S., and Sarret, P. (2021). Mechanistic insights into the role of the chemokine CCL2/CCR2 axis in dorsal root ganglia to peripheral inflammation and pain hypersensitivity. J Neuroinflammation *18*. https://doi.org/10.1186/s12974-021-02125-y.

51. Qiao, Q., Bai, R., Song, W., Gao, H., Zhang, M., Lu, J., Hong, M., Zhang, X., Sun, P., Zhang, Q., et al. (2021). Human α-defensin 5 suppressed colon cancer growth by targeting PI3K pathway. Exp Cell Res *407*. https://doi.org/10.1016/j.yexcr.2021.112809.

52. Li, M.D., Ruan, H. Bin, Singh, J.P., Zhao, L., Zhao, T., Azarhoush, S., Wu, J., Evans, R.M., and Yang, X. (2012). O-GlcNAc transferase is involved in glucocorticoid receptor-mediated transrepression. Journal of Biological Chemistry *287*, 12904–12912. https://doi.org/10.1074/jbc.M111.303792.

53. Shibabaw, T., Molla, M.D., Teferi, B., and Ayelign, B. (2020). Role of ifn and complements system: Innate immunity in sars-cov-2. Preprint at Dove Medical Press Ltd, https://doi.org/10.2147/JIR.S267280 https://doi.org/10.2147/JIR.S267280.

54. Glaviano, A., Foo, A.S.C., Lam, H.Y., Yap, K.C.H., Jacot, W., Jones, R.H., Eng, H., Nair, M.G., Makvandi, P., Geoerger, B., et al. (2023). PI3K/AKT/mTOR signaling transduction pathway and targeted therapies in cancer. Preprint at BioMed Central Ltd, https://doi.org/10.1186/s12943-023-01827-6 https://doi.org/10.1186/s12943-023-01827-6.
55. Wu, C., Xue, Y., Wang, P., Lin, L., Liu, Q., Li, N., Xu, J., and Cao, X. (2014). IFN-γ Primes Macrophage Activation by Increasing Phosphatase and Tensin Homolog via Downregulation of miR-3473b. The Journal of Immunology *193*, 3036–3044. https://doi.org/10.4049/jimmunol.1302379.
56. Zegeye, M.M., Lindkvist, M., Fälker, K., Kumawat, A.K., Paramel, G., Grenegård, M., Sirsjö, A., and Ljungberg, L.U. (2018). Activation of the JAK/STAT3 and PI3K/AKT pathways are crucial for IL-6 trans-signaling-mediated pro-inflammatory response in human vascular endothelial cells. Cell Communication and Signaling *16*. https://doi.org/10.1186/s12964-018-0268-4.
57. Yoshida, S., Yamada, S., Yokose, K., Matsumoto, H., Fujita, Y., Asano, T., Matsuoka, N., Temmoku, J., Sato, S., Yoshiro-Furuya, M., et al. (2021). Interferon-γ induces interleukin-6 production by neutrophils via the Janus kinase (JAK)-signal transducer and activator of transcription (STAT) pathway. BMC Res Notes *14*. https://doi.org/10.1186/s13104-021-05860-w.
58. Shi, J.H., and Sun, S.C. (2018). Tumor necrosis factor receptor-associated factor regulation of nuclear factor κB and mitogen-activated protein kinase pathways. Preprint at Frontiers Media S.A., https://doi.org/10.3389/fimmu.2018.01849 https://doi.org/10.3389/fimmu.2018.01849.
59. Carlini, V., Noonan, D.M., Abdalalem, E., Goletti, D., Sansone, C., Calabrone, L., and Albini, A. (2023). The multifaceted nature of IL-10: regulation, role in immunological homeostasis and its relevance to cancer, COVID-19 and post-COVID conditions. Preprint at Frontiers Media S.A., https://doi.org/10.3389/fimmu.2023.1161067 https://doi.org/10.3389/fimmu.2023.1161067.
60. Piecyk, M., Ferraro-Peyret, C., Laville, D., Perros, F., and Chaveroux, C. (2024). Novel insights into the GCN2 pathway and its targeting. Therapeutic value in cancer and lessons from lung fibrosis development. Preprint at John

Wiley and Sons Inc, https://doi.org/10.1111/febs.17203 https://doi.org/10.1111/febs.17203.

61. Levick, S.P., and Goldspink, P.H. (2014). Could interferon-gamma be a therapeutic Target for treating heart failure? Heart Fail Rev *19*, 227–236. https://doi.org/10.1007/s10741-013-9393-8.
62. Sobti Awtarrkrishannganjuu, R.C. Biomedical Translational Research From Disease Diagnosis tooTreatment.
63. Mingze Dong CINEMA-OT tutorial. https://github.com/vandijklab/CINEMA-OT/blob/main/cinemaot_tutorial.ipynb.
64. Clifton, C., Niemeyer, B.F., Novak, R., Can, U.I., Hainline, K., and Benam, K.H. (2022). BPIFA1 is a secreted biomarker of differentiating human airway epithelium. Front Cell Infect Microbiol *12*. https://doi.org/10.3389/fcimb.2022.1035566.
65. Kruzel, M.L., Zimecki, M., and Actor, J.K. (2017). Lactoferrin in a context of inflammation-induced pathology. Preprint at Frontiers Media S.A., https://doi.org/10.3389/fimmu.2017.01438 https://doi.org/10.3389/fimmu.2017.01438.
66. Afridi, R., Kim, J.H., Bhusal, A., Lee, W.H., and Suk, K. (2024). Lipocalin-2 as a mediator of neuroimmune communication. Preprint at Oxford University Press, https://doi.org/10.1093/jleuko/qiad157 https://doi.org/10.1093/jleuko/qiad157.
67. Xia, P., Ji, X., Yan, L., Lian, S., Chen, Z., and Luo, Y. (2024). Roles of S100A8, S100A9 and S100A12 in infection, inflammation and immunity. Preprint at John Wiley and Sons Inc, https://doi.org/10.1111/imm.13722 https://doi.org/10.1111/imm.13722.
68. Chowdhury, M.A., Kuivaniemi, H., Romero, R., Edwin, S., Chaiworapongsa, T., and Tromp, G. (2006). Identification of novel functional sequence variants in the gene for peptidase inhibitor 3. BMC Med Genet *7*. https://doi.org/10.1186/1471-2350-7-49.
69. Tintó-Font, E., Michel-Todó, L., Russell, T.J., Casas-Vila, N., Conway, D.J., Bozdech, Z., Llinás, M., and Cortés, A. A heat-shock response regulated by the PfAP2-HS transcription factor protects human malaria parasites from febrile temperatures. https://doi.org/10.5281/zenodo.4775988.

70. Yu, M., Kumar, T.R.S., Nkrumah, L.J., Coppi, A., Retzlaff, S., Li, C.D., Kelly, B.J., Moura, P.A., Lakshmanan, V., Freundlich, J.S., et al. (2008). The Fatty Acid Biosynthesis Enzyme FabI Plays a Key Role in the Development of Liver-Stage Malarial Parasites. Cell Host Microbe *4*, 567–578. https://doi.org/10.1016/j.chom.2008.11.001.
71. Suradji, E.W., Hatabu, T., Kobayashi, K., Yamazaki, C., Abdulah, R., Nakazawa, M., Nakajima-Shimada, J., and Koyama, H. (2011). Selenium-induced apoptosis-like cell death in Plasmodium falciparum. Parasitology *138*, 1852–1862. https://doi.org/10.1017/S0031182011001399.
72. Hampel, U., Schröder, A., Mitchell, T., Brown, S., Snikeris, P., Garreis, F., Kunnen, C., Willcox, M., and Paulsen, F. (2015). Serum-induced keratinization processes in an immortalized human meibomian gland epithelial cell line. PLoS One *10*. https://doi.org/10.1371/journal.pone.0128096.
73. Aldehlawi, H., Usman, S., Lalli, A., Ahmad, F., Williams, G., Teh, M.T., and Waseem, A. (2020). Serum lipids, retinoic acid and phenol red differentially regulate expression of keratins K1, K10 and K2 in cultured keratinocytes. Sci Rep *10*. https://doi.org/10.1038/s41598-020-61640-9.
74. Pang, B., Zhu, Z., Xiao, C., Luo, Y., Fang, H., Bai, Y., Sun, Z., Ma, J., Dang, E., and Wang, G. (2022). Keratin 17 Is Required for Lipid Metabolism in Keratinocytes and Benefits Epidermal Permeability Barrier Homeostasis. Front Cell Dev Biol *9*. https://doi.org/10.3389/fcell.2021.779257.
75. Jorge M Santos, Saskia Egarter, Vanessa Zuzarte-Luis, and Hirdesh Kumar (2017). Malaria parasite LIMPprotein regulates sporozoite gliding motility and infectivity in mosquito and mammalian hosts. Preprint, https://doi.org/10.7554/eLife.24109.001 https://doi.org/10.7554/eLife.24109.001.
76. Ono, T., Yamaguchi, Y., Nakashima, H., Nakashima, M., Ishikiriyama, T., Seki, S., and Kinoshita, M. (2021). Lipopolysaccharide Preconditioning Augments Phagocytosis of Malaria-Parasitized Red Blood Cells by Bone Marrow-Derived Macrophages in the Liver, Thereby Increasing the Murine Survival after Plasmodium yoelii Infection. Infect Immun *89*. https://doi.org/10.1128/IAI.00249-21.

77. Asad, M., Yamaryo-Botté, Y., Hossain, M.E., Thakur, V., Jain, S., Datta, G., Botté, C.Y., and Mohmmed, A. (2021). An essential vesicular-trafficking phospholipase mediates neutral lipid synthesis and contributes to hemozoin formation in Plasmodium falciparum. BMC Biol *19*. https://doi.org/10.1186/s12915-021-01042-z.

- ## Declarations
- ## Ethics approval and consent to participate

For the ORBIT data, all participants provided written, informed consent. The study protocol ORBIT [14] was approved by the West of Scotland Research Ethics Committee on 3/11/2009 (REC reference number: 09/S0703/109/ EudraCT number: 2009-011268-13)

For other studies, data were published.

- ## Consent for publication

We have consent for publication.

- ## Availability of data and materials

The code of can be found https://github.com/tangmingcan/RNAchat.

The RNA-Seq data from ORBIT can be found under the accession numbers Pending waiting for the publication of RNAcare, which is currently under review by BMC Medicine.

- ## Competing interests

The project is developed and some of its presumption is based on RNAcare, which is now under review by BMC Medicine.

- ## Funding

MT was funded by the IMID-Bio-UK (MRC: MR/R014191/1) project.

- ## Authors' contributions

MT – Construction of tool. Data analysis. Writing of first draft.

- ## Acknowledgements

Mingcan previously worked at the School of Infection & Immunity, University of Glasgow, UK, where the data for this study originated from his prior research. We extend our gratitude to Professor Thomas D. Otto and Professor Stefan Siebert from the School of Infection & Immunity for their invaluable support during his tenure.

We also thank Senior Lecturer Tim Storer at computing science, University of Glassgow, Professor James Pan and Jan Chow from the Business Analytics Department at the National University of Singapore for their helps to this paper.

Appendix I

We can also plot the diagram based on metagenes colored by 4 batches with a designated threshold controlling the frequency of two interacted metagenes existing in the metapathways. As we see in the Figure 1, metagene_9_mock interacts with metagene_4_cse under CSE/MOCK; metagene_9_mock interacts with metagene_6_rvcse under RVCSE/MOCK and metagene_4_cse interacts with metagene_6_rvcse under RVCSE/CSE. Therefore, we can know the relationships (promotion/suppression) of the 3 metagenes by just further plotting a Pearson matrix plot of these metagenes.

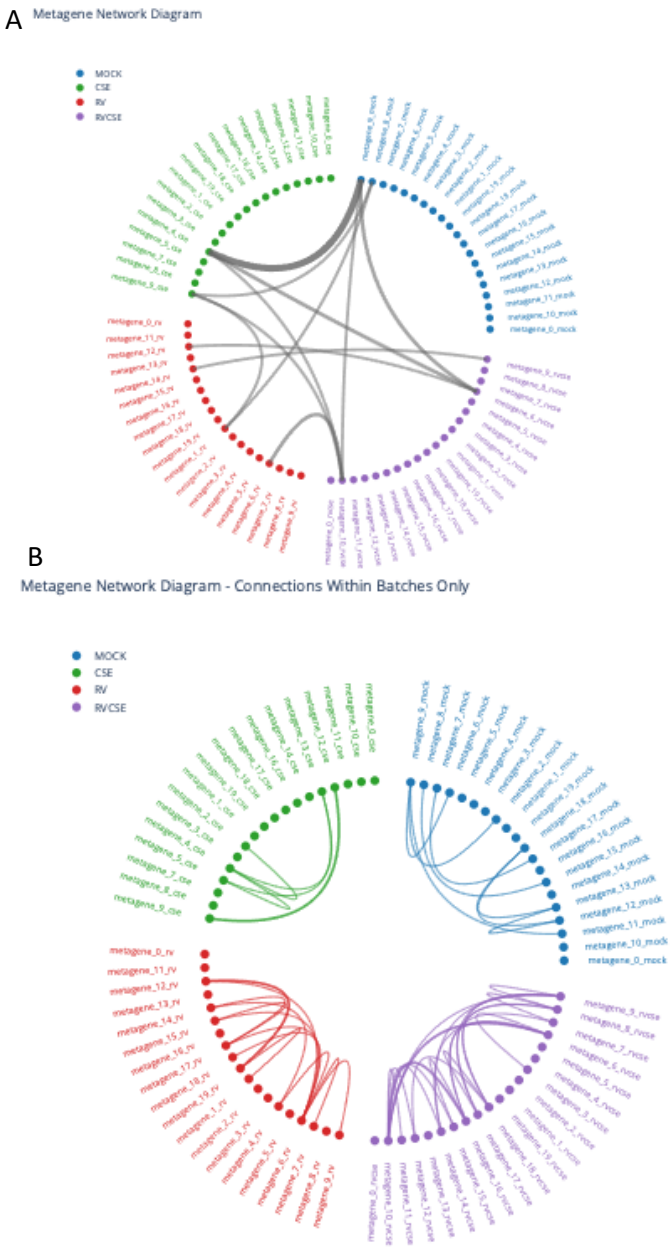

Figure 1. (A) Relationship of metagenes under different perturbations; (B) Relationship of metagenes under same perturbation.

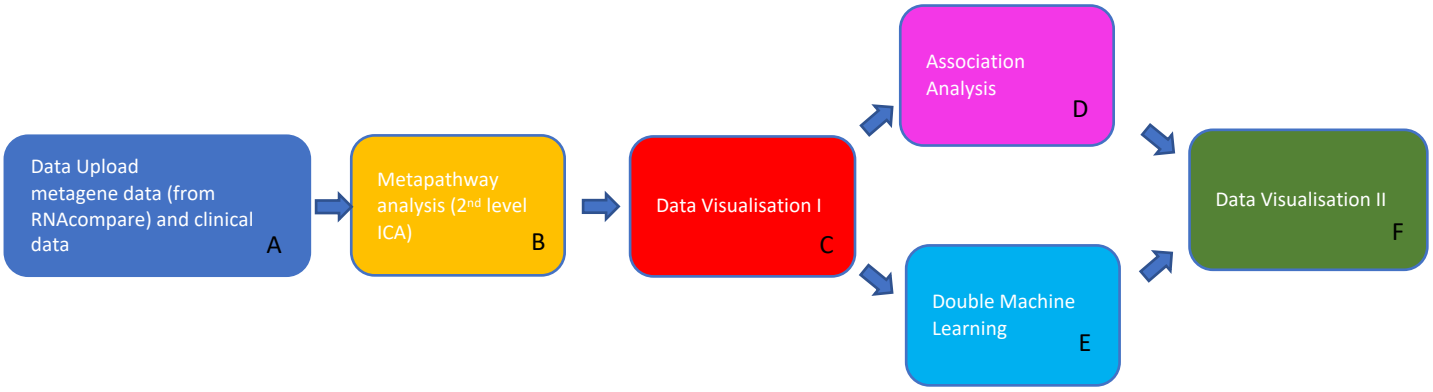
Data Upload
metagene data (from RNAcompare) and clinical data
A
Metapathway analysis (2nd level ICA)
B
Data Visualisation I
C
Association Analysis
D
Double Machine Learning
E
Data Visualisation II
F

A

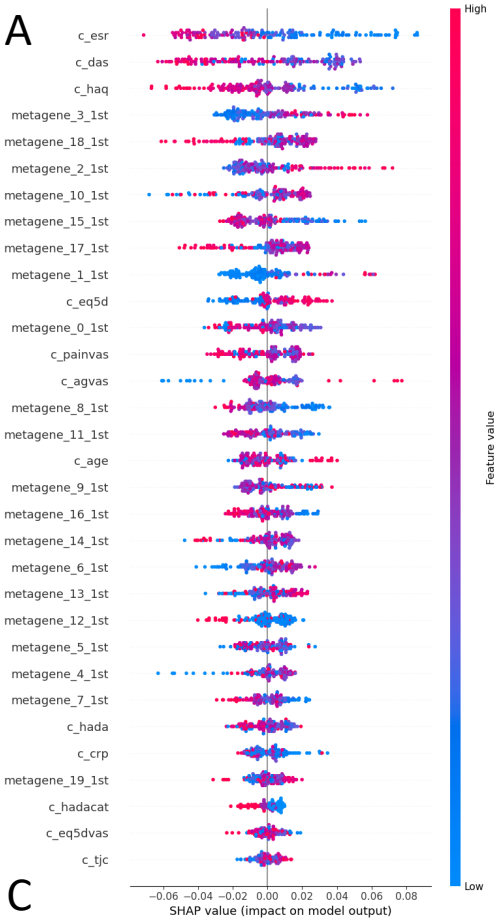

B

Name	PValue
REACTOME_INTERFERON_SIGNALING	1.476452e-46
REACTOME_INTERFERON_ALPHA_BETA_SIGNALING	1.071163e-45
REACTOME_INTERFERON_GAMMA_SIGNALING	9.851463e-32
WP_IMMUNE_RESPONSE_TO_TUBERCULOSIS	7.511500e-17
WP_TYPE_II_INTERFERON_SIGNALING	1.861285e-16
WP_TYPE_II_INTERFERON_SIGNALING_IFNG	4.031285e-13

C

	inputs
meta_0	[metagene_1_1st, metagene_0_1st, metagene_10_1st, metagene_4_1st, metagene_7_1st]
meta_1	[metagene_2_1st, metagene_0_1st, metagene_13_1st, metagene_6_1st]
meta_2	[metagene_16_1st, metagene_14_1st, metagene_7_1st, metagene_3_1st, metagene_17_1st, metagene_8_1st, metagene_0_1st]
meta_3	[metagene_18_1st, metagene_17_1st, metagene_4_1st, metagene_8_1st, metagene_10_1st]
meta_4	[metagene_19_1st, metagene_17_1st, metagene_4_1st, metagene_14_1st, metagene_9_1st, metagene_8_1st]
meta_5	[metagene_8_1st, metagene_15_1st, metagene_6_1st, metagene_19_1st, metagene_7_1st]
meta_6	[metagene_6_1st, metagene_17_1st, metagene_15_1st, metagene_8_1st]

D

	inputs
meta_0	[metagene_2_1st, metagene_0_1st, metagene_14_1st, metagene_5_1st, metagene_6_1st]
meta_1	[metagene_12_1st, metagene_14_1st, metagene_11_1st, metagene_9_1st, metagene_13_1st, metagene_15_1st, metagene_10_1st, metagene_18_1st]
meta_2	[metagene_16_1st, metagene_14_1st, metagene_7_1st, metagene_17_1st, metagene_8_1st]
meta_3	[metagene_18_1st, metagene_17_1st, metagene_8_1st, metagene_4_1st]
meta_4	[metagene_8_1st, metagene_15_1st, metagene_6_1st, metagene_19_1st, metagene_7_1st, metagene_1_1st, metagene_18_1st]
meta_5	[metagene_19_1st, metagene_17_1st, metagene_14_1st, metagene_9_1st, metagene_4_1st, metagene_8_1st, metagene_15_1st, metagene_5_1st]
meta_6	[metagene_6_1st, metagene_17_1st, metagene_15_1st, metagene_8_1st, metagene_3_1st]

E

	inputs
meta_0	[metagene_1_1st, metagene_10_1st, metagene_0_1st, metagene_11_1st, metagene_12_1st, metagene_4_1st, metagene_14_1st, metagene_18_1st]
meta_1	[metagene_2_1st, metagene_13_1st, metagene_0_1st, metagene_16_1st, metagene_10_1st, metagene_6_1st]
meta_2	[metagene_18_1st, metagene_4_1st, metagene_17_1st, metagene_13_1st, metagene_8_1st, metagene_14_1st, metagene_7_1st, metagene_10_1st]
meta_3	[metagene_16_1st, metagene_14_1st, metagene_7_1st, metagene_8_1st, metagene_17_1st, metagene_3_1st, metagene_2_1st]
meta_4	[metagene_19_1st, metagene_17_1st, metagene_4_1st, metagene_9_1st, metagene_14_1st, metagene_8_1st]
meta_5	[metagene_8_1st, metagene_15_1st, metagene_9_1st, metagene_11_1st, metagene_19_1st, metagene_16_1st]
meta_6	[metagene_17_1st, metagene_6_1st, metagene_15_1st, metagene_5_1st]

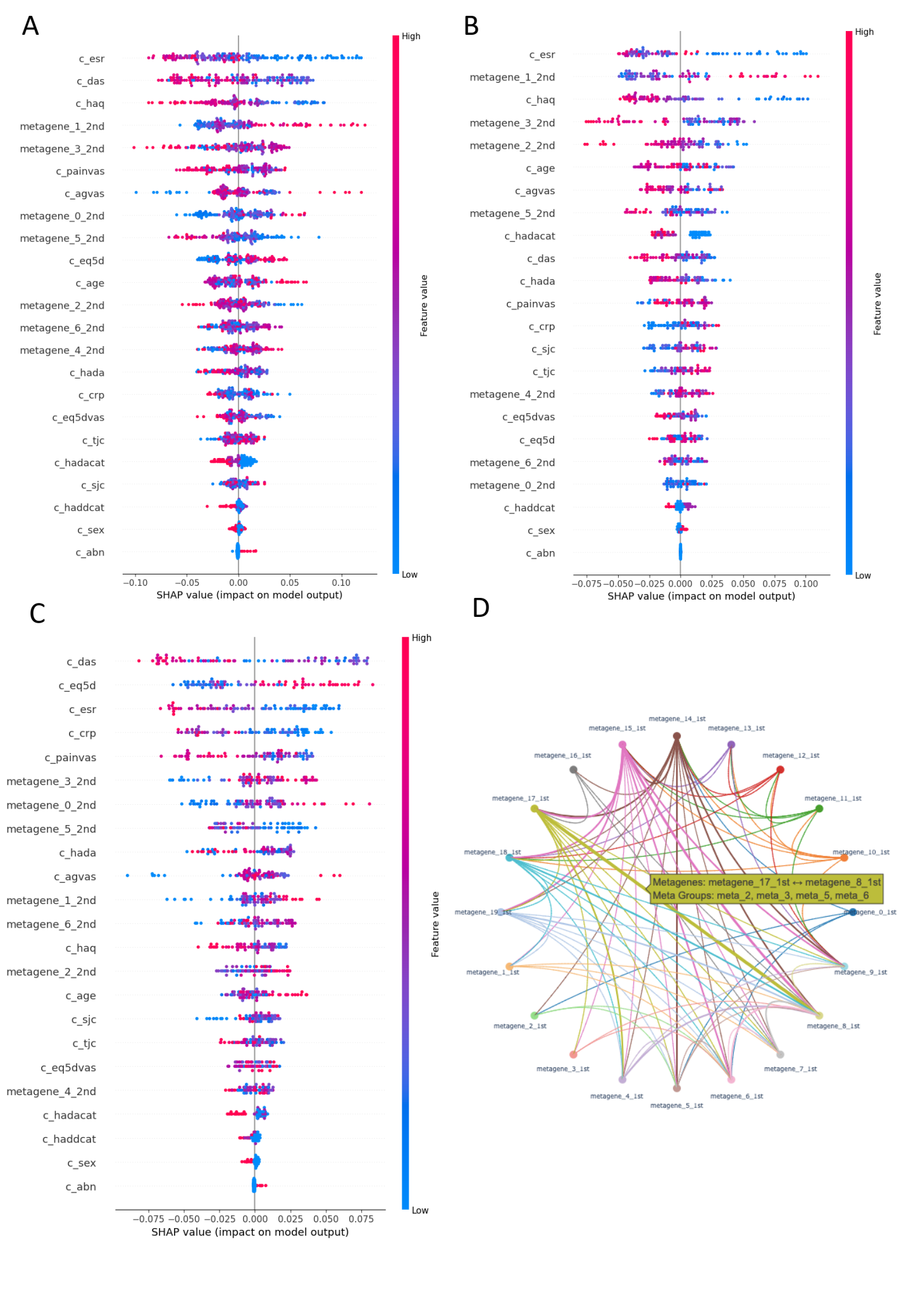
A
c_esr
c_das
c_haq
metagene_1_2nd
metagene_3_2nd
c_painvas
c_agvas
metagene_0_2nd
metagene_5_2nd
c_eq5d
c_age
metagene_2_2nd
metagene_6_2nd
metagene_4_2nd
c_hada
c_crp
c_eq5dvas
c_tjc
c_hadacat
c_sjc
c_haddcat
c_sex
c_abn
−0.10 −0.05 0.00 0.05 0.10
SHAP value (impact on model output)
High
Feature value
Low
B
c_esr
metagene_1_2nd
c_haq
metagene_3_2nd
metagene_2_2nd
c_age
c_agvas
metagene_5_2nd
c_hadacat
c_das
c_hada
c_painvas
c_crp
c_sjc
c_tjc
metagene_4_2nd
c_eq5dvas
c_eq5d
metagene_6_2nd
metagene_0_2nd
c_haddcat
c_sex
c_abn
−0.075 −0.050 −0.025 0.000 0.025 0.050 0.075 0.100
SHAP value (impact on model output)
High
Feature value
Low
C
c_das
c_eq5d
c_esr
c_crp
c_painvas
metagene_3_2nd
metagene_0_2nd
metagene_5_2nd
c_hada
c_agvas
metagene_1_2nd
metagene_6_2nd
c_haq
metagene_2_2nd
c_age
c_sjc
c_tjc
c_eq5dvas
metagene_4_2nd
c_hadacat
c_haddcat
c_sex
c_abn
−0.075 −0.050 −0.025 0.000 0.025 0.050 0.075
SHAP value (impact on model output)
High
Feature value
Low
D
metagene_14_1st
metagene_15_1st
metagene_13_1st
metagene_16_1st
metagene_12_1st
metagene_17_1st
metagene_11_1st
metagene_18_1st
metagene_10_1st
Metagenes: metagene_17_1st ↔ metagene_8_1st
Meta Groups: meta_2, meta_3, meta_5, meta_6
metagene_19_1st
metagene_0_1st
metagene_1_1st
metagene_9_1st
metagene_2_1st
metagene_8_1st
metagene_3_1st
metagene_7_1st
metagene_4_1st
metagene_6_1st
metagene_5_1st

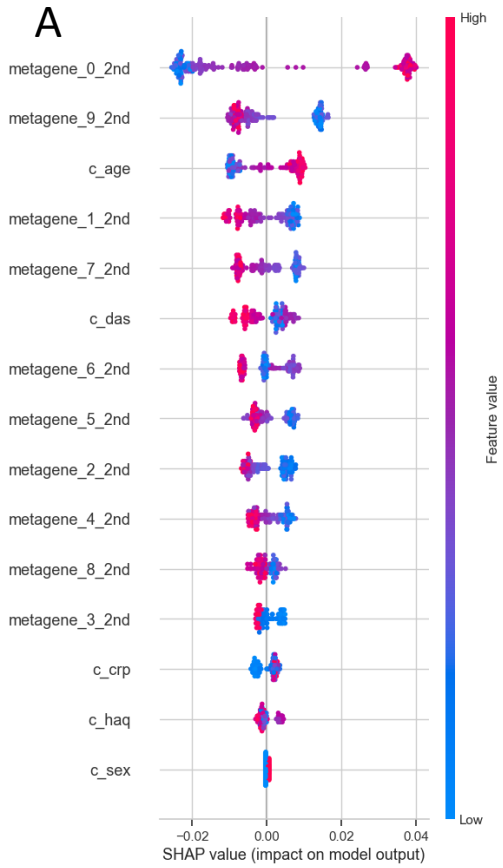

B

	inputs
meta_0	[metagene_3_orb, metagene_5_orb]
meta_1	[metagene_5_orb, metagene_8_pea, metagene_3_pea, metagene_7_orb, metagene_4_pea]
meta_2	[metagene_0_orb, metagene_3_pea]
meta_3	[metagene_2_orb, metagene_0_pea, metagene_5_pea]
meta_4	[metagene_4_orb, metagene_9_pea, metagene_5_pea, metagene_8_orb, metagene_5_orb, metagene_2_pea]
meta_5	[metagene_7_orb, metagene_5_pea, metagene_4_pea, metagene_2_pea, metagene_5_orb]
meta_6	[metagene_1_orb, metagene_8_pea, metagene_9_pea, metagene_0_orb, metagene_2_pea, metagene_8_orb]
meta_7	[metagene_8_orb, metagene_5_pea, metagene_8_pea, metagene_2_pea, metagene_4_pea, metagene_6_pea, metagene_0_pea, metagene_4_orb, metagene_1_pea]
meta_8	[metagene_9_orb, metagene_2_pea]
meta_9	[metagene_6_orb, metagene_6_pea, metagene_9_orb, metagene_9_pea, metagene_7_orb, metagene_1_orb, metagene_2_orb, metagene_0_orb, metagene_3_orb, metagene_5_orb]

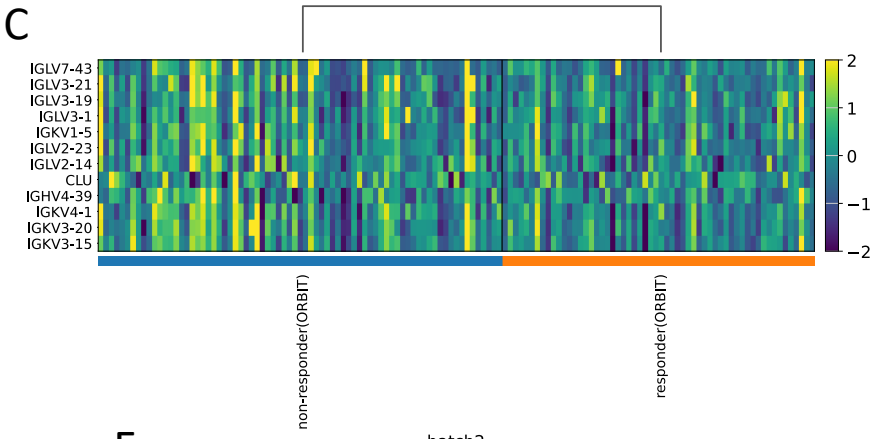

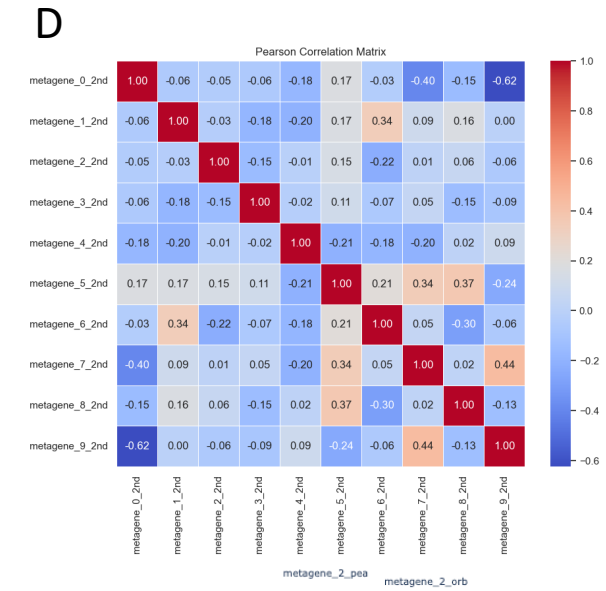

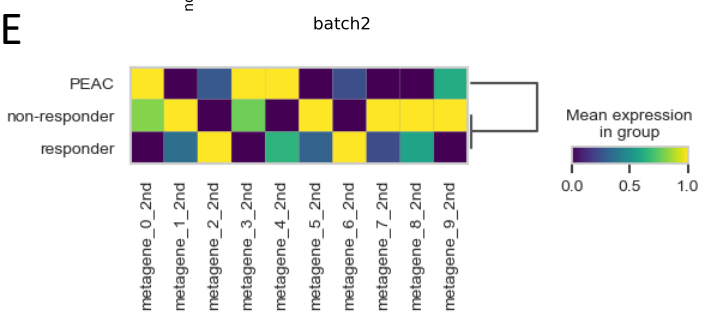

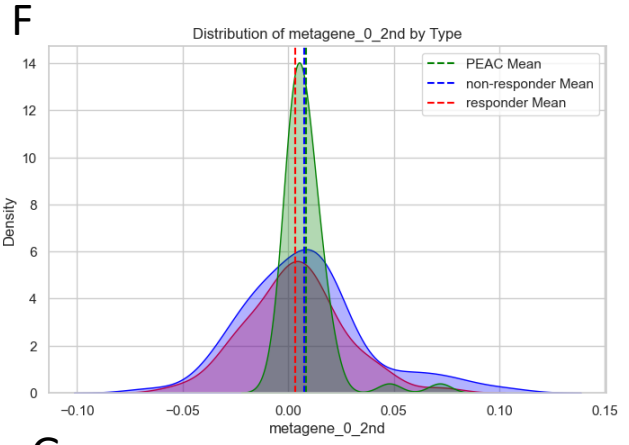

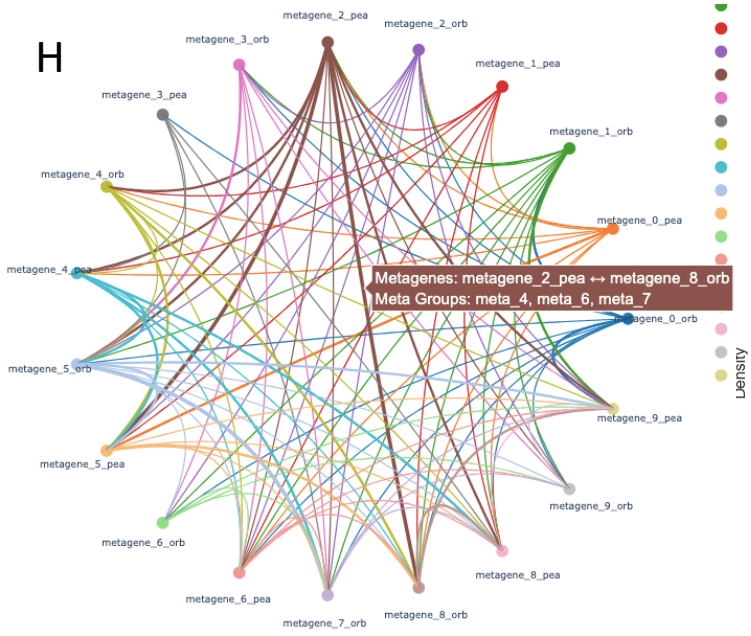

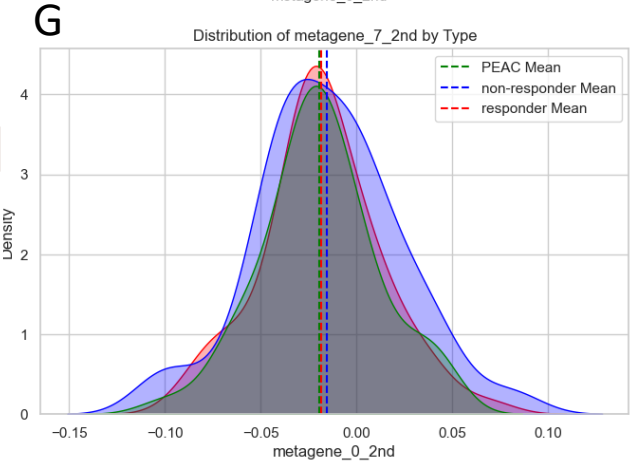

A

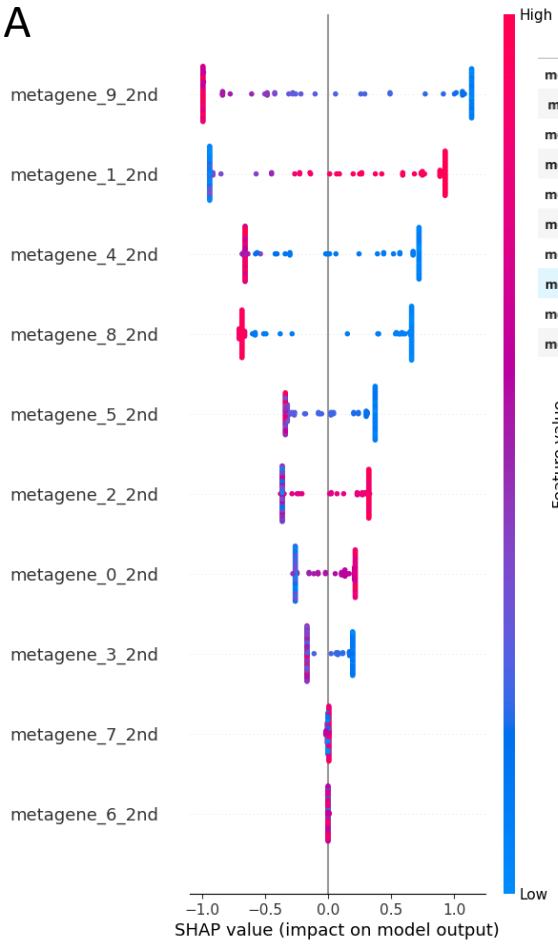

B

	inputs
meta_0	[metagene_2_syn, metagene_4_syn, metagene_0_whl]
meta_1	[metagene_0_syn, metagene_8_whl, metagene_9_whl, metagene_8_syn, metagene_7_syn, metagene_4_whl]
meta_2	[metagene_5_syn, metagene_1_whl, metagene_0_whl, metagene_4_syn, metagene_8_whl]
meta_3	[metagene_9_syn, metagene_6_whl, metagene_3_whl, metagene_0_whl]
meta_4	[metagene_6_syn, metagene_7_whl, metagene_1_syn, metagene_3_whl, metagene_1_whl]
meta_5	[metagene_3_syn, metagene_6_whl, metagene_1_syn, metagene_7_whl]
meta_6	[metagene_8_syn, metagene_0_whl, metagene_2_whl, metagene_6_syn, metagene_0_syn]
meta_7	[metagene_7_syn, metagene_7_whl, metagene_1_syn, metagene_3_whl]
meta_8	[metagene_7_whl, metagene_4_syn, metagene_2_whl, metagene_0_whl, metagene_9_whl, metagene_6_syn, metagene_9_syn]
meta_9	[metagene_4_syn, metagene_3_whl, metagene_6_whl, metagene_2_whl, metagene_4_whl, metagene_6_syn]

C

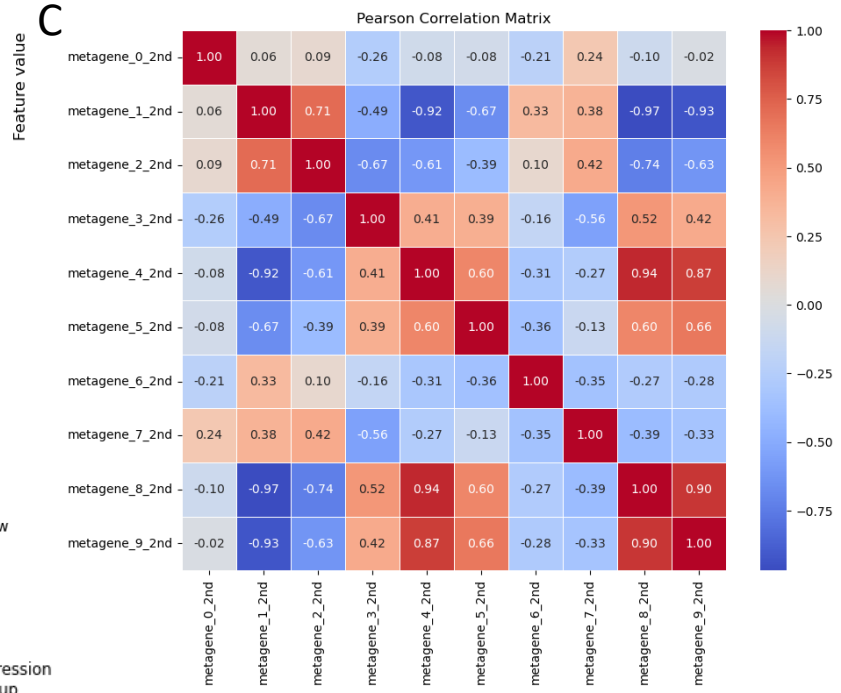

D

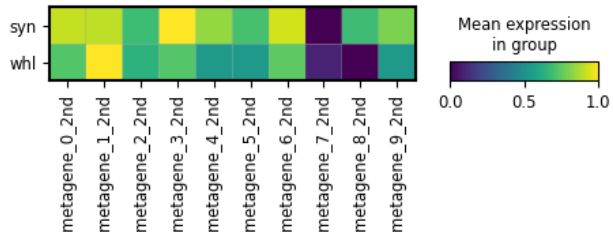

E

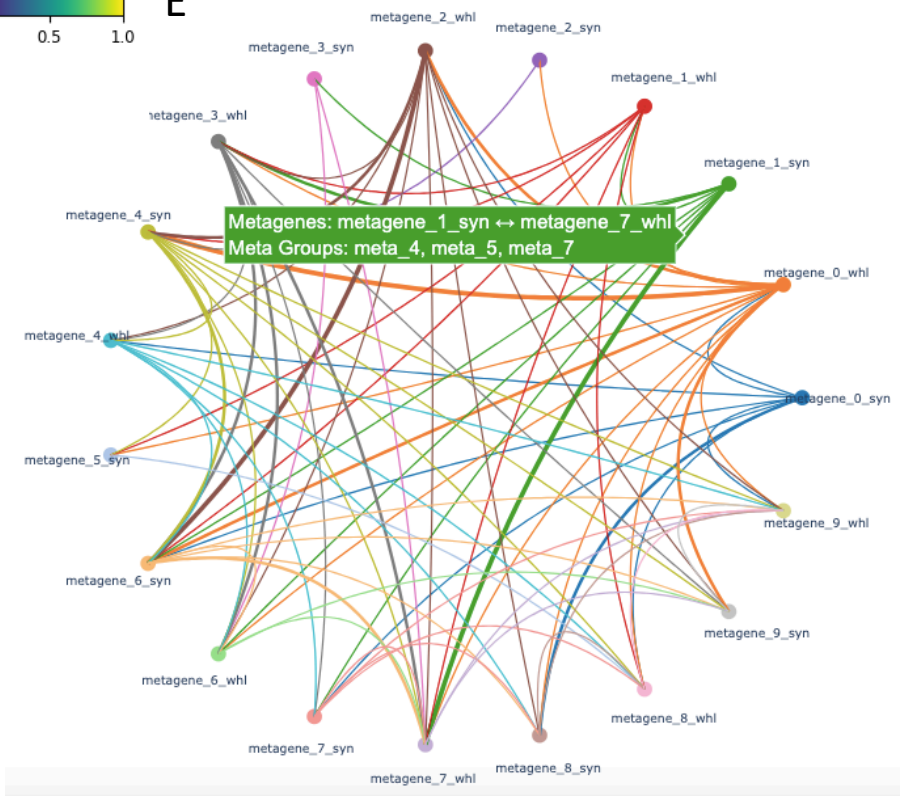

A

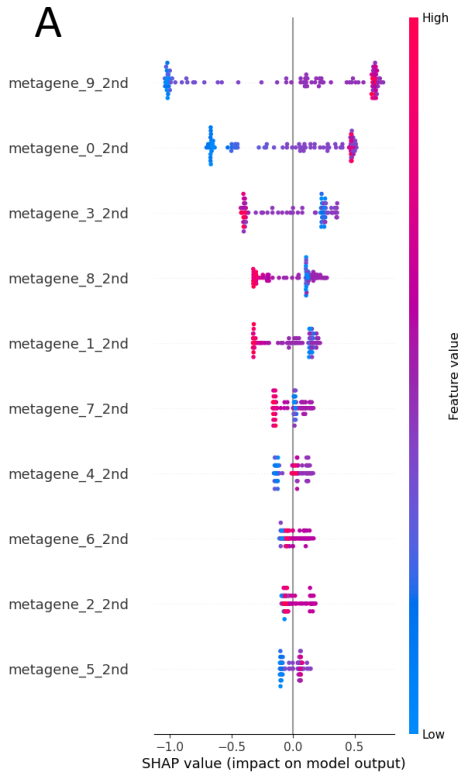

B

	inputs
meta_0	[metagene_0_pr, metagene_0_tr]
meta_1	[metagene_1_pr]
meta_2	[metagene_4_pr]
meta_3	[metagene_2_pr]
meta_4	[metagene_3_pr]
meta_5	[metagene_5_pr]
meta_6	[metagene_6_pr]
meta_7	[metagene_1_tr, metagene_9_tr, metagene_7_tr]
meta_8	[metagene_5_tr, metagene_3_tr, metagene_9_tr, metagene_4_tr, metagene_2_tr]
meta_9	[metagene_4_tr, metagene_0_tr, metagene_3_tr, metagene_5_tr, metagene_7_tr, metagene_0_pr]

C

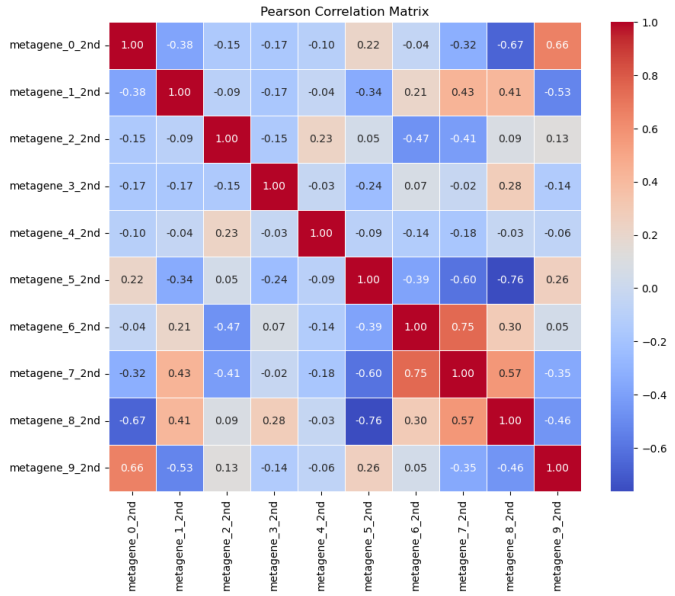

D

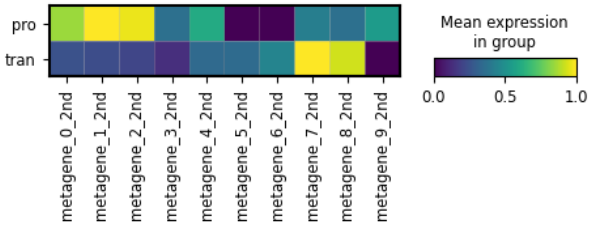

E

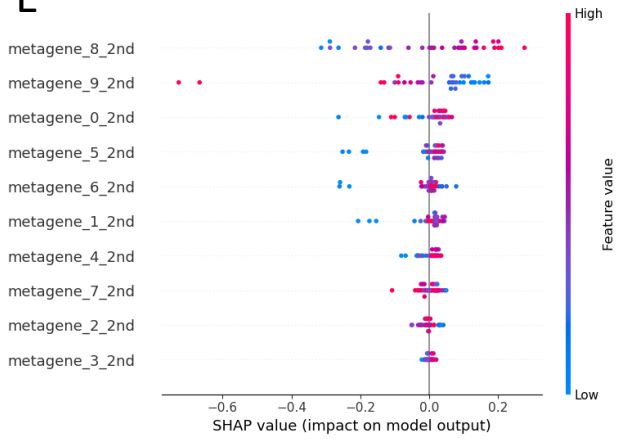

F

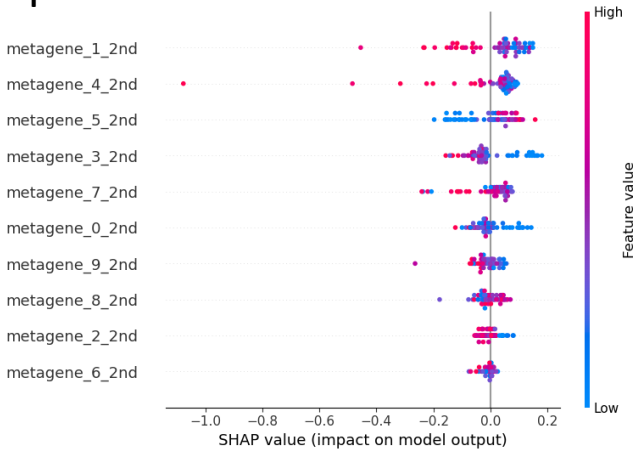

G

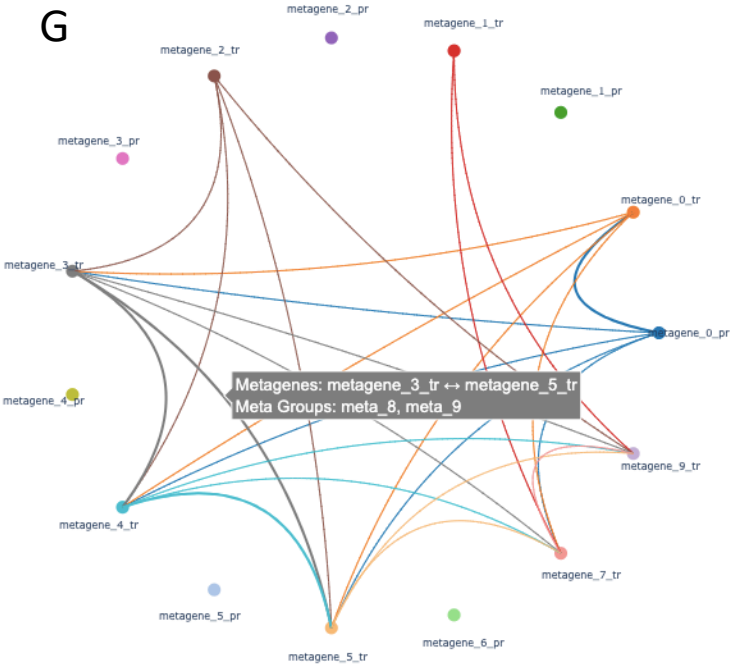

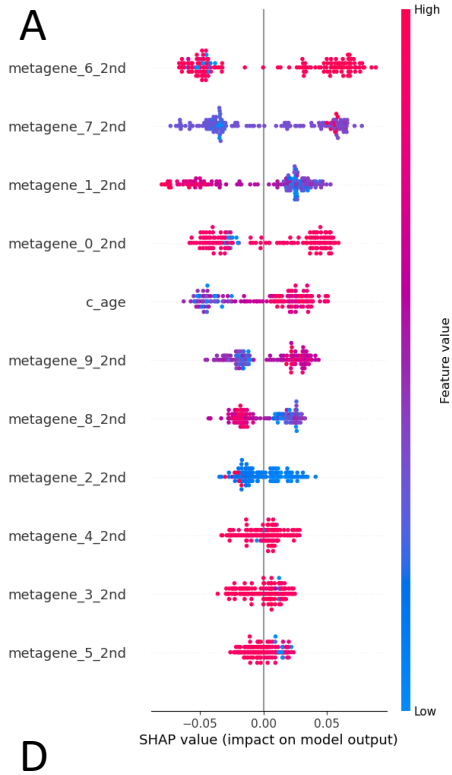

B

	inputs
meta_0	[metagene_3_hf, metagene_4_op]
meta_1	[metagene_6_op, metagene_2_op]
meta_2	[metagene_6_hf]
meta_3	[metagene_5_hf]
meta_4	[metagene_1_hf]
meta_5	[metagene_4_hf]
meta_6	[metagene_2_hf]
meta_7	[metagene_0_hf]
meta_8	[metagene_8_op, metagene_7_op, metagene_9_op, metagene_2_op]
meta_9	[metagene_4_op, metagene_5_op, metagene_1_op, metagene_0_op, metagene_6_op, metagene_3_hf, metagene_6_hf, metagene_5_hf, metagene_2_hf, metagene_1_hf, metagene_4_hf, metagene_0_hf]

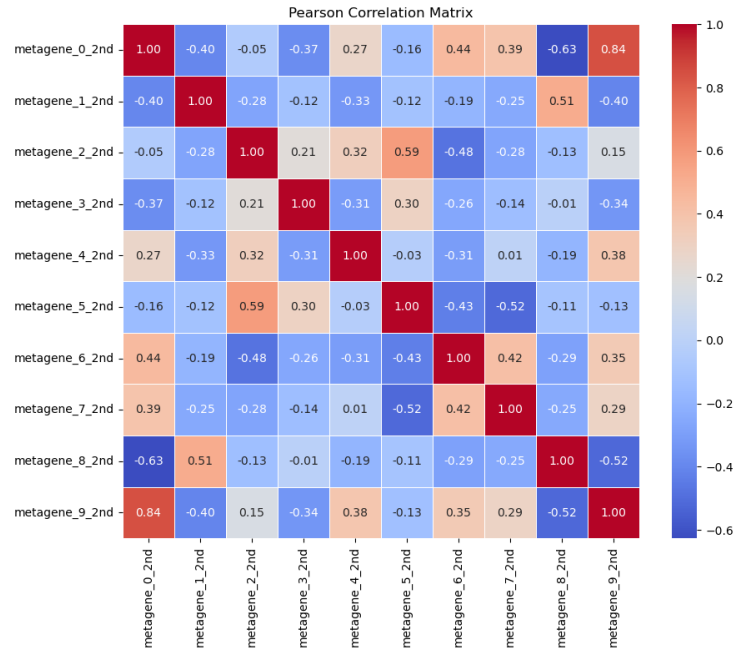

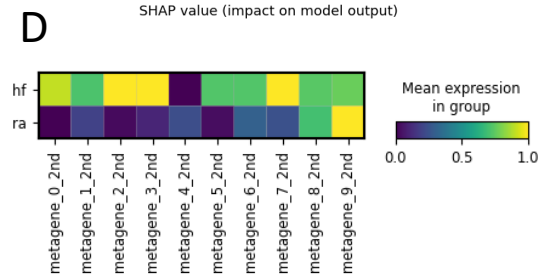

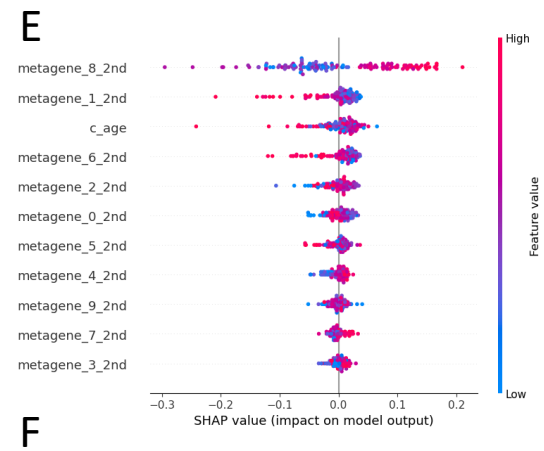

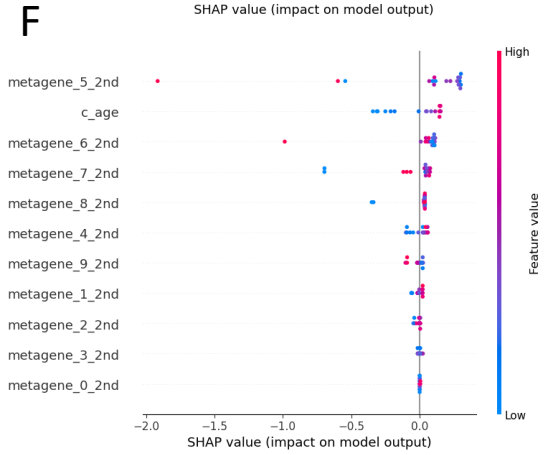

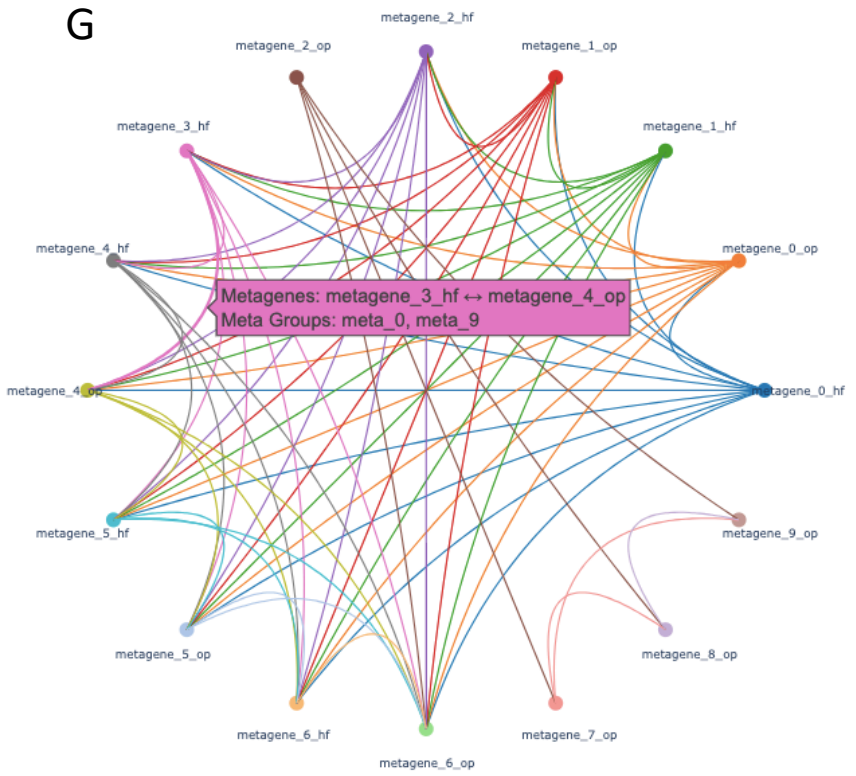

A

	inputs
meta_0	[cell_type_Doublet, cell_type_Pre-ciliated, cell_type_Ionocyte, metagene_12_r4, metagene_10_r2, metagene_14_r2, metagene_11_r4, cell_type_Brush+PNEC, metagene_17_r1]
meta_1	[cell_type_Basal, metagene_12_r4, metagene_15_r1, cell_type_Pre-ciliated, metagene_9_r3, metagene_10_r4, metagene_8_r1, metagene_19_r2, metagene_12_r3, cell_type_Ionocyte, metagene_1_r2, metagene_10_r2, metagene_18_r4, metagene_16_r2, metagene_18_r2, metagene_12_r1, metagene_7_r3, metagene_3_r2, metagene_4_r4, cell_type_Ciliated]
meta_2	[cell_type_Hillock, metagene_13_r1, metagene_6_r2, metagene_10_r4, metagene_15_r2, cell_type_Pre-ciliated, metagene_19_r2, metagene_17_r3, metagene_9_r3, metagene_18_r4, metagene_16_r4, cell_type_Ionocyte]
meta_3	[metagene_11_r3, metagene_6_r1, metagene_13_r4, metagene_17_r2, metagene_15_r2, metagene_10_r4, cell_type_Brush+PNEC, metagene_14_r4, metagene_6_r4, metagene_14_r2, cell_type_Pre-ciliated, metagene_12_r2, metagene_9_r4, metagene_19_r2, metagene_9_r1, metagene_4_r3, metagene_5_r1, metagene_9_r2, metagene_7_r4, metagene_2_r2, metagene_16_r2, metagene_4_r1, metagene_12_r1, metagene_8_r4, metagene_1_r4]
meta_4	[cell_type_Secretory, metagene_15_r2]

B

```
['cell_type_Doublet', 'cell_type_Pre-ciliated', 'cell_type_Ionocyte', 'cell_type_Brush+PNEC']
['cell_type_Basal', 'cell_type_Pre-ciliated', 'cell_type_Ionocyte', 'cell_type_Ciliated']
['cell_type_Hillock', 'cell_type_Pre-ciliated', 'cell_type_Ionocyte']
['cell_type_Brush+PNEC', 'cell_type_Pre-ciliated']
['cell_type_Secretory']
['cell_type_Cycling basal', 'cell_type_Ionocyte', 'cell_type_Pre-ciliated', 'cell_type_Ciliated']
['cell_type_Ciliated', 'cell_type_Brush+PNEC', 'cell_type_Cycling basal', 'cell_type_Ionocyte', 'cell_type_Basal']
['cell_type_Ionocyte', 'cell_type_Pre-ciliated']
['cell_type_Brush+PNEC', 'cell_type_Pre-ciliated']
['cell_type_Brush+PNEC', 'cell_type_Pre-ciliated', 'cell_type_Cycling basal']
['cell_type_Pre-ciliated', 'cell_type_Brush+PNEC']
['cell_type_Myoepithelial']
['cell_type_Ionocyte']
['cell_type_Brush+PNEC', 'cell_type_Cycling basal']
['cell_type_Brush+PNEC']
['cell_type_Brush+PNEC', 'cell_type_Myoepithelial', 'cell_type_Ionocyte']
['cell_type_Brush+PNEC']
['cell_type_Ionocyte', 'cell_type_Myoepithelial']
[]
['cell_type_Brush+PNEC', 'cell_type_Cycling basal', 'cell_type_Basal', 'cell_type_Doublet', 'cell_type_Hillock']
```

C

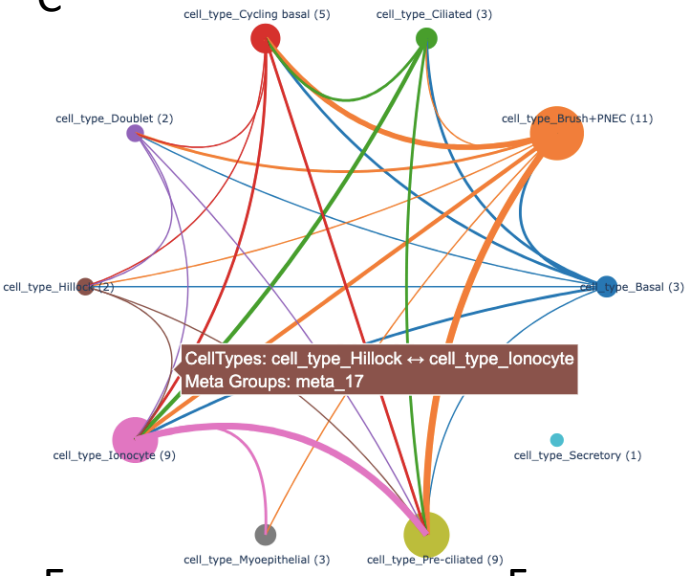

D

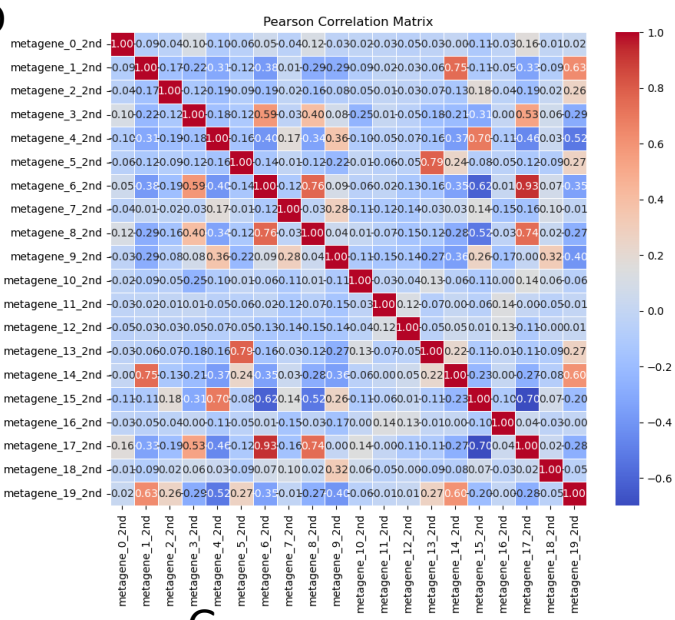

E

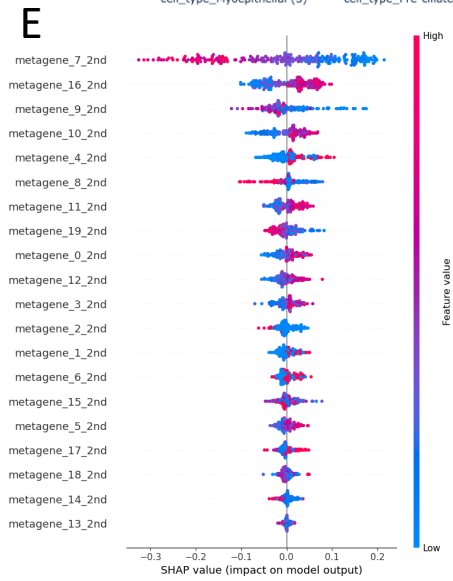

F

G

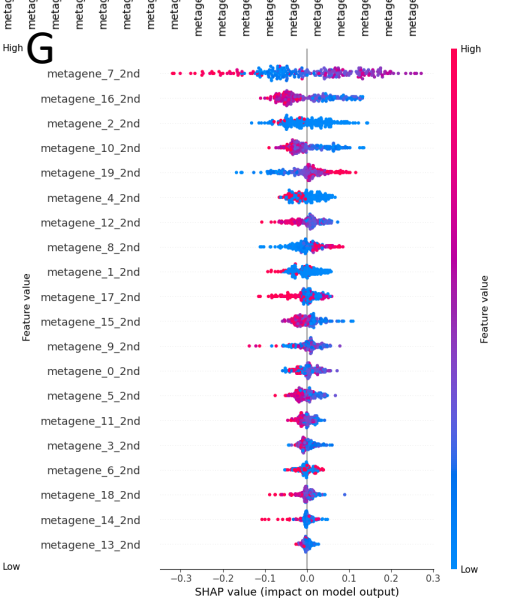

A

	inputs
meta_0	[metagene_4_hum, metagene_9_hum, metagene_0_hum, metagene_4_plas, metagene_2_hum, metagene_3_plas, metagene_6_plas, metagene_8_plas]
meta_1	[metagene_6_hum]
meta_2	[metagene_3_hum]
meta_3	[metagene_2_hum, metagene_4_hum, metagene_5_hum, metagene_8_hum]
meta_4	[metagene_0_hum, metagene_1_plas, metagene_5_hum, metagene_2_plas, metagene_0_plas, metagene_4_hum, metagene_9_plas]
meta_5	[metagene_7_hum, metagene_5_hum, metagene_9_hum, metagene_4_hum]
meta_6	[metagene_1_hum, metagene_9_hum, metagene_8_hum, metagene_5_hum, metagene_4_hum]

B

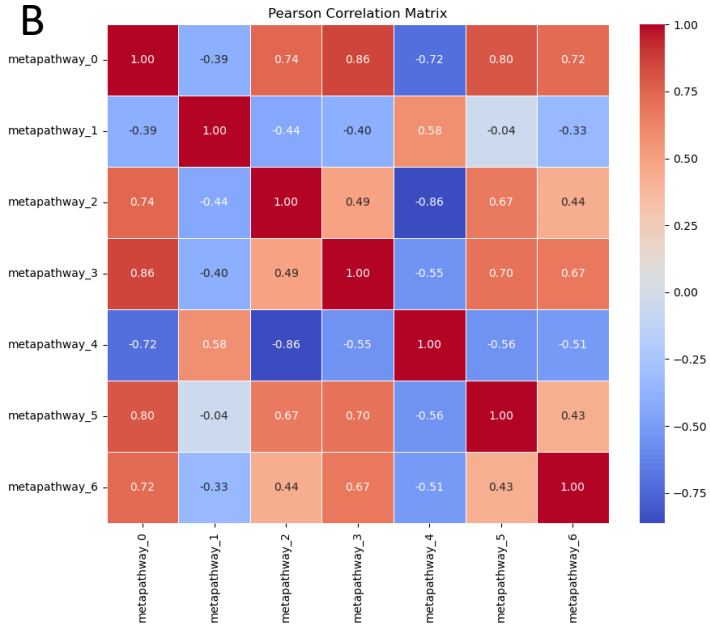

C

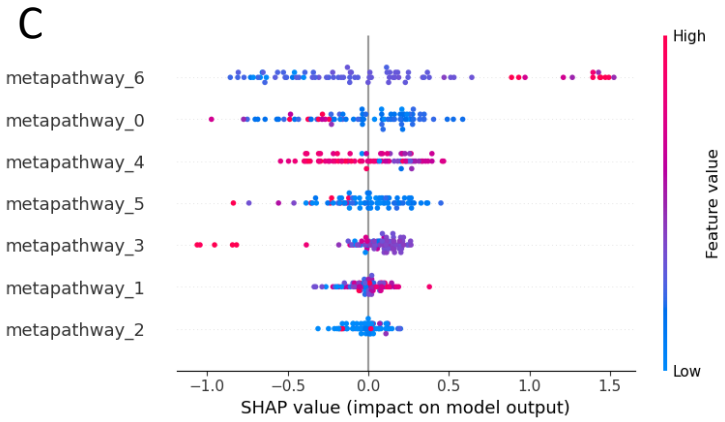

A

Metagene Network Diagram

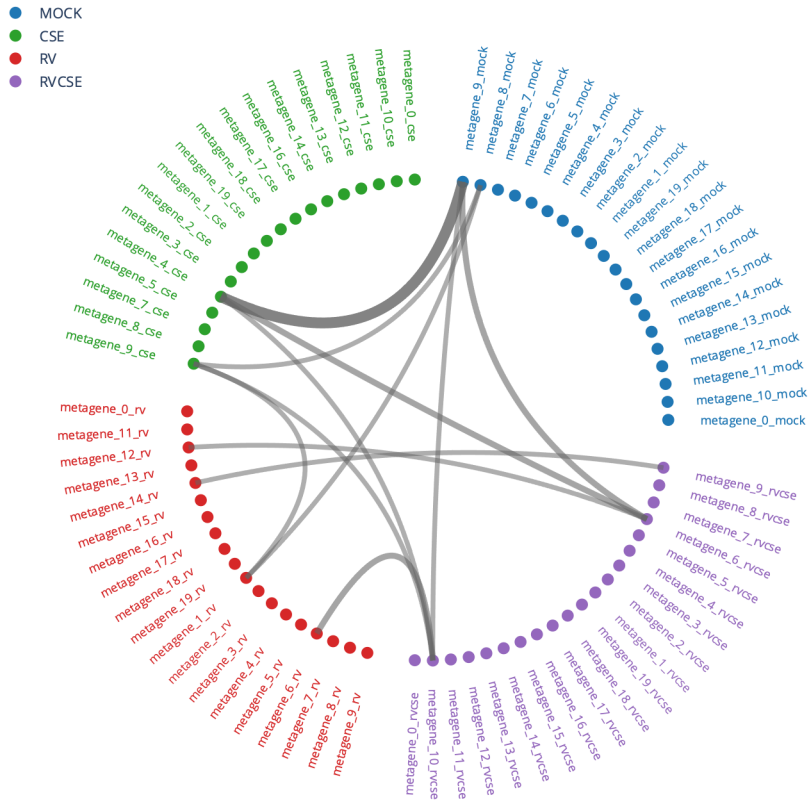

B
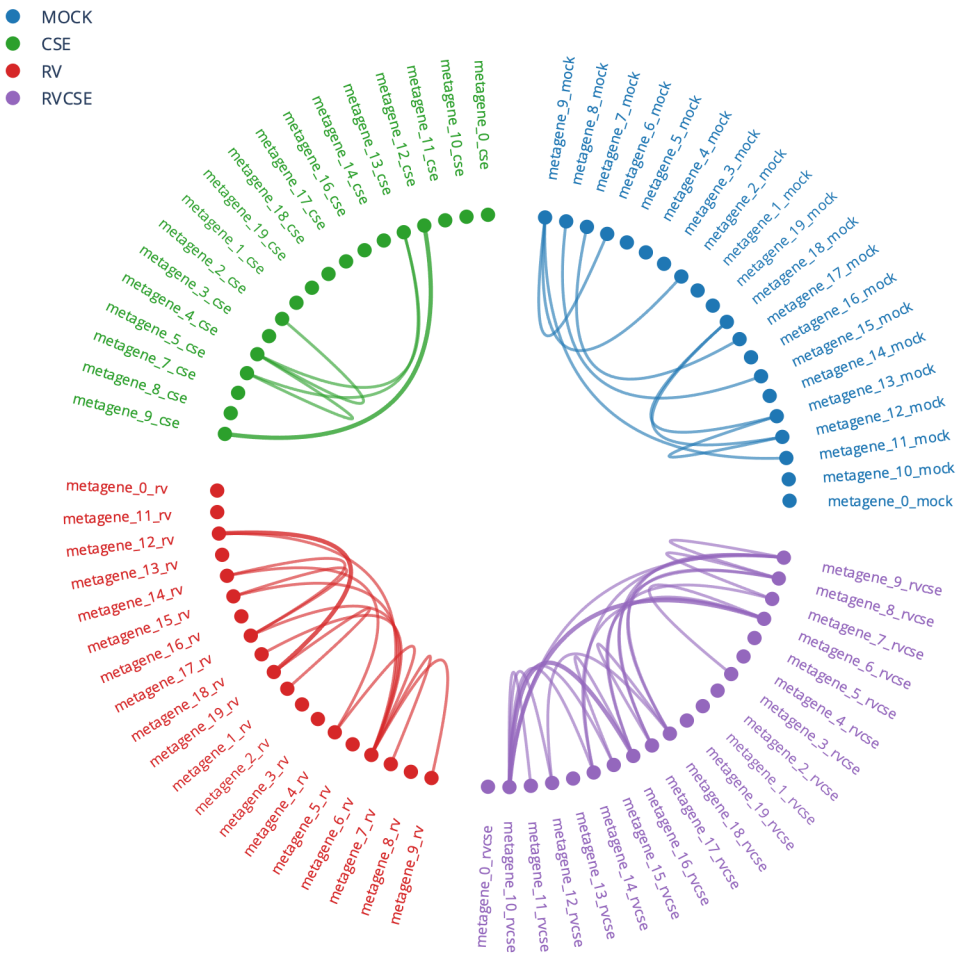
Metagene Network Diagram - Connections Within Batches Only